

Momentum-space resummation for transverse observables and the Higgs p_{\perp} at $N^3\text{LL}+\text{NNLO}$

Wojciech Bizon^a, Pier Francesco Monni^b, Emanuele Re^{b,c}, Luca Rottoli^a, Paolo Torrielli^d

^a*Rudolf Peierls Centre for Theoretical Physics, University of Oxford, Keble Road, Oxford OX1 3NP, UK*

^b*CERN, Theoretical Physics Department, CH-1211 Geneva 23, Switzerland*

^c*LAPTh, CNRS, Université Savoie Mont Blanc, BP110, F-74941 Annecy-le-Vieux Cedex, France*

^d*Dipartimento di Fisica, Università di Torino and INFN, Sezione di Torino, Via P. Giuria 1, I-10125, Turin, Italy*

E-mail: wojciech.bizon@physics.ox.ac.uk, pier.monni@cern.ch,
emanuele.re@lapth.cnrs.fr, luca.rottoli@physics.ox.ac.uk,
torriell@to.infn.it

ABSTRACT: We present an approach to the momentum-space resummation of global, recursive infrared and collinear safe observables featuring kinematic zeros away from the Sudakov limit. In the hadro-production of a generic colour singlet, we consider the family of inclusive observables which do not depend on the rapidity of the radiation, prime examples being the transverse momentum of the singlet, and ϕ^* in Drell-Yan pair production. We derive a resummation formula valid up to next-to-next-to-next-to-leading-logarithmic accuracy for the considered observables. This formula reduces exactly to the customary resummation performed in impact-parameter space in the known cases, and it also predicts the correct power-behaved scaling of the cross section in the limit of small value of the observable. We show how this formalism is efficiently implemented by means of Monte Carlo techniques in a fully exclusive generator that allows one to apply arbitrary cuts on the Born variables for any colour singlet, as well as to automatically match the resummed results to fixed-order calculations. As a phenomenological application, we present state-of-the-art predictions for the Higgs-boson transverse-momentum spectrum at the LHC at next-to-next-to-next-to-leading-logarithmic accuracy matched to fixed next-to-next-to-leading order.

Contents

1	Introduction	1
2	Derivation of the master formula	3
2.1	Cancellation of IRC divergences and NLL resummation	3
2.2	Structure of higher-order corrections	9
2.3	Treatment of parton densities and master formula for initial-state radiation	11
2.3.1	Hard-collinear emissions and treatment of recoil	11
2.3.2	Resummed formula for initial-state radiation	14
2.4	Equivalence with impact-parameter-space formulation	18
3	Evaluation up to N³LL	21
3.1	Momentum-space formulation	21
3.2	Perturbative scaling in the $p_t \rightarrow 0$ regime	28
4	Numerical implementation	30
4.1	Unitarity constraint and resummation-scale dependence	30
4.2	Matching to fixed order	33
4.3	Event generation	35
4.4	Predictions for Higgs-boson production at 13 TeV pp collisions	36
5	Conclusions	38
6	Acknowledgements	40
A	Connection with the backward-evolution algorithm at NLL	40
B	Analytic formulae for the N³LL radiator	42

1 Introduction

After the discovery of the Higgs boson [1, 2], the precise measurements from Run 2 of the LHC programme have so far confirmed the Standard Model with remarkable precision. Given that signals of new physics will most likely be elusive, it is important to define and study observables that can be both experimentally measured and theoretically predicted with a few-percent uncertainty. In this scenario, a prominent role is played by processes featuring the production of a colour singlet of high invariant mass, for instance gluon-fusion Higgs and Drell-Yan, where quantities like the transverse momentum of the singlet or angular observables defined on its decay products have been studied with increasing accuracy in the last decades.

The differential study of these processes not only is important from a purely phenomenological perspective, but also because it represents the ideal baseline for a more fundamental understanding of the underlying theory. Their structural simplicity indeed allows one to provide predictions that include several orders of perturbative corrections, hence probing in depth many non-trivial features of QCD.

In this paper, we consider the hadro-production of a heavy colour singlet, and in particular we study a class of observables that do not depend on the rapidity distribution of the initial-state QCD radiation. We refer to these as to *transverse* observables, and henceforth use the symbol v to denote them. Although the formalism that we present in this work can be extended to all transverse observables in colour-singlet hadro-production, we focus on one particular class of this family, namely the *inclusive* observables. Specifically, we consider the transverse-momentum distribution of a Higgs boson in gluon fusion. The derived formulae can be applied to any other observable belonging to this class like, for instance, the ϕ^* angle in Drell-Yan pair production.

Inclusive and differential distributions for gluon-fusion Higgs production are nowadays known with very high precision. The inclusive cross section is now known at next-to-next-to-next-to-leading-order (N³LO) accuracy in QCD [3, 4] in the heavy top-quark limit. The N³LO correction amounts to a few percent of the total cross section, indicating that the perturbative series has started to manifest convergence and that missing higher-order corrections are now getting under theoretical control. Current estimates show that they are very moderate in size [5]. The state-of-the-art results for the Higgs transverse-momentum spectrum in fixed-order perturbation theory are the next-to-next-to-leading-order (NNLO) computations of refs. [6–9], which have been obtained in the heavy top-quark limit. The impact of quark masses on differential distributions in the large-transverse-momentum limit is still poorly known beyond leading order, while in the moderate- p_t region, next-to-leading-order (NLO) QCD corrections to the top-bottom interference contribution were recently computed [10–12].

Although fixed-order results are crucial to obtain reliable theoretical predictions away from the soft and collinear regions of the phase space ($v \sim 1$), it is well known that regions dominated by soft and collinear QCD radiation — which give rise to the bulk of the total cross section — are affected by large logarithmic terms of the form $\alpha_s^n \ln^k(1/v)/v$, with $k \leq 2n - 1$, which spoil the convergence of the perturbative series at small v . In order to have a finite calculation in this limit, the subtraction of the infrared and collinear divergences requires an all-order resummation of the logarithmically divergent terms. The logarithmic accuracy is commonly defined in terms of the perturbative series of the *logarithm* of the cumulative cross section Σ

$$\Sigma(v) = \int_0^v dv' \frac{d\sigma(v')}{dv'}.$$

One refers to the dominant terms $\alpha_s^n \ln^{n+1}(1/v)$ as leading logarithmic (LL), to terms $\alpha_s^n \ln^n(1/v)$ as next-to-leading logarithmic (NLL), to $\alpha_s^n \ln^{n-1}(1/v)$ as next-to-next-to-leading logarithmic (NNLL), and so on.

The resummation of the p_t spectrum of a heavy colour singlet was first analysed in the seminal work by Parisi and Petronzio [13], where it was shown that in the low- p_t region the spectrum vanishes as $d\sigma/dp_t \sim p_t$, instead of vanishing exponentially as suggested by Sudakov suppression. This power-law behaviour is due to configurations in which p_t vanishes due to kinematic cancellations among the non-vanishing transverse momenta of all emissions. Around and below the peak of the distribution, this mechanism dominates with respect to kinematical configurations where p_t becomes small due to all the emissions having a small transverse momentum, i.e. the configurations which would yield an exponential suppression. In order to properly deal with these two competing mechanisms, in ref. [14] it was proposed to perform the resummation in the impact-parameter (b) space, where both effects leading to a vanishing p_t are handled through a Fourier transform.

Using the b -space formulation, the Higgs p_t spectrum was resummed at NNLL accuracy in [15, 16] using the formalism developed in [14, 17], as well as in [18] by means of a soft-collinear-effective-theory (SCET) approach [19, 20]. A study of the related theory uncertainties in the SCET formulation was presented in ref. [21]. More recently, all the necessary ingredients for the N³LL resummation were computed [22–25], paving the way to more precise predictions for transverse

observables in the infrared region. The impact of both threshold and high-energy resummation on the small-transverse-momentum region was also studied in detail in refs. [26–34].

The problem of the resummation of the transverse momentum distribution in direct (p_t) space received substantial attention throughout the years [35, 36], but remained unsolved until recently. Due to the vectorial nature of these observables, it is indeed not possible to define a resummed cross section at a given logarithmic accuracy in direct space that is simultaneously free of any subleading contributions and of spurious singularities at finite values of $p_t > 0$. Last year some of us proposed a solution to this problem by formulating a resummation formalism in direct space up to NNLL order [37], and used it to match the NNLL resummation to the NNLO Higgs p_t spectrum. The problem of direct-space resummation for the transverse-momentum distribution was also considered more recently in ref. [38] following a SCET approach. In this article we explain in detail the formalism introduced in [37]. Furthermore, we extend it to N³LL, and formulate it in general terms, so that a direct application at this logarithmic accuracy to all transverse, inclusive observables is possible.

The paper is structured as follows: in Section 2.1 we derive a NLL formula in the case of frozen parton densities using an extension of the formalism developed in ref. [39], and in Section 2.2 we discuss the structure of higher-order corrections. In Section 2.3, we discuss how to include the evolution of the parton densities and how to treat hard-collinear radiation, thereby extending the formalism to the case of initial-state radiation. In Section 2.4 we prove that our method is formally equivalent to the more common b -space formulation for the transverse momentum resummation. Section 3 shows how to evaluate our formula to N³LL order and in Section 3.2 we present a study of the scaling property of the differential distribution in the $p_t \rightarrow 0$ limit, and compare our findings to the classic result by Parisi and Petronzio [13]. Finally, in Section 4 we discuss the matching to NNLO, and in Section 4.4 we present N³LL accurate predictions for the Higgs-boson transverse momentum spectrum at the LHC, matched to NNLO.

In Appendix A we show that, at NLL, the approach used here is equivalent to a backward-evolution algorithm for this class of observables, while Appendix B collects some of the relevant equations used in the article.

2 Derivation of the master formula

We consider the resummation of a continuously global, recursive infrared and collinear (rIRC) safe [39] observable V in the reaction $pp \rightarrow B$, B being a generic colourless system with high invariant mass M . It is instructive to work out in detail the case of NLL resummation first, in the approximation of scale-independent parton densities; the correct treatment of the parton luminosity will be dealt with in Section 2.3.

2.1 Cancellation of IRC divergences and NLL resummation

To set up the notation, we start by denoting the momenta of the incoming partons in the rest frame of the colour singlet, meaning the innermost momenta entering the hard scattering after all radiation has taken place, as

$$\tilde{p}_1 = \frac{M}{2}(1, 0, 0, 1), \quad \tilde{p}_2 = \frac{M}{2}(1, 0, 0, -1), \quad (2.1)$$

where M is the invariant mass of the colour singlet produced in the scattering with momentum p_B

$$p_B = \tilde{p}_1 + \tilde{p}_2. \quad (2.2)$$

Beyond the Born level, radiation of gluons and quarks takes place, so that the final state consists in general of n partons with *outgoing* momenta k_1, \dots, k_n , and of the colour singlet. Due to this

radiation, the singlet acquires a transverse momentum with respect to the beam direction. We express the final-state momenta by means of the Sudakov parametrisation

$$k_i = (1 - y_i^{(1)})\tilde{p}_1 + (1 - y_i^{(2)})\tilde{p}_2 + \tilde{\kappa}_{ti}, \quad (2.3)$$

where $\tilde{\kappa}_{ti}$ are space-like four-vectors, orthogonal to both \tilde{p}_1 and \tilde{p}_2 . In the reference frame (2.1) each $\tilde{\kappa}_{ti}$ has no time-like component, and can be written as $\tilde{\kappa}_{ti} = (0, \vec{k}_{ti})$, such that $\tilde{\kappa}_{ti}^2 = -\vec{k}_{ti}^2$. Notice that since k_i is massless

$$\tilde{\kappa}_{ti}^2 = (1 - y_i^{(1)})(1 - y_i^{(2)})M^2 = \frac{2(\tilde{p}_1 k_i)2(\tilde{p}_2 k_i)}{2(\tilde{p}_1 \tilde{p}_2)}.$$

In the chosen parametrisation, the emission's (pseudo-)rapidity η_i in this frame is

$$\eta_i = \frac{1}{2} \ln \frac{1 - y_i^{(1)}}{1 - y_i^{(2)}}. \quad (2.4)$$

The observable V is in general a function of all momenta, and we denote it by $V(\{\tilde{p}\}, k_1, \dots, k_n)$; without loss of generality we assume that it vanishes in Born-like kinematic configurations. The observables considered in this paper obey the following general parametrisation for a single soft emission k collinear to leg ℓ :

$$V(\{\tilde{p}\}, k) \equiv V(k) = d_\ell g_\ell(\phi) \left(\frac{k_t}{M} \right)^a, \quad (2.5)$$

where k_t is the transverse momentum with respect to the beam axis, ϕ is the angle that \vec{k}_t forms with a fixed reference vector \vec{n} orthogonal to the beam axis, d_ℓ is a normalisation factor, and $a > 0$ by collinear and infrared safety. In particular, in this work we focus on the family of inclusive observables that will be defined in the next section. Examples of such observables are the transverse momentum of the colour-singlet system (corresponding to $d_\ell = g_\ell(\phi) = a = 1$)¹, and ϕ^* [40] (corresponding to $d_\ell = a = 1$, $g_\ell(\phi) = |\sin(\phi)|$). In the latter case, the reference vector \vec{n} is chosen along the direction of the dilepton system in Z -boson production.

The transverse momentum of the parametrisation (2.3) is related to the one relative to the beam axis, which enters the definition of the observable, by recoil effects due to hard-collinear emissions off the same leg ℓ ; under the convention of outgoing momenta we find

$$\vec{k}_{ti} = \vec{k}_{ti} - \frac{1 - y_i^{(\ell)}}{1 + \sum_{j \in \ell} (1 - y_j^{(\ell)})} \left(\sum_{j \in \ell} \vec{k}_{tj} \right), \quad (2.6)$$

where with the notation $j \in \ell$ we refer to partons that are emitted off the same leg \tilde{p}_ℓ as k_i . When only one emission is present, the above relation reduces to

$$\vec{k}_{ti} = \frac{\vec{k}_{ti}}{2 - y_i^{(\ell)}}. \quad (2.7)$$

In the soft approximation the two quantities coincide as $y_i^{(\ell)} \simeq 1$. In the present section we work under the assumption of soft kinematics in order to introduce the notation and derive the NLL result. The treatment of hard-collinear emissions will be discussed in detail in Section 2.3, where we extend the results derived here to the general case of initial-state radiation.

¹Without loss of generality we have introduced a dimensionless version of the transverse momentum by dividing by the singlet's mass.

The central quantity under study is the resummed cumulative cross section for V smaller than some value v , $\Sigma(v)$, defined as

$$\Sigma(v) = \int_0^v dv' \frac{d\sigma(v')}{dv'}. \quad (2.8)$$

In the infrared and collinear (IRC) limit, $\Sigma(v)$ is described by either virtual corrections or soft and/or collinear real emissions. In the limit $v \rightarrow 0$ the external legs are in their mass shell and the IRC divergences of the UV-renormalised virtual corrections exponentiate at all orders. We denote the latter by $\mathcal{V}(M^2)$ in the following discussion. In order to formulate an all-order treatment, it is thus necessary to devise a scheme to perform the cancellation of the real IRC divergences against the exponential virtual corrections.

The first step in this direction is to build an explicit logarithmic counting for the squared matrix elements. The renormalised squared amplitude for n real emissions ($pp \rightarrow B + n$ gluons) can be conveniently decomposed as

$$\begin{aligned} |M(\tilde{p}_1, \tilde{p}_2, k_1, \dots, k_n)|^2 &= |M_B(\tilde{p}_1, \tilde{p}_2)|^2 \left\{ \left(\frac{1}{n!} \prod_{i=1}^n |M(k_i)|^2 \right) + \right. \\ &\left[\sum_{a>b} \frac{1}{(n-2)!} \left(\prod_{\substack{i=1 \\ i \neq a, b}}^n |M(k_i)|^2 \right) |\tilde{M}(k_a, k_b)|^2 + \right. \\ &\left. \sum_{\substack{a>b \\ c>d \\ c, d \neq a, b}} \frac{1}{(n-4)!2!} \left(\prod_{\substack{i=1 \\ i \neq a, b, c, d}}^n |M(k_i)|^2 \right) |\tilde{M}(k_a, k_b)|^2 |\tilde{M}(k_c, k_d)|^2 + \dots \right] \\ &\left. + \left[\sum_{a>b>c} \frac{1}{(n-3)!} \left(\prod_{\substack{i=1 \\ i \neq a, b, c}}^n |M(k_i)|^2 \right) |\tilde{M}(k_a, k_b, k_c)|^2 + \dots \right] + \dots \right\}, \quad (2.9) \end{aligned}$$

where we have introduced the n -particle correlated matrix elements squared $|\tilde{M}(k_a, \dots, k_n)|^2$, which are defined recursively as follows

$$\begin{aligned} |\tilde{M}(k_a)|^2 &= \frac{|M(\tilde{p}_1, \tilde{p}_2, k_a)|^2}{|M_B(\tilde{p}_1, \tilde{p}_2)|^2} = |M(k_a)|^2, \\ |\tilde{M}(k_a, k_b)|^2 &= \frac{|M(\tilde{p}_1, \tilde{p}_2, k_a, k_b)|^2}{|M_B(\tilde{p}_1, \tilde{p}_2)|^2} - \frac{1}{2!} |M(k_a)|^2 |M(k_b)|^2, \\ |\tilde{M}(k_a, k_b, k_c)|^2 &= \frac{|M(\tilde{p}_1, \tilde{p}_2, k_a, k_b, k_c)|^2}{|M_B(\tilde{p}_1, \tilde{p}_2)|^2} - \frac{1}{3!} |M(k_a)|^2 |M(k_b)|^2 |M(k_c)|^2 \\ &\quad - |\tilde{M}(k_a, k_b)|^2 |M(k_c)|^2 - |\tilde{M}(k_a, k_c)|^2 |M(k_b)|^2 - |\tilde{M}(k_b, k_c)|^2 |M(k_a)|^2, \quad (2.10) \end{aligned}$$

and so on. These represent the contributions to the n -particle squared matrix element that vanish in strongly-ordered kinematic configurations, for which the full squared amplitude can not be factorised in terms of lower-multiplicity squared amplitudes. The decomposition above can be extended to the case in which some of the n emissions are quarks by properly changing the multiplicity factors in front of each term. The correlated squared amplitudes admit a perturbative expansion

$$|\tilde{M}(k_a, \dots, k_n)|^2 \equiv \sum_{j=0}^{\infty} \left(\frac{\alpha_s(\mu)}{2\pi} \right)^{n+j} n\text{PC}^{(j)}, \quad (2.11)$$

where μ is a common renormalisation scale, and α_s is the strong coupling constant in the $\overline{\text{MS}}$ scheme. The notation $n\text{PC}$ in Eq. (2.9) stands for “ n -particle correlated” and it will be used throughout the article.

The rIRC safety of the observables considered here guarantees a hierarchy between the different blocks in the decomposition (2.9), in the sense that, generally, correlated blocks with n particles start contributing at one logarithmic order higher than correlated blocks with $n-1$ particles [39, 41]. This, for instance, means that leading-logarithmic terms of the form $\alpha_s^n \ln^{2n}(1/v)$ entirely arise from $1\text{PC}^{(0)}$ blocks, in particular from their soft-collinear part. The cross section (2.8) therefore reduces to

$$\Sigma(v) = \sigma^{(0)} \mathcal{V}(M^2) \sum_{n=0}^{\infty} \frac{1}{n!} \int \prod_i [dk_i] |M(k_i)|^2 \Theta(v - V(\{\tilde{p}\}, k_1, \dots, k_n)), \quad (2.12)$$

where $\sigma^{(0)}$ is the Born cross section and, for the time being, we assumed that the parton densities in $\sigma^{(0)}$ do not depend on the energy scale.

If one wants to control all terms of order $\alpha_s^n \ln^{n+1}(1/v)$ in the *logarithm* of $\Sigma(v)$ then the leading (soft-collinear) term of the $1\text{PC}^{(1)}$ and $2\text{PC}^{(0)}$ blocks must be included as well. These contributions in the soft region can be entirely encoded in the running of the coupling through a proper choice of the scale at which the latter is evaluated, which turns out to be the k_t (equal to \tilde{k}_t for soft radiation) of each emission k in the parametrisation (2.3) [42, 43]. As such, they can be completely absorbed into the $1\text{PC}^{(0)}$ blocks with coupling $\alpha_s(k_t)$. The $1\text{PC}^{(0)}$ block and phase space controlling all $\alpha_s^n \ln^{n+1}(1/v)$ terms are thus

$$\begin{aligned} [dk] |M(k)|^2 &= [dk] M_{\text{sc}}^2(k) \\ &+ \sum_{\ell=1,2} \frac{dk_t^2}{k_t^2} \frac{dz^{(\ell)}}{1-z^{(\ell)}} \frac{\alpha_s(k_t)}{2\pi} \left((1-z^{(\ell)}) P^{(0)}(z^{(\ell)}) - \lim_{z^{(\ell)} \rightarrow 1} [(1-z^{(\ell)}) P^{(0)}(z^{(\ell)})] \right), \end{aligned} \quad (2.13)$$

where we split the squared amplitude in a soft-collinear term defined as

$$[dk] M_{\text{sc}}^2(k) = \sum_{\ell=1,2} 2C_\ell \frac{\alpha_s(k_t)}{\pi} \frac{dk_t}{k_t} \frac{dz^{(\ell)}}{1-z^{(\ell)}} \Theta\left((1-z^{(\ell)}) - k_t/M\right) \Theta(z^{(\ell)}) \frac{d\phi}{2\pi}, \quad (2.14)$$

and a hard-collinear term that involves a generic collinear splitting function $P^{(0)}(z^{(\ell)})^2$ minus its soft-collinear limit. Their expression is reported in Appendix B. We denoted by C_ℓ the Casimir relative to the emitting leg ($C_\ell = C_F$ for quarks, and $C_\ell = C_A$ for gluons).

For initial-state radiation, the argument of the splitting kernels is $z^{(\ell)}$, with $1-z^{(\ell)}$ being the fraction of the incoming momentum (entering the emission vertex) that is carried by the emitted parton. This will in general differ from the $y^{(\ell)}$ fractions of the Sudakov parametrisation (2.3) when some emissions are not soft. In particular, while $(1-z^{(\ell)}) \leq 1$, this is not true in general for the $(1-y^{(\ell)})$ appearing in our initial parametrisation. However, in the soft limit, the energy of the emission is much smaller than the singlet's mass M , which restricts $y_i^{(\ell)}$ to positive values in this limit.

For a single emission, the two variables are related by

$$1 - y^{(\ell)} = \frac{1 - z^{(\ell)}}{z^{(\ell)}}, \quad (2.15)$$

from which is clear that in the soft limit $z^{(\ell)} \simeq 1$ one has $z^{(\ell)} \simeq y^{(\ell)}$. The upper bound for $z^{(\ell)}$ in the single-emission case can be worked out by imposing that $y^{(\ell)} < 1 - \tilde{k}_t/M$, and subsequently relating \tilde{k}_t to k_t relative to the beam axis. This yields

$$z^{(\ell)} < 1 - k_t/M + \mathcal{O}(k_t^2). \quad (2.16)$$

²For emissions off gluonic legs, $P^{(0)}$ receives contributions from both $P_{gg}^{(0)}$ and $P_{gq}^{(0)}$, as it will be discussed in Sec. 2.3. In this case, we implicitly exploit the symmetry of $P_{gg}^{(0)}$ under $z \leftrightarrow 1-z$ to recast it such that it has only a $z \rightarrow 1$ singularity.

To extend the above discussion to all NLL terms of order $\alpha_s^n \ln^n(1/v)$ in the *logarithm* of $\Sigma(v)$, we must include the less singular part of the 1PC⁽¹⁾ and 2PC⁽⁰⁾ blocks in the soft limit. For rIRC safe observables, it can be shown [39, 41, 44] that at NLL one can treat the soft 2PC⁽⁰⁾ amplitude inclusively (i.e. integrating over the invariant mass of the two correlated final-state partons). Once again this simply amounts to correcting Eq. (2.14) as

$$[dk]M_{\text{sc}}^2(k) = \sum_{\ell=1,2} 2C_\ell \frac{\alpha_s(k_t)}{\pi} \left(1 + \frac{\alpha_s(k_t)}{2\pi} K \right) \frac{dk_t}{k_t} \frac{dz^{(\ell)}}{1-z^{(\ell)}} \Theta \left((1-z^{(\ell)}) - k_t/M \right) \Theta(z^{(\ell)}) \frac{d\phi}{2\pi}, \quad (2.17)$$

where

$$K = \left(\frac{67}{18} - \frac{\pi^2}{6} \right) C_A - \frac{5}{9} n_f. \quad (2.18)$$

The above operation defines the Catani-Marchesini-Webber (CMW) scheme [45] for the running coupling.

Once the logarithmic counting for the squared amplitude has been set up, as a next step we need to discuss the cancellation of the exponentiated divergences of virtual origin against the real ones. At all perturbative orders at a given logarithmic accuracy, we need to single out the IRC singularities of the real matrix elements, which can again be achieved by exploiting [39, 41, 44] the rIRC safety of the observable $V(\{\tilde{p}\}, k_1, \dots, k_n)$ that we are computing. We start by considering configurations where the hardest emission k_1 ($V(k_1) > V(k_i)$ for $i > 1$) has occurred. The rIRC safety of the observable allows us to introduce a resolution parameter $\epsilon \ll 1$ independent of the observable such that all emissions k_i with $V(k_i) < \epsilon V(k_1)$ can be neglected in the computation of the observable up to power-suppressed corrections $\mathcal{O}(\epsilon^p V(k_1))$. Real emissions k coming from the 1PC^(m) blocks are categorised as *resolved* if $V(k) > \epsilon V(k_1)$, or *unresolved* if $V(k) < \epsilon V(k_1)$.

The collinear-safe extension of the definition of the resolution parameter to any $n\text{PC}^{(m)}$ block requires considering the content of each block inclusively. One possible scheme to do this is to refer to a $n\text{PC}^{(m)}$ block as unresolved if $V(k^{\text{inclusive}}) < \epsilon V(k_1)$, $k^{\text{inclusive}}$ being a light-like four-vector defined as

$$\vec{k}_{t1} + \vec{k}_{t2} + \dots + \vec{k}_{tn} = \vec{k}_t^{\text{inclusive}}, \quad (2.19)$$

$$Y_{1\dots n} = Y^{\text{inclusive}}, \quad (2.20)$$

where $Y_{1\dots n}$ is the rapidity of the $k_1 + k_2 + \dots + k_n$ system in the centre-of-mass frame of the collision.

The phase space of the unresolved real ensemble is now solely constrained by the upper resolution scale, since it does not contribute to the evaluation of the observable. As a consequence, it can be exponentiated and employed to cancel the divergences of the virtual corrections $\mathcal{V}(M^2)$. The combination of unresolved real and virtual contributions is thus finite and gives rise to a Sudakov suppression factor. At NLL accuracy, this amounts to $\exp\{-R(\epsilon V(k_1))\}$ where R is the radiator which at this order reads [39, 41]

$$R(v) \simeq R_{\text{NLL}}(v) \equiv \int [dk] M_{\text{sc}}^2(k) \Theta \left(\ln \left(\frac{k_t}{M} \right)^a - \ln v \right) + \int [dk] M_{\text{sc}}^2(k) \ln \bar{d}_\ell \delta \left(\ln \left(\frac{k_t}{M} \right)^a - \ln v \right) \\ + \sum_{\ell=1,2} C_\ell B_\ell \int \frac{dk_t^2}{k_t^2} \frac{\alpha_s(k_t)}{2\pi} \Theta \left(\left(\frac{k_t}{M} \right)^a - v \right), \quad (2.21)$$

where

$$\ln \bar{d}_\ell = \int_0^{2\pi} \frac{d\phi}{2\pi} \ln d_\ell g_\ell(\phi), \quad (2.22)$$

and

$$C_\ell B_\ell = \int_0^1 \frac{dz^{(\ell)}}{1-z^{(\ell)}} \left((1-z^{(\ell)})P^{(0)}(z^{(\ell)}) - \lim_{z^{(\ell)} \rightarrow 1} [(1-z^{(\ell)})P^{(0)}(z^{(\ell)})] \right). \quad (2.23)$$

The next and final step is to treat the resolved real emissions k_i for which $V(k_i) > \epsilon V(k_1)$. It is therefore necessary to work out the kinematics and phase space in the presence of additional radiation, which modifies the relations (2.15) and (2.16). In order to study this, we need to introduce an ordering with which the emissions are radiated off the hard Born legs. Without loss of generality, we therefore impose that the radiation is ordered in $V(k_i)$, which is compatible with the definition of the resolution variable, and therefore ensures that the full phase space is covered. For a given emission k_i , one then has³

$$1 - y_i^{(\ell)} = \frac{1 - z_i^{(\ell)}}{z_1^{(\ell)} z_2^{(\ell)} \dots z_i^{(\ell)}}, \quad (2.24)$$

where emissions k_1, k_2, \dots, k_{i-1} have been radiated off the same hard leg before k_i . In general, this implies that the phase space available for each emission is changed by the previous radiation. At the NLL order considered in this section, the real-radiation kinematics can be approximated with its soft limit [39, 41]. This allows us to approximate $y_i^{(\ell)} \simeq z_i^{(\ell)}$ and $k_t \simeq \tilde{k}_t$ for all real emissions and therefore the phase space of each emission becomes in fact independent of the remaining radiation in the event.

The squared matrix element (2.13) and phase space for a resolved real emission can be parametrised by introducing the functions

$$\begin{aligned} R'_1 \left(\frac{v}{d_1 g_1(\bar{\phi})} \right) &= \int [dk] M^2(k) (2\pi) \delta(\phi - \bar{\phi}) v \delta(v - V(\{\tilde{p}\}, k)) \Theta(y^{(2)} - y^{(1)}), \\ R'_2 \left(\frac{v}{d_2 g_2(\bar{\phi})} \right) &= \int [dk] M^2(k) (2\pi) \delta(\phi - \bar{\phi}) v \delta(v - V(\{\tilde{p}\}, k)) \Theta(y^{(1)} - y^{(2)}), \end{aligned} \quad (2.25)$$

and

$$R'(v, \phi) = R'_1 \left(\frac{v}{d_1 g_1(\phi)} \right) + R'_2 \left(\frac{v}{d_2 g_2(\phi)} \right). \quad (2.26)$$

Using Eq. (2.13), the product of the single-particle phase space and the squared amplitude for an emission k_i becomes [39, 41]

$$[dk_i] M^2(k_i) = \frac{dv_i d\phi_i}{v_i 2\pi} \sum_{\ell_i=1,2} R'_{\ell_i} \left(\frac{v_i}{d_{\ell_i} g_{\ell_i}(\phi_i)} \right) = \frac{d\zeta_i d\phi_i}{\zeta_i 2\pi} \sum_{\ell_i=1,2} R'_{\ell_i} \left(\frac{\zeta_i v_i}{d_{\ell_i} g_{\ell_i}(\phi_i)} \right), \quad (2.27)$$

where we defined $v_i = V(k_i)$ and $\zeta_i = V(k_i)/V(k_1)$.

We are now ready to iterate the above picture at all orders to derive the NLL result. Given that the squared amplitude at this accuracy reduces to the product of single-emission probabilities given by Eqs. (2.13), (2.17), and that the phase space is identical for all secondary emissions k_i , $i > 1$, Eq. (2.12) can be recast as

$$\begin{aligned} \Sigma(v) &= \sigma^{(0)} \int \frac{dv_1}{v_1} \int_0^{2\pi} \frac{d\phi_1}{2\pi} e^{-R(\epsilon v_1)} \sum_{\ell_1=1,2} R'_{\ell_1} \left(\frac{v_1}{d_{\ell_1} g_{\ell_1}(\phi_1)} \right) \times \\ &\times \sum_{n=0}^{\infty} \frac{1}{n!} \prod_{i=2}^{n+1} \int_{\epsilon}^1 \frac{d\zeta_i}{\zeta_i} \int_0^{2\pi} \frac{d\phi_i}{2\pi} \sum_{\ell_i=1,2} R'_{\ell_i} \left(\frac{\zeta_i v_i}{d_{\ell_i} g_{\ell_i}(\phi_i)} \right) \Theta(v - V(\{\tilde{p}\}, k_1, \dots, k_{n+1})). \end{aligned} \quad (2.28)$$

Eq. (2.28) resembles equation (2.34) of ref. [39] which in turn leads to the general NLL formula of the CAESAR method for all global rIRC observables in processes with two hard legs. We remind

³See also discussion in the appendix of ref. [39].

the reader that additional corrections coming from the parton luminosities start at NLL order, and they will be discussed in Section 2.3.

In order to reproduce the NLL formula of ref. [39], a number of approximations can be further made on Eq. (2.28) with the purpose of neglecting all contributions beyond NLL accuracy. Specifically, in the resolved real squared matrix elements R'_ℓ one can ignore the second term in the r.h.s. of Eq. (2.13) which is irrelevant in the soft-collinear limit. Analogously, the observable can be treated in its soft-collinear approximation given that the real emissions constitute an ensemble of soft-collinear gluons at NLL. Moreover, for rIRC safe, global observables that only vanish in the Sudakov limit one can Taylor-expand both the Sudakov radiator $R(\epsilon v_1)$ and the real emission squared amplitudes R' about the observable's value v , retaining only terms that contribute at NLL order. Physically, this is equivalent to approximating the rapidity bounds of all emissions with a common bound that is set by the observable's value [39, 41]. This approximation allows one to evaluate the integral over v_1 analytically and to fully neglect subleading terms. This operation is described in detail in refs. [39, 41]. While the above approximations are not necessary, they define an unambiguous and rigorous procedure to neglect any contamination from terms beyond the desired logarithmic accuracy.

However, in order to perform the latter expansion around the observable's value v , one has to make sure that the ratio v_i/v remains of order one in the real-emission phase space. rIRC safety ensures that emissions with $v_i \ll v$ do not contribute to the observable, and are fully exponentiated and accounted for in the Sudakov radiator. Therefore, the condition $v_i/v \sim 1$ is fulfilled if there are no emissions for which $v_i \gg v$. While this condition holds true for most rIRC observables, it is clearly violated for observables that feature azimuthal cancellations away from the Sudakov limit. An example is given by the transverse momentum of a colour singlet, which can vanish even in the presence of several emissions with a finite (non-zero) transverse momentum. For such observables, Eq. (2.28) cannot be expanded around v . Therefore, while Eq. (2.28) is accurate at NLL order for such observables (as they are rIRC safe), subleading corrections beyond NLL cannot be entirely neglected.

Before concluding the present section, we would like to discuss further the choice of the resolution variable. A proper resolution variable has to guarantee, at all orders, the cancellation of the IRC divergences of the virtual corrections (and hence has to be rIRC safe) while, at the same time, reproducing the singular structure of the resolved real emission. This means that the difference between the actual observable one is computing and the observable used in the definition of the resolution variable has to be finite in four dimensions at any perturbative order. This implies that the two observables, due to rIRC safety, have the same leading-logarithmic structure and differ at higher logarithmic orders. It is therefore clear that one has some freedom in choosing the resolution variable, and several choices are possible. A particular choice is motivated by convenience in formulating the calculation. In particular, in the case studied in this section, as in refs. [39, 41, 46, 47], the resolution variable coincides with the observable itself computed in its soft-collinear limit, as discussed above. However, we note that for all observables of the type (2.5) one can equivalently choose $V(k) = (k_t/M)^a$ as a resolution variable. It is easy to verify that this indeed fulfills all the properties just described. Such a definition will lead to a common Sudakov radiator for all observables with the same a in Eq. (2.5), while the resolved real radiation will correctly encode the full observable dependence through the measurement function $\Theta(v - V(\{\hat{p}\}, k_1, \dots, k_{n+1}))$. In the present article, we adopt this choice, and we present explicitly the case for $a = 1$. The generalisation to any $a > 0$ is straightforward following our derivation.

2.2 Structure of higher-order corrections

In order to compute higher-order corrections to Eq. (2.28), one has to consider additional contributions to the all-order squared amplitudes beyond NLL accuracy. In the present article, we focus

on the family of inclusive observables V for which

$$V(\{\tilde{p}\}, k_1, \dots, k_n) = V(\{\tilde{p}\}, k_1 + \dots + k_n). \quad (2.29)$$

In this case, we can integrate the n PC blocks for $n > 1$ inclusively prior to evaluating the observable. Hence, starting from Eq. (2.9) for the pure gluonic case, we can replace it with the following squared amplitude

$$\begin{aligned} |M(\tilde{p}_1, \tilde{p}_2, k_1, \dots, k_n)|^2 &= |M_B(\tilde{p}_1, \tilde{p}_2)|^2 \\ &\times \frac{1}{n!} \left\{ \prod_{i=1}^n \left(|M(k_i)|^2 + \int [dk_a][dk_b] |\tilde{M}(k_a, k_b)|^2 \delta^{(2)}(\vec{k}_{ta} + \vec{k}_{tb} - \vec{k}_{ti}) \delta(Y_{ab} - Y_i) \right. \right. \\ &\left. \left. + \int [dk_a][dk_b][dk_c] |\tilde{M}(k_a, k_b, k_c)|^2 \delta^{(2)}(\vec{k}_{ta} + \vec{k}_{tb} + \vec{k}_{tc} - \vec{k}_{ti}) \delta(Y_{abc} - Y_i) + \dots \right) \right\}, \end{aligned} \quad (2.30)$$

where $Y_{abc\dots}$ is the rapidity of the $k_a + k_b + k_c + \dots$ system in the centre-of-mass frame of the collision. We refer to this treatment of the squared amplitude as to the *inclusive approximation*. For non-inclusive observables, namely the ones that do not fulfil Eq. (2.29), this reorganisation is not correct starting at NNLL. Therefore in that case one must correct for the non-inclusive nature of the observables. The full set of NNLL corrections for a generic global, rIRC safe observable is defined in refs. [41, 47]. In the rest of this article we refer to observables of the type (2.29).

Higher-order corrections require the inclusion of higher-multiplicity and higher-order blocks with respect to those relevant to Eq. (2.28). The relevant blocks necessary to a given order are summarised in Table 2.2. For instance, at NNLL, for the observables (2.29), one has to include

Logarithmic order	Blocks required
LL	{1PC ⁽⁰⁾ (sc)}
NLL	{1PC ⁽⁰⁾ , 1PC ⁽¹⁾ (sc)}; {2PC ⁽⁰⁾ (sc)}
NNLL	{1PC ^(m≤1) , 1PC ⁽²⁾ (sc)}; {2PC ⁽⁰⁾ , 2PC ⁽¹⁾ (sc)}; {3PC ⁽⁰⁾ (sc)}
N ³ LL	{1PC ^(m≤2) , 1PC ⁽³⁾ (sc)}; {2PC ^(m≤1) , 2PC ⁽²⁾ (sc)}; {3PC ⁽⁰⁾ , 3PC ⁽¹⁾ (sc)}; {4PC ⁽⁰⁾ (sc)}
⋮	⋮
N ^k LL	{1PC ^(m≤k-1) , 1PC ^(k) (sc)}; ⋯ ; {(k+1)PC ⁽⁰⁾ (sc)}

Table 1. Blocks to be included in the squared-amplitude decomposition at a given logarithmic order. At each order, the higher-rank blocks are to be included in the soft-collinear limit (“sc” in the table).

2PC⁽⁰⁾ (i.e. the fully correlated double emission), and 1PC⁽¹⁾ both in the soft and in the hard-collinear limit, and the fully inclusive contribution of the 3PC⁽⁰⁾, 2PC⁽¹⁾, and 1PC⁽²⁾ blocks in the soft-collinear limit.

In order to repeat the procedure that led to Eq. (2.28) at higher logarithmic accuracy, we need to handle the phase space in the multiple-emission kinematics. In the NLL case derived in the previous section, indeed, all resolved real emissions are soft and collinear and therefore they do not modify each other’s phase space. However, starting at NNLL one or more real emissions can be hard and collinear to the emitting leg and this changes the available phase space for subsequent real emissions. The kinematics and the proper treatment of hard-collinear emissions, still missing in our formulation, will be discussed in the following section.

2.3 Treatment of parton densities and master formula for initial-state radiation

In this section we formulate the treatment of initial-state, hard-collinear radiation and we derive the all-order formula for an inclusive observable v of the type (2.29).

2.3.1 Hard-collinear emissions and treatment of recoil

In order to correctly include the evolution of the hard-collinear radiation in our formulation, we first consider how initial-state radiation modifies the real-emission kernels, illustrating this in the single-emission case for the sake of clarity. Throughout this section and in the rest of this article we use the notation of ref. [48] for the flavour indices of the Altarelli-Parisi splitting kernels.

We start by formulating the single-emission probability for a gluon-initiated processes. We express the probability of emitting either a gluon or a quark off leg 1 (an analogous term can be written for an emission off leg 2), for an observable v , as

$$\begin{aligned}
\Sigma(v) &= |M_B|_{gg}^2 \int dx_1 dx_2 \delta(x_1 x_2 s - M^2) \int \frac{dk_t}{k_t} \frac{\alpha_s}{\pi} \frac{d\phi}{2\pi} \\
&\times \left(\int_{x_1}^{1-k_t/M} dz \left[2 \frac{P_{gg}^{(0)}(z)}{z} f_g(\mu_F, \frac{x_1}{z}) + \frac{P_{gq}^{(0)}(z)}{z} \left(f_q(\mu_F, \frac{x_1}{z}) + f_{\bar{q}}(\mu_F, \frac{x_1}{z}) \right) \right] f_g(\mu_F, x_2) \Theta(v - v(k)) \right. \\
&- \int_0^{1-k_t/M} dz \left[P_{gg}^{(0)}(z) + n_f P_{qg}^{(0)}(z) \right] f_g(\mu_F, x_1) f_g(\mu_F, x_2) \\
&\left. - \left(\hat{P}_{gg}^{(0)} \otimes f_g \right) (x_1) f_g(\mu_F, x_2) - \left(P_{gq}^{(0)} \otimes f_q \right) (\mu_F, x_1) f_g(\mu_F, x_2) - \left(P_{gq}^{(0)} \otimes f_{\bar{q}} \right) (\mu_F, x_1) f_g(\mu_F, x_2) \right), \tag{2.31}
\end{aligned}$$

where $f_g(\mu_F, x)$ is the gluon density renormalised in the $\overline{\text{MS}}$ scheme, evaluated at a factorisation scale μ_F , and \hat{P} denotes the regularised splitting function. Since $\hat{P}_{gq}^{(0)}(z) = P_{gq}^{(0)}(z)$ (see Appendix B), the regularised label “ $\hat{}$ ” applies only to $P_{gg}^{(0)}$. The second, third, and fourth line of Eq. (2.31) denote the real emission, the virtual corrections corresponding to the relative self-energy (in dispersive representation), and collinear counterterm, respectively. We stress that the upper bound in the z integral of the virtual corrections is in general different from the one in the real-emission term. This is because the virtual contribution features one less emission than the corresponding real correction. In the single-emission case treated in Eq. (2.31) one can use the fact that for the virtual corrections $\tilde{k}_t = k_t$ and therefore the limits of the z integral are identical to the ones in the real correction. For the sake of simplicity, for the time being we neglected NNLL constant parts in Eq. (2.31), arising from both the finite terms of the virtual form factor in $\overline{\text{MS}}$, and the $\mathcal{O}(\alpha_s)$ collinear coefficient functions. These will be included in our final formula.

We now add and subtract the term

$$\begin{aligned}
&|M_B|_{gg}^2 \int dx_1 dx_2 \delta(x_1 x_2 s - M^2) \int \frac{dk_t}{k_t} \frac{\alpha_s}{\pi} \frac{d\phi}{2\pi} \\
&\times \int_0^{1-k_t/M} dz \left[P_{gg}^{(0)}(z) + n_f P_{qg}^{(0)}(z) \right] (f_g(\mu_F, x_1) f_g(\mu_F, x_2) + \{x_1 \leftrightarrow x_2\}) \Theta(v - v(k)), \tag{2.32}
\end{aligned}$$

and recast Eq. (2.31) as

$$\begin{aligned}
\Sigma(v) &= |M_B|_{gg}^2 \int dx_1 dx_2 \delta(x_1 x_2 s - M^2) \int \frac{dk_t}{k_t} \frac{\alpha_s}{\pi} \frac{d\phi}{2\pi} \\
&\times \left(\int_{x_1}^{1-k_t/M} dz 2 \frac{P_{gg}^{(0)}(z)}{z} f_g(\mu_F, \frac{x_1}{z}) f_g(\mu_F, x_2) \Theta(v - v(k)) - \int_{x_1}^1 dz \frac{\hat{P}_{gg}^{(0)}(z)}{z} f_g(\mu_F, \frac{x_1}{z}) f_g(\mu_F, x_2) \right. \\
&\left. - \int_0^{1-k_t/M} dz \left[P_{gg}^{(0)}(z) + n_f P_{qg}^{(0)}(z) \right] f_g(\mu_F, x_1) f_g(\mu_F, x_2) \Theta(v - v(k)) \right)
\end{aligned}$$

$$\begin{aligned}
& + \int_0^{1-k_t/M} dz \left[P_{gg}^{(0)}(z) + n_f P_{qg}^{(0)}(z) \right] f_g(\mu_F, x_1) f_g(\mu_F, x_2) (\Theta(v - v(k)) - 1) \\
& + \int_{x_1}^1 dz \frac{P_{gq}^{(0)}(z)}{z} \left(f_q(\mu_F, \frac{x_1}{z}) + f_{\bar{q}}(\mu_F, \frac{x_1}{z}) \right) f_g(\mu_F, x_2) (\Theta(v - v(k)) - 1) \\
& - \int_{1-k_t/M}^1 dz \frac{P_{gq}^{(0)}(z)}{z} \left(f_q(\mu_F, \frac{x_1}{z}) + f_{\bar{q}}(\mu_F, \frac{x_1}{z}) \right) f_g(\mu_F, x_2) \Theta(v - v(k)) \Big). \tag{2.33}
\end{aligned}$$

By using the symmetry of the P_{gg} splitting function under $z \leftrightarrow 1 - z$, one finds that

$$\int_{x_1}^1 dz 2 \frac{P_{gg}^{(0)}(z)}{z} f_g(\mu_F, \frac{x_1}{z}) - \int_0^1 dz \left(P_{gg}^{(0)}(z) + n_f P_{qg}^{(0)}(z) \right) f_g(\mu_F, x_1) = \int_{x_1}^1 dz \frac{\hat{P}_{gg}^{(0)}(z)}{z} f_g(\mu_F, \frac{x_1}{z}), \tag{2.34}$$

which allows us to recast the previous equation as

$$\begin{aligned}
\Sigma(v) = & |M_B|_{gg}^2 \int dx_1 dx_2 \delta(x_1 x_2 s - M^2) \int \frac{dk_t}{k_t} \frac{\alpha_s}{\pi} \frac{d\phi}{2\pi} \\
& \times \left\{ \int_{x_1}^1 dz \frac{\hat{P}_{gg}^{(0)}(z)}{z} f_g(\mu_F, \frac{x_1}{z}) f_g(\mu_F, x_2) (\Theta(v - v(k)) - 1) \right. \\
& + \int_0^{1-k_t/M} dz \left[P_{gg}^{(0)}(z) + n_f P_{qg}^{(0)}(z) \right] f_g(\mu_F, x_1) f_g(\mu_F, x_2) (\Theta(v - v(k)) - 1) \\
& + \int_{x_1}^1 dz \frac{P_{gq}^{(0)}(z)}{z} \left(f_q(\mu_F, \frac{x_1}{z}) + f_{\bar{q}}(\mu_F, \frac{x_1}{z}) \right) f_g(\mu_F, x_2) (\Theta(v - v(k)) - 1) \\
& - \int_{1-k_t/M}^1 dz \left(2 \frac{P_{gg}^{(0)}(z)}{z} f_g(\mu_F, \frac{x_1}{z}) f_g(\mu_F, x_2) - \left[P_{gg}^{(0)}(z) + n_f P_{qg}^{(0)}(z) \right] f_g(\mu_F, x_1) f_g(\mu_F, x_2) \right. \\
& \left. \left. + \frac{P_{gq}^{(0)}(z)}{z} \left(f_q(\mu_F, \frac{x_1}{z}) + f_{\bar{q}}(\mu_F, \frac{x_1}{z}) \right) f_g(\mu_F, x_2) \right) \Theta(v - v(k)) \right\}. \tag{2.35}
\end{aligned}$$

Analogously, it is straightforward to show that the logarithmic part for a quark-initiated process with an emission off the leg 1 reads

$$\begin{aligned}
\Sigma(v) = & |M_B|_{q\bar{q}}^2 \int dx_1 dx_2 \delta(x_1 x_2 s - M^2) \int \frac{dk_t}{k_t} \frac{\alpha_s}{\pi} \frac{d\phi}{2\pi} \\
& \times \left\{ \int_{x_1}^1 dz \frac{P_{qg}^{(0)}(z)}{z} f_g(\mu_F, \frac{x_1}{z}) f_{\bar{q}}(\mu_F, x_2) (\Theta(v - v(k)) - 1) \right. \\
& + \int_0^{1-k_t/M} dz P_{qg}^{(0)}(z) f_q(\mu_F, x_1) f_{\bar{q}}(\mu_F, x_2) (\Theta(v - v(k)) - 1) \\
& + \int_{x_1}^1 dz \frac{\hat{P}_{qg}^{(0)}(z)}{z} f_q(\mu_F, \frac{x_1}{z}) f_{\bar{q}}(\mu_F, x_2) (\Theta(v - v(k)) - 1) \\
& - \int_{1-k_t/M}^1 dz \left(\frac{P_{qg}^{(0)}(z)}{z} f_q(\mu_F, \frac{x_1}{z}) f_{\bar{q}}(\mu_F, x_2) - P_{qg}^{(0)}(z) f_q(\mu_F, x_1) f_{\bar{q}}(\mu_F, x_2) \right. \\
& \left. \left. + \frac{P_{qg}^{(0)}(z)}{z} f_g(\mu_F, \frac{x_1}{z}) f_{\bar{q}}(\mu_F, x_2) \right) \Theta(v - v(k)) \right\}, \tag{2.36}
\end{aligned}$$

where we have set $\hat{P}_{qg}^{(0)}(z) = P_{qg}^{(0)}(z)$.

In Eqs. (2.35) and (2.36), the last integral from $1 - k_t/M$ to 1 gives rise to regular terms and can therefore be neglected. As far as the remaining terms are concerned, we notice that the squared matrix element for an initial-state emission, which corresponds to the terms containing a Θ function in Eqs. (2.35) and (2.36), can be separated into two pieces:

- The first one, encoded in the third line of Eqs. (2.35) and (2.36), modifies neither the flavour nor the momentum fraction of the incoming partons, and the bounds of the relative z integration are those of the corresponding virtual phase space. This contribution is fully analogous to the case treated in Sec. 2.2, that gives rise to R' in Eq. (2.28). When evaluating this term explicitly, we can further split it, as done in Eq. (2.13), into a sum of a soft term and a hard-collinear contribution. The exact upper bound of the z integral is only relevant in the soft contribution and it can be extended up to 1 in the hard-collinear term up to regular (non logarithmic) terms.
- The second one (second and fourth lines of Eqs. (2.35) and (2.36)) does modify both flavour and momentum fraction. This contribution corresponds to an exclusive step of DGLAP evolution. The corresponding z integration can be extended up to the soft limit ($z = 1$) as it is regularised by the plus distribution. We stress once again that this approximation is correct up to regular terms that are ignored in our treatment.

This decomposition is only a convenient way of expressing the squared amplitude and phase space for an initial-state emission, and only the sum of all logarithmic terms in Eqs. (2.35) and (2.36) is physically well defined. The considerations above will be useful in the rest of this section when the all-order kinematics is discussed.

Following the discussion of Sec. 2.2, in order to achieve N³LL accuracy, in addition to the soft ensembles described with the proper squared amplitudes (as in Table 2.2), one has to consider configurations with up to two hard-collinear emissions and any number of soft partons in the final state. We therefore study how the presence of the hard-collinear emission affects the phase space of the remaining radiation in the all-order picture.⁴ We consider again the emissions ordered according to their transverse momentum. In this picture, the relation between the $z^{(\ell)}$ variable and the Sudakov variable $y^{(\ell)}$ for a given emission k will be modified by the radiation that occurred before k as described in Eq. (2.24).

We consider the case of an ensemble of resolved emissions off a leg ℓ of which a single one is hard and collinear, while all the remaining radiation is soft. We can divide the event into three regions: the soft emissions that occur before the hard-collinear parton is emitted (i.e. at larger transverse momenta), the hard-collinear emission itself, and the soft emissions that occur after the hard-collinear one (at smaller transverse momenta). The soft radiation emitted before the hard-collinear emission has $z_i^{(\ell)} \simeq y_i^{(\ell)} \simeq 1$ and therefore $k_{ti} \simeq \tilde{k}_{ti}$, so its phase space boundaries are as described in Section 2.1. For the hard-collinear emission k^{hc} the relation between $z_{hc}^{(\ell)}$ and $y_{hc}^{(\ell)}$ is reported in Eq. (2.15) and the corresponding $z_{hc}^{(\ell)}$ integration bound is in Eq. (2.16). Finally, soft emissions that occur after the hard-collinear one will again have $k_{ti} \simeq \tilde{k}_{ti}$ but now $1 - y_i^{(\ell)} \simeq (1 - z_i^{(\ell)})/z_{hc}^{(\ell)}$. The upper bound of their $z_i^{(\ell)}$ integral is therefore

$$z_i^{(\ell)} < 1 - z_{hc}^{(\ell)} k_{ti}/M. \quad (2.37)$$

From the above equation we see that the phase space of the soft radiation emitted after the hard-collinear emission is modified by the presence of the latter. However, the squared amplitude and phase space for emissions in the soft limit only depend on $z_i^{(\ell)}$ through $dz_i^{(\ell)}/(1 - z_i^{(\ell)})$. Therefore, using the relation

$$\frac{dz_i^{(\ell)}}{1 - z_i^{(\ell)}} = \frac{dy_i^{(\ell)}}{1 - y_i^{(\ell)}}, \quad (2.38)$$

⁴We thank A. Banfi for fruitful discussions on this point.

and using the fact that $k_{ti} \simeq \tilde{k}_{ti}$ for these emissions, we can replace the integral over $z_i^{(\ell)}$ with an integral over $y_i^{(\ell)}$ whose upper bound is given by

$$y_i^{(\ell)} < 1 - k_{ti}/M. \quad (2.39)$$

This allows one to disentangle the phase space of all emissions in the considered kinematic configuration and, hence, to iterate the procedure at all orders.

The remaining kinematic configuration to be considered in a N³LL resummation is given by an ensemble of soft-collinear emissions accompanied by two hard-collinear ones. We therefore repeat the above discussion in this case. We label the two hard collinear emissions by k_1^{hc} and k_2^{hc} and we assume, without any loss of generality, that k_1^{hc} is emitted before k_2^{hc} (hence it has a larger transverse momentum in our picture). The upper bounds of the corresponding $z^{(\ell)}$ integrations for the real contribution will now be complicated functions of the transverse momenta k_{t1}^{hc} and k_{t2}^{hc} that can be obtained starting from Eqs. (2.6), (2.24). However, things are much simplified if we use the decomposition described in the first part of this section. We recall that the real matrix element can be decomposed as a sum of a term whose $z^{(\ell)}$ integration bounds are the same as for the virtual correction, and it is proportional to R' , and an actual hard-collinear correction which modifies the momentum fraction of the emitting leg. In the latter term, the upper bound of the $z^{(\ell)}$ integration can be extended to 1 since the soft limit is regularised by the plus prescription. Furthermore, as discussed above, the R' contributions relative to k_1^{hc} and k_2^{hc} will be further decomposed into the sum of a soft-collinear term and a term that contains the hard-collinear matrix element and does not modify the momentum fraction of the emitting leg. Once again, in the latter contribution the $z^{(\ell)}$ integration can be extended to 1, while in the soft contribution one can simply replace the $z^{(\ell)}$ integral with an integral over $y^{(\ell)}$ by means of Eq. (2.38). Moreover, using the fact that in the virtual phase space $\tilde{k}_t \simeq k_t$, the corresponding upper bound of the $y^{(\ell)}$ integral can be replaced by $1 - k_t/M$.

This procedure allows one to disentangle completely the phase space of soft radiation from the phase space of hard-collinear radiation when several emissions are considered. The phase space of different hard-collinear emissions, however, will still be entangled as each of them modifies significantly the momentum available for the subsequent hard-collinear ones. The above treatment of the double-hard-collinear case is valid up to regular terms. In this section we neglected the constant terms that arise from the finite part of the renormalised form factor, and from the collinear coefficient functions, which are relevant already for a NNLL resummation. For inclusive observables considered in this article, the collinear coefficient functions factorise in front of the Sudakov factor and, for the processes considered here, they were computed to $\mathcal{O}(\alpha_s^2)$ in refs. [22–24]. These will be introduced in the following section when we iterate the arguments discussed here at all perturbative orders in α_s .

2.3.2 Resummed formula for initial-state radiation

The arguments derived in the previous section can be used to formulate the structure of the cross section at all orders by iterating the single-emission probability defined above. As shown in the previous section, the contribution from each emission to the cross section can be split into a term that does not modify either the momentum fraction or the flavour of the emitting leg, and a contribution that modifies both, which corresponds to an exclusive DGLAP-evolution step. To precisely formulate this concept, we start by discussing the scale at which the parton densities are to be evaluated. This can be done by means of physical arguments based on rIRC safety. We stress that the formulation that follows is valid at least up to N³LL.

The parton densities are initially evaluated at a scale μ_0 that is assumed to be smaller than all transverse momenta in the event. We consider the situation in which the first (hardest) emission

k_1 occurred. The phase-space diagram for any secondary emission k_i with $i > 1$ is depicted in Fig. 1 in the $\ln(k_t/M) - \eta$ (Lund) plane, where now η denotes the rapidity in the centre-of-mass frame of the incoming partons which are extracted from the proton at a factorisation scale μ_0 . The corresponding transverse momentum k_t is taken with respect to the beam direction. As stated in Section 2.1, due to rIRC safety, only emissions that take place in the strip between ϵk_{t1} and k_{t1} modify the observable significantly and are resolved. The remaining unresolved real emissions ($k_{ti} < \epsilon k_{t1}$) are combined with the virtual corrections, which populate the whole region below the two diagonal lines that denote the upper rapidity limits. The result of this combination is indeed the Sudakov form factor associated with the first emission that vetoes secondary emissions in the yellow region of the Lund plane. In addition, the combination of virtual and unresolved emissions gives also rise to a constant term that multiplies the Sudakov and encodes both the finite part of the virtual corrections and the constant contribution due to soft and/or collinear emissions exactly at the edges of their phase space.

In the initial-state-radiation case at hand, hard-collinear emissions define the evolution of the parton densities. These emissions live on a strip (blue region in Fig. 1) along the upper rapidity bounds, and their evolution is encoded in the DGLAP equations. In the unresolved region, up

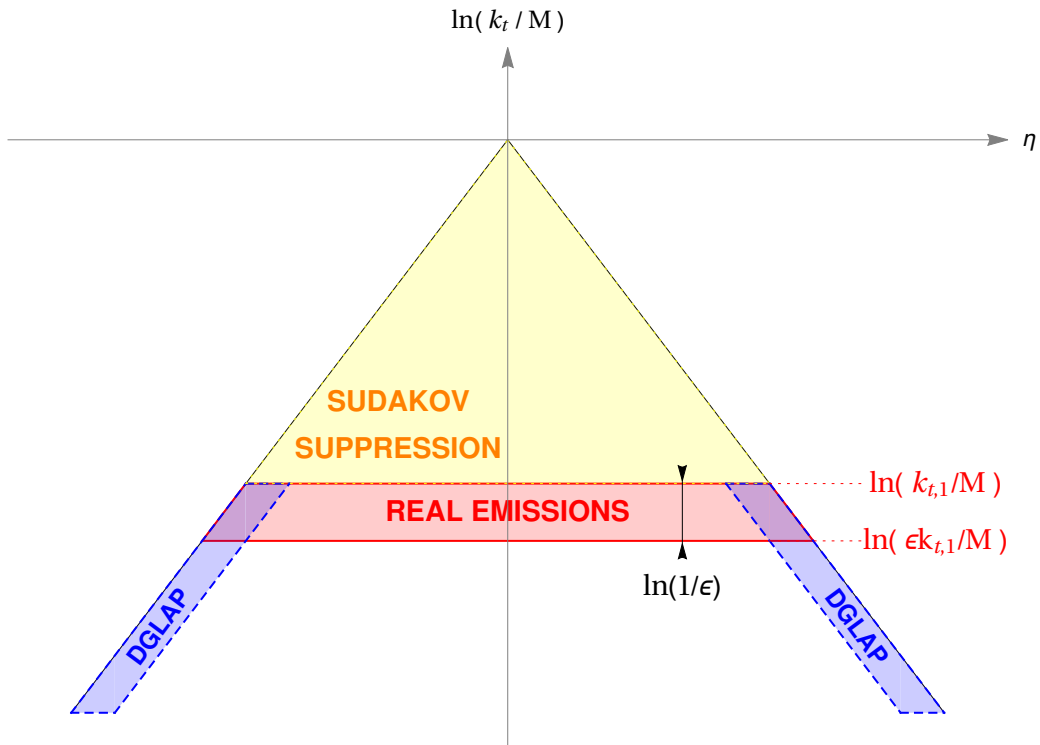


Figure 1. Phase space for a secondary real emission.

to ϵk_{t1} , the DGLAP evolution can be performed *inclusively* since emissions in this phase-space region do not affect the observable. On the other hand, when $k_{t1} > k_{ti} > \epsilon k_{t1}$ the corresponding hard-collinear emissions modify significantly the observable's value and therefore must be treated *exclusively*, namely unintegrated in k_t .

In addition to the parton densities, starting at $\mathcal{O}(\alpha_s)$, one needs to include the coefficient functions that emerge from their renormalisation, and originate from emissions that live at the edges of the phase space. The coefficient functions contribute to the logarithmic structure only through the scale of their running coupling, which is the transverse momentum of the emission(s)

they are associated with. As done for the parton densities, one can evaluate them initially at a scale μ_0 smaller than any transverse momentum in the event, and subsequently evolve them inclusively up to the resolution scale ϵk_{t1} . Their evolution must be instead treated exclusively in the resolved strip $k_{t1} > k_{ti} > \epsilon k_{t1}$.

In order to introduce the all-order result, it is convenient to simplify the flavour structure of the evolution for the time being. We neglect real-emission kernels that modify the flavour of the emitting leg, namely those that do not have a soft singularity P_{qg} and P_{gq} . This ensures that the flavour of the initial parton densities is only modified by the coefficient functions and is conserved by the real radiation. This approximation is made without any loss of generality, and for the only sake of simplicity. The extension to the full flavour case will be trivial once the final formula is obtained.

For the remaining part of the section, it is useful to introduce a matrix notation to simplify the structure of our expressions in flavour space. We define \mathbf{f} as the array containing the $2n_f + 1$ partonic densities, where n_f denotes the number of light flavours. To handle different Born configurations with different incoming flavours c_ℓ , we then define the coefficient-function matrix \mathbf{C}^{c_ℓ} as a $(2n_f + 1) \times (2n_f + 1)$ diagonal matrix in flavour space whose entries are

$$[\mathbf{C}^{c_\ell}]_{ab} = C_{c_\ell f(a)} \delta_{ab}, \quad (2.40)$$

where C_{ij} are the collinear coefficient functions, c_ℓ is the flavour of the leg ℓ entering the Born process, and $f(a)$ is the flavour corresponding to the a -th entry of the parton-density array. For instance, we explicitly show the above convention in the case of Higgs production, considering only a single quark flavour q . By defining the array $\mathbf{f} = (f_g, f_q, f_{\bar{q}})^T$, the matrix \mathbf{C}^g reads

$$\mathbf{C}^g = \begin{pmatrix} C_{gg} & 0 & 0 \\ 0 & C_{gq} & 0 \\ 0 & 0 & C_{g\bar{q}} \end{pmatrix}. \quad (2.41)$$

The evolution of (2.40) between two scales is entirely encoded in the evolution of the running coupling. By introducing the corresponding anomalous-dimension matrix $\mathbf{\Gamma}^{(C)}$

$$\mathbf{\Gamma}^{(C)}(\alpha_s(k_t)) = 2\beta(\alpha_s(k_t)) \frac{d \ln \mathbf{C}^{c_\ell}(\alpha_s(k_t))}{d\alpha_s(k_t)}, \quad (2.42)$$

we can write the Renormalisation-Group evolution (RGE) of the coefficient function matrix as

$$\mathbf{C}^{c_\ell}(\alpha_s(\mu)) = \exp \left\{ - \int_{\mu}^{\mu_0} \frac{dk_t}{k_t} \mathbf{\Gamma}^{(C)}(\alpha_s(k_t)) \right\} \mathbf{C}^{c_\ell}(\alpha_s(\mu_0)). \quad (2.43)$$

In principle, the matrix $\mathbf{\Gamma}^{(C)}$ should also explicitly carry a label c_ℓ to specify that it evolves the coefficient function \mathbf{C}^{c_ℓ} associated with the Born flavour c_ℓ . We omit this label in the following as the notation in what follows is unambiguous.

The iterative structure of the squared amplitudes appears more transparent if we work in Mellin space, where convolutions become products. We therefore introduce the Mellin transform of a function $g(x)$ as

$$g_{N_\ell} \equiv \int_0^1 dx x^{N_\ell - 1} g(x). \quad (2.44)$$

The DGLAP [49–51] evolution of the parton-density vector \mathbf{f} can be conveniently written in Mellin space as

$$\mathbf{f}_{N_\ell}(\mu) = \mathcal{P} \exp \left\{ - \int_{\mu}^{\mu_0} \frac{dk_t}{k_t} \frac{\alpha_s(k_t)}{\pi} \mathbf{\Gamma}_{N_\ell}(\alpha_s(k_t)) \right\} \mathbf{f}_{N_\ell}(\mu_0). \quad (2.45)$$

In the previous equation \mathcal{P} is the path-ordering symbol, and the matrix $\mathbf{\Gamma}$ is defined as

$$[\mathbf{\Gamma}_{N_\ell}(\alpha_s(\mu))]_{ab} = \int_0^1 dz z^{N_\ell-1} \hat{P}_{f(a)f(b)}(z, \alpha_s(\mu)) \equiv \gamma_{N_\ell;f(a)f(b)} = \sum_{n=0}^{\infty} \left(\frac{\alpha_s(\mu)}{2\pi} \right)^n \gamma_{N_\ell;f(a)f(b)}^{(n)}, \quad (2.46)$$

where $\hat{P}_{f(a)f(b)}$ are the regularised splitting functions (see Appendix B). We stress that, within the simplifying assumption made above on flavour-conserving real-emission kernels, no splitting functions involving a real quark emission are involved, therefore the matrix $\mathbf{\Gamma}$ is diagonal. Within this assumption, the path ordering in Eq. (2.45) can be lifted.

With this notation, the hadronic cumulative cross section, differential with respect to the Born phase space Φ_B , can be written as

$$\frac{d\Sigma(v)}{d\Phi_B} = \int_{\mathcal{C}_1} \frac{dN_1}{2\pi i} \int_{\mathcal{C}_2} \frac{dN_2}{2\pi i} x_1^{-N_1} x_2^{-N_2} \sum_{c_1, c_2} \frac{d|M_B|_{c_1 c_2}^2}{d\Phi_B} \mathbf{f}_{N_1}^T(\mu_0) \hat{\Sigma}_{N_1, N_2}^{c_1, c_2}(v) \mathbf{f}_{N_2}(\mu_0), \quad (2.47)$$

where the sum runs over all possible Born configurations and we employed a double inverse Mellin transform. The contours \mathcal{C}_1 and \mathcal{C}_2 are understood to lie along the imaginary axis to the right of all singularities of the integrand.

The matrix $\hat{\Sigma}$ encodes the effect of the all-order radiation that evolves the partonic cross section and the corresponding parton densities. To write down an all-order expression for $\hat{\Sigma}$ for the observables (2.29), we need to iterate the single-emission probability derived in the previous section. Given that the phase spaces of the soft and hard-collinear emissions are completely disentangled, this operation can be performed straightforwardly in Mellin space, yielding

$$\begin{aligned} \hat{\Sigma}_{N_1, N_2}^{c_1, c_2}(v) &= \left[\mathbf{C}_{N_1}^{c_1; T}(\alpha_s(\mu_0)) H(\mu_R) \mathbf{C}_{N_2}^{c_2}(\alpha_s(\mu_0)) \right] \int_0^M \frac{dk_{t1}}{k_{t1}} \int_0^{2\pi} \frac{d\phi_1}{2\pi} \\ &\times e^{-\mathbf{R}(\epsilon k_{t1})} \exp \left\{ - \sum_{\ell=1}^2 \left(\int_{\epsilon k_{t1}}^{\mu_0} \frac{dk_t}{k_t} \frac{\alpha_s(k_t)}{\pi} \mathbf{\Gamma}_{N_\ell}(\alpha_s(k_t)) + \int_{\epsilon k_{t1}}^{\mu_0} \frac{dk_t}{k_t} \mathbf{\Gamma}_{N_\ell}^{(C)}(\alpha_s(k_t)) \right) \right\} \\ &\sum_{\ell_1=1}^2 \left(\mathbf{R}'_{\ell_1}(k_{t1}) + \frac{\alpha_s(k_{t1})}{\pi} \mathbf{\Gamma}_{N_{\ell_1}}(\alpha_s(k_{t1})) + \mathbf{\Gamma}_{N_{\ell_1}}^{(C)}(\alpha_s(k_{t1})) \right) \\ &\times \sum_{n=0}^{\infty} \frac{1}{n!} \prod_{i=2}^{n+1} \int_{\epsilon}^1 \frac{d\zeta_i}{\zeta_i} \int_0^{2\pi} \frac{d\phi_i}{2\pi} \sum_{\ell_i=1}^2 \left(\mathbf{R}'_{\ell_i}(k_{ti}) + \frac{\alpha_s(k_{ti})}{\pi} \mathbf{\Gamma}_{N_{\ell_i}}(\alpha_s(k_{ti})) + \mathbf{\Gamma}_{N_{\ell_i}}^{(C)}(\alpha_s(k_{ti})) \right) \\ &\times \Theta(v - V(\{\bar{p}\}, k_1, \dots, k_{n+1})), \end{aligned} \quad (2.48)$$

where now $\zeta_i = k_{ti}/k_{t1}$ since we are using the transverse momentum as a resolution and ordering variable. \mathbf{R}'_{ℓ} is a diagonal matrix in flavour space: given the flavour c_ℓ of the Born leg ℓ , it describes the flavour-conserving resolved radiation off leg ℓ . It is defined as

$$[\mathbf{R}'_{\ell}]_{ab} = R'_{\ell} \delta_{ab}, \quad (2.49)$$

and R'_{ℓ} is defined in Eq. (2.25). The Sudakov operator \mathbf{R} is then defined as

$$\mathbf{R}(\epsilon k_{t1}) = \sum_{\ell=1}^2 \int_{\epsilon k_{t1}}^M \frac{dk_t}{k_t} \mathbf{R}'_{\ell}(k_t). \quad (2.50)$$

The terms proportional to \mathbf{R}' in Eq. (2.48) encode the contribution of the radiation which is flavour-diagonal, and does not modify the momentum fraction of the incoming partons. This is the analogous of what has been derived in Sec. 2.1 in the case of frozen parton densities. In addition,

the real emission probability now involves the exclusive evolution step for the parton densities and coefficient functions.

The matrices $\hat{\Sigma}^{c_1, c_2}$ are diagonal in flavour space within the flavour assumption that we are making here. The first line of Eq. (2.48) contains the factor $\left[\mathbf{C}_{N_1}^{c_1; T}(\alpha_s(\mu_0)) H(\mu_R) \mathbf{C}_{N_2}^{c_2}(\alpha_s(\mu_0)) \right]$ that encodes the hard-virtual corrections to the form factor and the collinear coefficient functions. Explicit expressions for these quantities will be given later (see Sec. 3.1 and references therein). As discussed above, the coupling of the coefficient functions here is evaluated at μ_0 and subsequently evolved up to ϵk_{t1} by the operator containing the diagonal matrix $\mathbf{\Gamma}_{N_\ell}^{(C)}$ in the second line of (2.48). Similarly, the parton densities are evolved from μ_0 up to ϵk_{t1} . As it was shown in ref. [52], starting at a given order in perturbation theory one needs to include the contribution from the gluon collinear correlation functions \mathbf{G} . Such a contribution starts at $\mathcal{O}(\alpha_s^2)$ (i.e. N³LL) for gluon-fusion processes, and at yet higher orders for quark-initiated ones. It is included in the above formulation by simply adding to Eq. (2.48) an analogous term where one makes the replacements

$$\left[\mathbf{C}_{N_1}^{c_1; T}(\alpha_s(\mu_0)) H(\mu_R) \mathbf{C}_{N_2}^{c_2}(\alpha_s(\mu_0)) \right] \rightarrow \left[\mathbf{G}_{N_1}^{c_1; T}(\alpha_s(\mu_0)) H(\mu_R) \mathbf{G}_{N_2}^{c_2}(\alpha_s(\mu_0)) \right], \quad (2.51)$$

and

$$\mathbf{\Gamma}_{N_\ell}^{(C)}(\alpha_s(k_t)) \rightarrow \mathbf{\Gamma}_{N_\ell}^{(G)}(\alpha_s(k_t)), \quad (2.52)$$

where $\mathbf{\Gamma}_{N_\ell}^{(G)}$ is defined analogously to Eq. (2.42), and the flavour structure of \mathbf{G} is analogous to the one of the \mathbf{C} matrix. In what follows this contribution, whenever not reported, is understood.

Eq. (2.48) has been derived by iterating the single-emission probability. For the observables discussed in this article defined in Eq. (2.29), higher-order blocks, contributing to subleading-logarithmic corrections, can be included by simply redefining the squared amplitudes in the inclusive approximation as discussed in Section 2.2. Specifically, this amounts to including higher-order logarithmic corrections to the radiator R and its derivative R' , as well as in the anomalous dimensions which drive the evolution of the parton densities and coefficient functions.

We conclude the discussion by pointing out that even if the all-order formulation has been conveniently obtained in Mellin space, it is possible to evaluate Eq. (2.47) directly in momentum space at any given logarithmic order. We will describe how to do this in Sec. 3.1. Eq. (2.48) holds for all inclusive observables (see definition in Sec. 2.2) that do not depend on the rapidity of the initial-state radiation. In the remaining part of this article we specialise to the study of the transverse-momentum case, but analogous conclusions will apply to other observables of the same class.

2.4 Equivalence with impact-parameter-space formulation

In this section we show how to relate our Eq. (2.47) to the impact-parameter-space formulation of [13]. We show the equivalence for the differential partonic cross section (2.48) in the case of the transverse momentum p_t . An analogous proof can be carried out in the case of the ϕ^* .

Our starting point is the differential partonic cross section, where we now set $\mu_0 = \mu_R = M$ without loss of generality:

$$\begin{aligned} \frac{d}{d^2 \vec{p}_t} \hat{\Sigma}_{N_1, N_2}^{c_1, c_2}(p_t) &= \mathbf{C}_{N_1}^{c_1; T}(\alpha_s(M)) H(M) \mathbf{C}_{N_2}^{c_2}(\alpha_s(M)) \int_0^M \frac{dk_{t1}}{k_{t1}} \int_0^{2\pi} \frac{d\phi_1}{2\pi} \\ &\times e^{-\mathbf{R}(\epsilon k_{t1})} \exp \left\{ - \sum_{\ell=1}^2 \left(\int_{\epsilon k_{t1}}^M \frac{dk_t}{k_t} \frac{\alpha_s(k_t)}{\pi} \mathbf{\Gamma}_{N_\ell}(\alpha_s(k_t)) + \int_{\epsilon k_{t1}}^M \frac{dk_t}{k_t} \mathbf{\Gamma}_{N_\ell}^{(C)}(\alpha_s(k_t)) \right) \right\} \\ &\times \sum_{\ell_1=1}^2 \left(\mathbf{R}'_{\ell_1}(k_{t1}) + \frac{\alpha_s(k_{t1})}{\pi} \mathbf{\Gamma}_{N_{\ell_1}}(\alpha_s(k_{t1})) + \mathbf{\Gamma}_{N_{\ell_1}}^{(C)}(\alpha_s(k_{t1})) \right) \end{aligned}$$

$$\begin{aligned}
& \times \sum_{n=0}^{\infty} \frac{1}{n!} \prod_{i=2}^{n+1} \int_{\epsilon}^1 \frac{d\zeta_i}{\zeta_i} \int_0^{2\pi} \frac{d\phi_i}{2\pi} \sum_{\ell_i=1}^2 \left(\mathbf{R}'_{\ell_i}(k_{ti}) + \frac{\alpha_s(k_{ti})}{\pi} \Gamma_{N_{\ell_i}}(\alpha_s(k_{ti})) + \Gamma_{N_{\ell_i}}^{(C)}(\alpha_s(k_{ti})) \right) \\
& \times \delta^{(2)} \left(\vec{p}_t - \left(\vec{k}_{t1} + \dots + \vec{k}_{t(n+1)} \right) \right). \tag{2.53}
\end{aligned}$$

We transform the δ function into b -space as

$$\delta^{(2)} \left(\vec{p}_t - \left(\vec{k}_{t1} + \dots + \vec{k}_{t(n+1)} \right) \right) = \int \frac{d^2\vec{b}}{4\pi^2} e^{-i\vec{b}\cdot\vec{p}_t} \prod_{i=1}^{n+1} e^{i\vec{b}\cdot\vec{k}_{ti}}, \tag{2.54}$$

and we evaluate the azimuthal integrals, which simply amounts to replacing each of the factors $e^{\pm i\vec{b}\cdot\vec{k}_t}$ with a Bessel function $J_0(bk_t)$. It is now straightforward to see that the sum in Eq. (2.53) give rises to an exponential function, yielding

$$\begin{aligned}
\frac{d}{dp_t} \hat{\Sigma}_{N_1, N_2}^{c_1 c_2}(p_t) &= \mathbf{C}_{N_1}^{c_1; T}(\alpha_s(M)) H(M) \mathbf{C}_{N_2}^{c_2}(\alpha_s(M)) p_t \int b db J_0(p_t b) \int_0^M \frac{dk_{t1}}{k_{t1}} \\
& \times \sum_{\ell_1=1}^2 \left(\mathbf{R}'_{\ell_1}(k_{t1}) + \frac{\alpha_s(k_{t1})}{\pi} \Gamma_{N_{\ell_1}}(\alpha_s(k_{t1})) + \Gamma_{N_{\ell_1}}^{(C)}(\alpha_s(k_{t1})) \right) J_0(bk_{t1}) \\
& \times \exp \left\{ - \sum_{\ell=1}^2 \int_{k_{t1}}^M \frac{dk_t}{k_t} \left(\mathbf{R}'_{\ell}(k_t) + \frac{\alpha_s(k_t)}{\pi} \Gamma_{N_{\ell}}(\alpha_s(k_t)) + \Gamma_{N_{\ell}}^{(C)}(\alpha_s(k_t)) \right) J_0(bk_t) \right\} \\
& \times \exp \left\{ - \sum_{\ell=1}^2 \int_{\epsilon k_{t1}}^M \frac{dk_t}{k_t} \left(\mathbf{R}'_{\ell}(k_t) + \frac{\alpha_s(k_t)}{\pi} \Gamma_{N_{\ell}}(\alpha_s(k_t)) + \Gamma_{N_{\ell}}^{(C)}(\alpha_s(k_t)) \right) (1 - J_0(bk_t)) \right\}. \tag{2.55}
\end{aligned}$$

We finally notice that we can set $\epsilon \rightarrow 0$ in the above formula, given that now the cancellation of divergences is manifest. The k_{t1} integrand is a total derivative and it integrates to one, leaving

$$\begin{aligned}
\frac{d}{dp_t} \hat{\Sigma}_{N_1, N_2}^{c_1 c_2}(p_t) &= \mathbf{C}_{N_1}^{c_1; T}(\alpha_s(M)) H(M) \mathbf{C}_{N_2}^{c_2}(\alpha_s(M)) p_t \int b db J_0(p_t b) \\
& \times \exp \left\{ - \sum_{\ell=1}^2 \int_0^M \frac{dk_t}{k_t} \left(\mathbf{R}'_{\ell}(k_t) + \frac{\alpha_s(k_t)}{\pi} \Gamma_{N_{\ell}}(\alpha_s(k_t)) + \Gamma_{N_{\ell}}^{(C)}(\alpha_s(k_t)) \right) (1 - J_0(bk_t)) \right\}. \tag{2.56}
\end{aligned}$$

We now insert the resulting partonic cross section back into the definition of the hadronic cross section (2.47), and use the second and third terms in the exponent of Eq. (2.56) to evolve the parton densities and the coefficient functions down to b_0/b , with $b_0 = 2e^{-\gamma_E}$. After performing the inverse Mellin transform, and neglecting N^4 LL terms, we obtain (hereafter we simplify the notation for the parton densities by omitting their x_1 and x_2 dependence, which is determined by the Born kinematics Φ_B)

$$\begin{aligned}
\frac{d^2\Sigma(v)}{d\Phi_B dp_t} &= \sum_{c_1, c_2} \frac{d|M_B|_{c_1 c_2}^2}{d\Phi_B} \int b db p_t J_0(p_t b) \mathbf{f}^T(b_0/b) \mathbf{C}_{N_1}^{c_1; T}(\alpha_s(b_0/b)) H(M) \mathbf{C}_{N_2}^{c_2}(\alpha_s(b_0/b)) \mathbf{f}(b_0/b) \\
& \times \exp \left\{ - \sum_{\ell=1}^2 \int_0^M \frac{dk_t}{k_t} \mathbf{R}'_{\ell}(k_t) (1 - J_0(bk_t)) \right\}. \tag{2.57}
\end{aligned}$$

Eq. (2.57) represents indeed the b -space formulation of transverse-momentum resummation. Commonly, it is expressed in the equivalent form [14]⁵

$$\frac{d^2\Sigma(v)}{d\Phi_B dp_t} = \sum_{c_1, c_2} \frac{d|M_B|_{c_1 c_2}^2}{d\Phi_B} \int b db p_t J_0(p_t b) \mathbf{f}^T(b_0/b) \mathbf{C}_{N_1}^{c_1; T}(\alpha_s(b_0/b)) H_{\text{CSS}}(M) \mathbf{C}_{N_2}^{c_2}(\alpha_s(b_0/b)) \mathbf{f}(b_0/b)$$

⁵This corresponds to a change of scheme of the type discussed in ref. [53].

$$\times \exp \left\{ - \sum_{\ell=1}^2 \int_0^M \frac{dk_t}{k_t} \mathbf{R}'_{\text{CSS},\ell}(k_t) \Theta(k_t - \frac{b_0}{b}) \right\}. \quad (2.58)$$

where $\mathbf{R}'_{\text{CSS},\ell}$ and $H_{\text{CSS}}(M)$ are the Sudakov and hard function commonly used for a b -space formulation [14]. As shown in ref. [52], and as already stressed above, both Eqs. (2.57) and (2.58) receive an extra contribution due to the azimuthal correlations which are parametrised by the \mathbf{G} coefficient functions. We omit them in this comparison for the sake of simplicity, however it is clear that analogous considerations apply in that case. The comparison between Eqs. (2.57) and (2.58) allows us to extract the N³LL ingredients from the latter formulation as obtained in refs. [22, 23, 25], that will be reported in the next section.

We start by using the relation⁶

$$(1 - J_0(bk_t)) \simeq \Theta(k_t - \frac{b_0}{b}) + \frac{\zeta_3}{12} \frac{\partial^3}{\partial \ln(Mb/b_0)^3} \Theta(k_t - \frac{b_0}{b}) + \dots, \quad (2.59)$$

where we ignored N⁴LL terms. In the above formula the derivative in the second term of the right-hand-side is meant to act on the integral whose bounds are set by $\Theta(k_t - \frac{b_0}{b})$. This yields, at N³LL,

$$\begin{aligned} \frac{d^2 \Sigma(v)}{d\Phi_B dp_t} &= \sum_{c_1, c_2} \frac{d|M_B|_{c_1 c_2}^2}{d\Phi_B} \int b db p_t J_0(p_t b) \mathbf{f}^T(b_0/b) \mathbf{C}_{N_1}^{c_1; T}(\alpha_s(b_0/b)) H(M) \mathbf{C}_{N_2}^{c_2}(\alpha_s(b_0/b)) \mathbf{f}(b_0/b) \\ &\times \exp \left\{ - \sum_{\ell=1}^2 \left(\int_{b_0/b}^M \frac{dk_t}{k_t} \mathbf{R}'_{\ell}(k_t) + \frac{\zeta_3}{12} \frac{\partial^3}{\partial \ln(Mb/b_0)^3} \int_{b_0/b}^M \frac{dk_t}{k_t} \mathbf{R}'_{\ell}(k_t) \right) \right\}. \end{aligned} \quad (2.60)$$

The second term in the exponent of Eq. (2.60) starts at N³LL, so up to NNLL the two definitions (the one in terms of a J_0 and the one in terms of the theta function) are manifestly equivalent. To relate the two formulations we recall the definition of \mathbf{R}' in Eq. (2.49) and we express the Sudakov radiators as (2.50)

$$\begin{aligned} R(b) &= \sum_{\ell=1}^2 \left(\int_{b_0/b}^M \frac{dk_t}{k_t} R'_{\ell}(k_t) + \frac{\zeta_3}{12} \frac{\partial^3}{\partial \ln(Mb/b_0)^3} \int_{b_0/b}^M \frac{dk_t}{k_t} R'_{\ell}(k_t) \right) \\ &= \sum_{\ell=1}^2 \int_{b_0/b}^M \frac{dk_t}{k_t} \left(A_{\ell}(\alpha_s(k_t)) \ln \frac{M^2}{k_t^2} + B_{\ell}(\alpha_s(k_t)) \right), \\ R_{\text{CSS}}(b) &= \sum_{\ell=1}^2 \int_{b_0/b}^M \frac{dk_t}{k_t} R'_{\text{CSS},\ell}(k_t) = \sum_{\ell=1}^2 \int_{b_0/b}^M \frac{dk_t}{k_t} \left(A_{\text{CSS},\ell}(\alpha_s(k_t)) \ln \frac{M^2}{k_t^2} + B_{\text{CSS},\ell}(\alpha_s(k_t)) \right), \end{aligned} \quad (2.61)$$

where we neglected N⁴LL corrections. The anomalous dimensions A_{ℓ} and B_{ℓ} relative to leg ℓ and the hard function H admit an expansion in the strong coupling as

$$A_{\ell}(\alpha_s) = \sum_{n=1}^4 \left(\frac{\alpha_s}{2\pi} \right)^n A_{\ell}^{(n)}, \quad B_{\ell}(\alpha_s) = \sum_{n=1}^3 \left(\frac{\alpha_s}{2\pi} \right)^n B_{\ell}^{(n)}, \quad H(M) = 1 + \sum_{n=1}^2 \left(\frac{\alpha_s(M)}{2\pi} \right)^n H^{(n)}(M). \quad (2.62)$$

The relation between the coefficients that enter at N³LL can be deduced by equating Eqs. (2.57) and (2.58), obtaining

$$A_{\ell}^{(4)} = A_{\text{CSS},\ell}^{(4)} + 32 A_{\ell}^{(1)} \pi^3 \beta_0^3 \zeta_3,$$

⁶See appendix of ref. [54] for a derivation.

$$\begin{aligned}
B_\ell^{(3)} &= B_{\text{CSS},\ell}^{(3)} + 16A_\ell^{(1)}\pi^2\beta_0^2\zeta_3, \\
H^{(2)}(M) &= H_{\text{CSS}}^{(2)}(M) + \frac{8}{3}\pi\beta_0\zeta_3 \sum_{\ell=1}^2 A_\ell^{(1)}.
\end{aligned} \tag{2.63}$$

The above equations constitute the ingredients for our N³LL resummation.

3 Evaluation up to N³LL

In this section we evaluate our all-order master formulae (2.47) and (2.48) explicitly up to N³LL accuracy. The latter equations can already be evaluated as they are by means of Monte Carlo techniques; however, at any given logarithmic order it is possible, and convenient, to further manipulate them in order to evaluate them *directly in momentum space*, without the need of the Mellin transform.

3.1 Momentum-space formulation

We firstly focus on the partonic cross section (2.48). There are three main ingredients: the Sudakov radiator and its derivative, the block containing coefficient functions $C(\alpha_s)$ and hard-virtual corrections to the form factor $H(\mu_R)$, and the anomalous dimensions that rule the evolution of parton densities and coefficient functions.

For colour-singlet production, the coefficients entering the Sudakov radiator satisfy $A_1^{(n)} = A_2^{(n)} = A^{(n)}/2$, and $B_1^{(n)} = B_2^{(n)} = B^{(n)}/2$. Coefficients $A^{(1)}$, $A^{(2)}$, $A^{(3)}$, $B^{(1)}$, $B^{(2)}$ have been known for several years [19, 55, 56], and they are collected, for instance, in the appendix of ref. [54]. The N³LL coefficient $B^{(3)}$ can be extracted from the recent result [25]. For gluon processes it reads:

$$\begin{aligned}
B^{(3)} &= C_A^3 \left(\frac{22\zeta_3\zeta_2}{3} - \frac{799\zeta_2}{81} - \frac{5\pi^2\zeta_3}{9} - \frac{2533\zeta_3}{54} - \frac{77\zeta_4}{12} + 20\zeta_5 - \frac{319\pi^4}{1080} + \frac{6109\pi^2}{1944} + \frac{34219}{1944} \right) \\
&+ C_A^2 n_f \left(\frac{103\zeta_2}{81} + \frac{202\zeta_3}{27} - \frac{5\zeta_4}{6} + \frac{41\pi^4}{540} - \frac{599\pi^2}{972} - \frac{10637}{1944} \right) + C_A C_F n_f \left(2\zeta_4 - \frac{\pi^4}{45} - \frac{\pi^2}{12} + \frac{241}{72} \right) \\
&- \frac{1}{4} C_F^2 n_f + C_A n_f^2 \left(-\frac{2\zeta_3}{27} + \frac{5\pi^2}{162} + \frac{529}{1944} \right) - \frac{11}{36} C_F n_f^2 + 32 C_A \pi^2 \beta_0^2 \zeta_3 \\
&\approx -492.908 + 32 C_A \pi^2 \beta_0^2 \zeta_3,
\end{aligned} \tag{3.1}$$

while for quark processes

$$\begin{aligned}
B^{(3)} &= C_A^2 C_F \left(\frac{22\zeta_3\zeta_2}{3} - \frac{799\zeta_2}{81} - \frac{11\pi^2\zeta_3}{9} + \frac{2207\zeta_3}{54} - \frac{77\zeta_4}{12} - 10\zeta_5 - \frac{83\pi^4}{360} - \frac{7163\pi^2}{1944} + \frac{151571}{3888} \right) \\
&+ C_F^3 \left(\frac{4\pi^2\zeta_3}{3} - 17\zeta_3 + 60\zeta_5 - \frac{2\pi^4}{5} - \frac{3\pi^2}{4} - \frac{29}{8} \right) + C_F^2 n_f \left(\frac{34\zeta_3}{3} + 2\zeta_4 - \frac{7\pi^4}{54} - \frac{13\pi^2}{36} + \frac{23}{4} \right) \\
&+ C_A C_F^2 \left(-\frac{2}{3}\pi^2\zeta_3 - \frac{211\zeta_3}{3} - 30\zeta_5 + \frac{247\pi^4}{540} + \frac{205\pi^2}{36} - \frac{151}{16} \right) \\
&+ C_A C_F n_f \left(\frac{103\zeta_2}{81} - \frac{128\zeta_3}{27} - \frac{5\zeta_4}{6} + \frac{11\pi^4}{180} + \frac{1297\pi^2}{972} - \frac{3331}{243} \right) + C_F n_f^2 \left(\frac{10\zeta_3}{27} - \frac{5\pi^2}{54} + \frac{1115}{972} \right) \\
&+ 32 C_F \pi^2 \beta_0^2 \zeta_3 \approx -116.685 + 32 C_F \pi^2 \beta_0^2 \zeta_3.
\end{aligned} \tag{3.2}$$

The remaining N³LL anomalous dimension $A^{(4)}$ is currently incomplete given that the four-loop cusp anomalous dimension is still unknown. Here we compute $A^{(4)}$ according to Eq. (71) of ref. [19] or Eq. (4.6) of ref. [57], using the results of ref. [25] for the soft anomalous dimension, and setting the four-loop cusp anomalous dimension to zero. For gluon-initiated processes we get

$$A^{(4)} = C_A^4 \left(\frac{121}{3} \zeta_3 \zeta_2 - \frac{8789\zeta_2}{162} - \frac{19093\zeta_3}{54} - \frac{847\zeta_4}{24} + 132\zeta_5 + \frac{3761815}{11664} \right)$$

$$\begin{aligned}
& + C_A^3 n_f \left(-\frac{22}{3} \zeta_3 \zeta_2 + \frac{2731 \zeta_2}{162} + \frac{4955 \zeta_3}{54} + \frac{11 \zeta_4}{6} - 24 \zeta_5 - \frac{31186}{243} \right) \\
& + C_A^2 C_F n_f \left(\frac{272 \zeta_3}{9} + 11 \zeta_4 - \frac{7351}{144} \right) + C_A^2 n_f^2 \left(-\frac{103 \zeta_2}{81} - \frac{47 \zeta_3}{27} + \frac{5 \zeta_4}{6} + \frac{13819}{972} \right) \\
& + C_A C_F n_f^2 \left(-\frac{38 \zeta_3}{9} - 2 \zeta_4 + \frac{215}{24} \right) + C_A n_f^3 \left(-\frac{4 \zeta_3}{9} - \frac{232}{729} \right) + 64 C_A \pi^3 \beta_0^3 \zeta_3 \\
& \approx -2675.68 + 64 C_A \pi^3 \beta_0^3 \zeta_3,
\end{aligned} \tag{3.3}$$

while for quark-initiated ones

$$\begin{aligned}
A^{(4)} & = C_A^3 C_F \left(\frac{121}{3} \zeta_3 \zeta_2 - \frac{8789 \zeta_2}{162} - \frac{19093 \zeta_3}{54} - \frac{847 \zeta_4}{24} + 132 \zeta_5 + \frac{3761815}{11664} \right) \\
& + C_A^2 C_F n_f \left(-\frac{22}{3} \zeta_3 \zeta_2 + \frac{2731 \zeta_2}{162} + \frac{4955 \zeta_3}{54} + \frac{11 \zeta_4}{6} - 24 \zeta_5 - \frac{31186}{243} \right) \\
& + C_A C_F^2 n_f \left(\frac{272 \zeta_3}{9} + 11 \zeta_4 - \frac{7351}{144} \right) + C_A C_F n_f^2 \left(-\frac{103 \zeta_2}{81} - \frac{47 \zeta_3}{27} + \frac{5 \zeta_4}{6} + \frac{13819}{972} \right) \\
& + C_F^2 n_f^2 \left(-\frac{38 \zeta_3}{9} - 2 \zeta_4 + \frac{215}{24} \right) + C_F n_f^3 \left(-\frac{4 \zeta_3}{9} - \frac{232}{729} \right) + 64 C_F \pi^3 \beta_0^3 \zeta_3 \\
& \approx -1189.19 + 64 C_F \pi^3 \beta_0^3 \zeta_3.
\end{aligned} \tag{3.4}$$

We have left the additional terms arising from Eq. (2.63) unexpanded to facilitate the comparison to the existing literature. The remaining quantities are evaluated with $n_f = 5$.

As above, we define R' as the logarithmic derivative of R (2.50), i.e.

$$R'_\ell(k_{t1}) = \frac{dR_\ell(k_{t1})}{dL}, \tag{3.5}$$

where we defined

$$L = \ln \frac{M}{k_{t1}}. \tag{3.6}$$

Since the ratios k_{ti}/k_{t1} for all resolved emissions are of order 1, we can expand R and its derivative about k_{t1} , retaining terms that contribute at the desired logarithmic accuracy. At N³LL one has

$$\begin{aligned}
R(\epsilon k_{t1}) & = R(k_{t1}) + R'(k_{t1}) \ln \frac{1}{\epsilon} + \frac{1}{2!} R''(k_{t1}) \ln^2 \frac{1}{\epsilon} + \frac{1}{3!} R'''(k_{t1}) \ln^3 \frac{1}{\epsilon} + \dots \\
R'(k_{ti}) & = R'(k_{t1}) + R''(k_{t1}) \ln \frac{1}{\zeta_i} + \frac{1}{2!} R'''(k_{t1}) \ln^2 \frac{1}{\zeta_i} + \dots,
\end{aligned} \tag{3.7}$$

where the dots denote N⁴LL terms, and we have employed the usual notation $\zeta_i = k_{ti}/k_{t1}$.

The above equation corresponds to an expansion of the rapidity bound of each emission k_i , $\ln(M/k_{ti})$, about the one of the leading emission $\ln(M/k_{t1})$. We recall that the transverse momenta of emissions in the resolved ensemble are parametrically of the same order. This is because rIRC safety ensures that emissions k with $k_t \ll k_{t1}$ do not contribute to the observable and are encoded in the Sudakov radiator. Therefore, since $\ln(1/\zeta_i)$ in the above formula is the logarithm of an $\mathcal{O}(1)$ quantity, each term in the right-hand-side of Eq. (3.7) is logarithmically subleading with respect to the one to its left.

The logarithms $\ln(1/\epsilon)$ in the first line of Eq. (3.7) are a parametrisation of the IRC divergences arising from the combination of real-unresolved emissions and virtual corrections, expanded at a given logarithmic order. The ϵ dependence exactly cancels against the corresponding terms in the resolved real corrections (denoted by the same-order derivative of R) upon integration over ζ_i , as it will be shown below. This is a convenient way to recast the subtraction of IRC divergences at each logarithmic order in our formulation.

The terms proportional to $R'(k_{t1})$ are to be retained starting at NLL, those proportional to $R''(k_{t1})$ contribute at NNLL and, finally, the ones proportional to $R'''(k_{t1})$ are needed at N³LL. Starting from the NLL ensemble, we note that correcting a single emission with respect to its $R'(k_{t1})$ approximation (i.e. including for that emission the subleading terms of Eq. (3.7)) gives rise at most to a NNLL correction of order $\mathcal{O}(\alpha_s^n L^{n-1})$ in our counting. Modifying two emissions would lead to a relative correction of order $\mathcal{O}(\alpha_s^n L^{n-2})$, i.e. N³LL, and so on. Therefore, at any given logarithmic order, it is sufficient to keep terms beyond the $R'(k_{t1})$ approximation only for a finite number of emissions (namely a single emission at NNLL, two emissions at N³LL, and so forth). Consistently, one has to expand out the corresponding terms in the Sudakov that cancel the ϵ divergences of the modified real emissions to the given logarithmic order. This prescription has been derived and discussed in detail at NNLL in ref. [41], and will be used later in this section.

As a next step we address the evolution of the parton densities and relative coefficient functions encoded Eq. (2.48), whose anomalous dimensions Γ_N and $\Gamma_N^{(C)}$ have been defined in Eqs. (2.45), and (2.43). Only a finite number of terms in their perturbative series needs to be retained for a given logarithmic accuracy: in particular, contributions from the $\mathcal{O}(\alpha_s^n)$ term in Γ_N enter for a Nⁿ⁺¹LL resummation (we recall that the series of Γ_N starts at $\mathcal{O}(\alpha_s^0)$, hence these terms start contributing at NLL). On the other hand, the contribution of the coefficient functions, and therefore of the corresponding anomalous dimension, starts at NNLL. Therefore the $\mathcal{O}(\alpha_s^m)$ term in $\Gamma_N^{(C)}$ is necessary at N^{m+1}LL, since its expansion starts at $\mathcal{O}(\alpha_s)$.

We can then repeat the treatment of the Sudakov radiator for the terms in Eq. (2.48) containing Γ and $\Gamma^{(C)}$. Up to N³LL we expand the exponent of the evolution operators as

$$\int_{\epsilon k_{t1}}^{\mu_0} \frac{dk_t}{k_t} \frac{\alpha_s(k_t)}{\pi} \mathbf{\Gamma}_{N_\ell}(\alpha_s(k_t)) = \int_{k_{t1}}^{\mu_0} \frac{dk_t}{k_t} \frac{\alpha_s(k_t)}{\pi} \mathbf{\Gamma}_{N_\ell}(\alpha_s(k_t)) + \frac{d}{dL} \int_{k_{t1}}^{\mu_0} \frac{dk_t}{k_t} \frac{\alpha_s(k_t)}{\pi} \mathbf{\Gamma}_{N_\ell}(\alpha_s(k_t)) \ln \frac{1}{\epsilon} + \frac{1}{2} \frac{d^2}{dL^2} \int_{k_{t1}}^{\mu_0} \frac{dk_t}{k_t} \frac{\alpha_s(k_t)}{\pi} \mathbf{\Gamma}_{N_\ell}(\alpha_s(k_t)) \ln^2 \frac{1}{\epsilon} + \dots \quad (3.8)$$

$$\int_{\epsilon k_{t1}}^{\mu_0} \frac{dk_t}{k_t} \mathbf{\Gamma}_{N_\ell}^{(C)}(\alpha_s(k_t)) = \int_{k_{t1}}^{\mu_0} \frac{dk_t}{k_t} \mathbf{\Gamma}_{N_\ell}^{(C)}(\alpha_s(k_t)) + \frac{d}{dL} \int_{k_{t1}}^{\mu_0} \frac{dk_t}{k_t} \mathbf{\Gamma}_{N_\ell}^{(C)}(\alpha_s(k_t)) \ln \frac{1}{\epsilon} + \dots, \quad (3.9)$$

and the corresponding resolved real-emission kernels as

$$\frac{\alpha_s(k_{tj})}{\pi} \mathbf{\Gamma}_{N_\ell}(\alpha_s(k_{tj})) = \frac{\alpha_s(k_{t1})}{\pi} \mathbf{\Gamma}_{N_\ell}(\alpha_s(k_{t1})) + \frac{d}{dL} \frac{\alpha_s(k_{t1})}{\pi} \mathbf{\Gamma}_{N_\ell}(\alpha_s(k_{t1})) \ln \frac{1}{\zeta_j} + \dots \quad (3.10)$$

$$\mathbf{\Gamma}_{N_\ell}^{(C)}(\alpha_s(k_{tj})) = \mathbf{\Gamma}_{N_\ell}^{(C)}(\alpha_s(k_{t1})) + \dots, \quad (3.11)$$

where as usual $L = \ln(M/k_{t1})$. The first terms on the right-hand side of Eqs. (3.8), and (3.9) represent the evolution operator that runs the parton densities and the coefficient functions, respectively, from μ_0 up to k_{t1} . The remaining terms describe the exclusive evolution of the parton densities and of the coefficient functions in the resolved strip. In particular, the ϵ -dependent terms completely cancel against the corresponding terms in the real-emission kernel of Eqs. (3.10), and (3.11) upon integration.

At NLL the coefficient functions are an identity matrix in flavour space, and therefore their evolution operator is trivial. The contribution of the $\mathbf{\Gamma}_N$ in the exponent starts at NLL, while the exclusive evolution of the parton densities in the resolved strip starts at NNLL since it corresponds to emissions in the hard-collinear edge of the phase space. Therefore, at NLL one only needs to retain the first term in the right-hand side of Eq. (3.8), and ignore everything else in Eqs. (3.8), (3.9), (3.10), and (3.11), which corresponds to evaluating the parton densities at $\mu_F = k_{t1}$. At this order, the evolution can be carried out by means of the tree-level anomalous dimension $\gamma_N^{(0)}$.

Similarly, at NNLL one needs to take into account the second term in the r.h.s. of Eq. (3.8) and the first term in the r.h.s. of Eq. (3.10), where now the anomalous dimension $\mathbf{\Gamma}_N$ is evaluated at

one-loop accuracy (i.e. including $\gamma_N^{(1)}$). At this order also the coefficient functions start contributing with their inclusive evolution, therefore one needs to add the first term in the r.h.s. of Eq. (3.9). The corresponding exclusive evolution in the resolved strip, encoded in the r.h.s. of Eq. (3.11) only starts at N³LL. At higher orders, one simply needs to add subsequent terms from the above equations, and evaluate the anomalous dimensions at the appropriate perturbative accuracy.

As discussed above for the Sudakov radiator, at any given logarithmic order beyond NLL, it is sufficient to include the extra ϵ -dependent terms from Eqs. (3.8), (3.9) in the exponent, and the corresponding terms in the resolved real radiation from Eqs. (3.10), (3.11) only for a finite number of emissions, namely a single emission at NNLL, two emissions at N³LL, and so forth.

Finally, we need to deal with the block $\mathbf{C}_{N_1}^{c_1;T}(\alpha_s(\mu_0))H(\mu_R)\mathbf{C}_{N_2}^{c_2}(\alpha_s(\mu_0))$ in Eq. (2.48). As discussed in the previous section, for a generic process this block receives a contribution from the gluon collinear correlations \mathbf{G} , as in Eq. (2.52). Since the contribution of the \mathbf{G} functions starts at N³LL, at this order one can drop the ϵ dependence in their evolution; namely, in the analogue of Eq. (3.9) with $\Gamma_N^{(C)} \rightarrow \Gamma_N^{(G)}$, only the first term on the right-hand side needs to be retained. This amounts to evaluating the coupling of the \mathbf{G} coefficient functions at k_{t1} .

With the expansions detailed above, Eq. (2.48) becomes

$$\begin{aligned}
\hat{\Sigma}_{N_1, N_2}^{c_1 c_2}(v) &= \mathbf{C}_{N_1}^{c_1;T}(\alpha_s(\mu_0))H(\mu_R)\mathbf{C}_{N_2}^{c_2}(\alpha_s(\mu_0)) \int_0^M \frac{dk_{t1}}{k_{t1}} \int_0^{2\pi} \frac{d\phi_1}{2\pi} \\
&\times e^{-\mathbf{R}(k_{t1}) - \mathbf{R}'(k_{t1}) \ln \frac{1}{\epsilon} - \frac{1}{2!} \mathbf{R}''(k_{t1}) \ln^2 \frac{1}{\epsilon} - \frac{1}{3!} \mathbf{R}'''(k_{t1}) \ln^3 \frac{1}{\epsilon} + \dots} \\
&\times \exp \left\{ - \sum_{\ell=1}^2 \left(\int_{k_{t1}}^{\mu_0} \frac{dk_t}{k_t} \frac{\alpha_s(k_t)}{\pi} \Gamma_{N_\ell}(\alpha_s(k_t)) + \frac{d}{dL} \int_{k_{t1}}^{\mu_0} \frac{dk_t}{k_t} \frac{\alpha_s(k_t)}{\pi} \Gamma_{N_\ell}(\alpha_s(k_t)) \ln \frac{1}{\epsilon} \right. \right. \\
&\quad \left. \left. + \frac{1}{2!} \frac{d^2}{dL^2} \int_{k_{t1}}^{\mu_0} \frac{dk_t}{k_t} \frac{\alpha_s(k_t)}{\pi} \Gamma_{N_\ell}(\alpha_s(k_t)) \ln^2 \frac{1}{\epsilon} + \dots \right. \right. \\
&\quad \left. \left. + \int_{k_{t1}}^{\mu_0} \frac{dk_t}{k_t} \Gamma_{N_\ell}^{(C)}(\alpha_s(k_t)) + \frac{d}{dL} \int_{k_{t1}}^{\mu_0} \frac{dk_t}{k_t} \Gamma_{N_\ell}^{(C)}(\alpha_s(k_t)) \ln \frac{1}{\epsilon} + \dots \right) \right\} \\
&\times \sum_{\ell_1=1}^2 \left(\mathbf{R}'_{\ell_1}(k_{t1}) + \frac{\alpha_s(k_{t1})}{\pi} \Gamma_{N_{\ell_1}}(\alpha_s(k_{t1})) + \Gamma_{N_{\ell_1}}^{(C)}(\alpha_s(k_{t1})) \right) \\
&\times \sum_{n=0}^{\infty} \frac{1}{n!} \prod_{i=2}^{n+1} \int_{\epsilon}^1 \frac{d\zeta_i}{\zeta_i} \int_0^{2\pi} \frac{d\phi_i}{2\pi} \sum_{\ell_i=1}^2 \left\{ \mathbf{R}'_{\ell_i}(k_{t1}) + \mathbf{R}''_{\ell_i}(k_{t1}) \ln \frac{1}{\zeta_i} + \frac{1}{2} \mathbf{R}'''_{\ell_i}(k_{t1}) \ln^2 \frac{1}{\zeta_i} + \dots \right. \\
&\quad \left. + \frac{\alpha_s(k_{t1})}{\pi} \Gamma_{N_{\ell_i}}(\alpha_s(k_{t1})) + \frac{d}{dL} \left(\frac{\alpha_s(k_{t1})}{\pi} \Gamma_{N_{\ell_i}}(\alpha_s(k_{t1})) \right) \ln \frac{1}{\zeta_i} + \dots \right. \\
&\quad \left. + \Gamma_{N_{\ell_i}}^{(C)}(\alpha_s(k_{t1})) + \dots \right\} \Theta(v - V(\{\tilde{p}\}, k_1, \dots, k_{n+1})) + \{\mathbf{C} \rightarrow \mathbf{G}; \Gamma^{(C)} \rightarrow \Gamma^{(G)}\}. \quad (3.12)
\end{aligned}$$

Following the procedure of ref. [41], we can express the $\ln(1/\epsilon)$ singularities in the exponent of Eq. (3.12) as integrals over dummy real emissions as follows

$$\ln \frac{1}{\epsilon} = \int_{\epsilon}^1 \frac{d\zeta}{\zeta}, \quad \frac{1}{2} \ln^2 \frac{1}{\epsilon} = \int_{\epsilon}^1 \frac{d\zeta}{\zeta} \ln \frac{1}{\zeta}, \quad \frac{1}{3!} \ln^3 \frac{1}{\epsilon} = \frac{1}{2} \int_{\epsilon}^1 \frac{d\zeta}{\zeta} \ln^2 \frac{1}{\zeta}, \quad (3.13)$$

and subsequently expand out the divergent part of the exponent, retaining the terms necessary at a given logarithmic order. We further introduce the average of a function $G(\{\tilde{p}\}, \{k_i\})$ over the measure $d\mathcal{Z}$

$$\int d\mathcal{Z}[\{R', k_i\}] G(\{\tilde{p}\}, \{k_i\}) = \epsilon^{R'(k_{t1})} \sum_{n=0}^{\infty} \frac{1}{n!} \prod_{i=2}^{n+1} \int_{\epsilon}^1 \frac{d\zeta_i}{\zeta_i} \int_0^{2\pi} \frac{d\phi_i}{2\pi} R'(k_{t1}) G(\{\tilde{p}\}, k_1, \dots, k_{n+1}), \quad (3.14)$$

where we simplified the notation by using

$$R'(k_{t1}) = \sum_{\ell=1,2} R'_\ell(k_{t1}). \quad (3.15)$$

The dependence on the regulator ϵ cancels exactly in Eq. (3.14).

We can transform back to momentum space, thus abandoning the matrix notation used so far. We define the derivatives of the parton densities by means of the DGLAP evolution equation

$$\frac{\partial f(\mu, x)}{\partial \ln \mu} = \frac{\alpha_s(\mu)}{\pi} \int_x^1 \frac{dz}{z} \hat{P}(z, \alpha_s(\mu)) f(\mu, \frac{x}{z}), \quad (3.16)$$

where $\hat{P}(z, \alpha_s(\mu))$ is the regularised splitting function

$$\hat{P}(z, \alpha_s(\mu)) = \hat{P}^{(0)}(z) + \frac{\alpha_s(\mu)}{2\pi} \hat{P}^{(1)}(z) + \left(\frac{\alpha_s(\mu)}{2\pi}\right)^2 \hat{P}^{(2)}(z) + \dots \quad (3.17)$$

Including terms up to N³LL, we can therefore recast Eqs. (3.12), (2.47) as

$$\begin{aligned} \frac{d\Sigma(v)}{d\Phi_B} &= \int \frac{dk_{t1}}{k_{t1}} \frac{d\phi_1}{2\pi} \partial_L \left(-e^{-R(k_{t1})} \mathcal{L}_{\text{N}^3\text{LL}}(k_{t1}) \right) \int d\mathcal{Z}[\{R', k_i\}] \Theta(v - V(\{\tilde{p}\}, k_1, \dots, k_{n+1})) \\ &+ \int \frac{dk_{t1}}{k_{t1}} \frac{d\phi_1}{2\pi} e^{-R(k_{t1})} \int d\mathcal{Z}[\{R', k_i\}] \int_0^1 \frac{d\zeta_s}{\zeta_s} \frac{d\phi_s}{2\pi} \left\{ \left(R'(k_{t1}) \mathcal{L}_{\text{NNLL}}(k_{t1}) - \partial_L \mathcal{L}_{\text{NNLL}}(k_{t1}) \right) \right. \\ &\times \left(R''(k_{t1}) \ln \frac{1}{\zeta_s} + \frac{1}{2} R'''(k_{t1}) \ln^2 \frac{1}{\zeta_s} \right) - R'(k_{t1}) \left(\partial_L \mathcal{L}_{\text{NNLL}}(k_{t1}) - 2 \frac{\beta_0}{\pi} \alpha_s^2(k_{t1}) \hat{P}^{(0)} \otimes \mathcal{L}_{\text{NLL}}(k_{t1}) \ln \frac{1}{\zeta_s} \right) \\ &\left. + \frac{\alpha_s^2(k_{t1})}{\pi^2} \hat{P}^{(0)} \otimes \hat{P}^{(0)} \otimes \mathcal{L}_{\text{NLL}}(k_{t1}) \right\} \left\{ \Theta(v - V(\{\tilde{p}\}, k_1, \dots, k_{n+1}, k_s)) - \Theta(v - V(\{\tilde{p}\}, k_1, \dots, k_{n+1})) \right\} \\ &+ \frac{1}{2} \int \frac{dk_{t1}}{k_{t1}} \frac{d\phi_1}{2\pi} e^{-R(k_{t1})} \int d\mathcal{Z}[\{R', k_i\}] \int_0^1 \frac{d\zeta_{s1}}{\zeta_{s1}} \frac{d\phi_{s1}}{2\pi} \int_0^1 \frac{d\zeta_{s2}}{\zeta_{s2}} \frac{d\phi_{s2}}{2\pi} R'(k_{t1}) \\ &\times \left\{ \mathcal{L}_{\text{NLL}}(k_{t1}) (R''(k_{t1}))^2 \ln \frac{1}{\zeta_{s1}} \ln \frac{1}{\zeta_{s2}} - \partial_L \mathcal{L}_{\text{NLL}}(k_{t1}) R''(k_{t1}) \left(\ln \frac{1}{\zeta_{s1}} + \ln \frac{1}{\zeta_{s2}} \right) \right. \\ &\left. + \frac{\alpha_s^2(k_{t1})}{\pi^2} \hat{P}^{(0)} \otimes \hat{P}^{(0)} \otimes \mathcal{L}_{\text{NLL}}(k_{t1}) \right\} \\ &\times \left\{ \Theta(v - V(\{\tilde{p}\}, k_1, \dots, k_{n+1}, k_{s1}, k_{s2})) - \Theta(v - V(\{\tilde{p}\}, k_1, \dots, k_{n+1}, k_{s1})) - \right. \\ &\left. \Theta(v - V(\{\tilde{p}\}, k_1, \dots, k_{n+1}, k_{s2})) + \Theta(v - V(\{\tilde{p}\}, k_1, \dots, k_{n+1})) \right\} + \mathcal{O}\left(\alpha_s^n \ln^{2n-6} \frac{1}{v}\right), \quad (3.18) \end{aligned}$$

where we defined $\partial_L = d/dL$.

Until now we have explicitly considered the case of flavour-conserving real emissions, for which we derived Eq. (3.18). We now turn to the inclusion of the flavour-changing splitting kernels, that enter purely in the hard-collinear limit and contribute to the DGLAP evolution. In order to include an arbitrary number of these splittings, one is forced to relax the assumption of k_t ordering that we made in our discussion of Section 2.3.⁷ Indeed, if some soft radiation occurs after the flavour-changing collinear emission has taken place, then it becomes quite cumbersome to determine the

⁷We are grateful to A. Banfi for a discussion about this aspect.

correct colour factor for the former. This is because coherence guarantees that a soft gluon feels the effective colour charge of the radiation at smaller angles, which now may involve combinations of different flavours. A correct solution to this problem requires to reformulate the evolution by ordering the radiation in angle. This ensures that the hard-collinear emissions contributing to the DGLAP evolution happen at last (see also the discussion in Appendix E.2 of ref. [39]), and the colour structure of the soft radiation is easily determined. An alternative solution, which we adopt here, relies on the observation that at a given logarithmic order only a finite number of hard-collinear emissions are actually necessary. As we mentioned several times in the above sections, at N³LL one needs to account for the effect of up to two hard-collinear resolved partons. Therefore, the inclusion of the flavour-changing kernels in Eq. (3.18) can be done directly at the level of the parton luminosity which are defined as follows

$$\mathcal{L}_{\text{NLL}}(k_{t1}) = \sum_{c,c'} \frac{d|M_B|_{cc'}^2}{d\Phi_B} f_c(k_{t1}, x_1) f_{c'}(k_{t1}, x_2), \quad (3.19)$$

$$\begin{aligned} \mathcal{L}_{\text{NNLL}}(k_{t1}) = & \sum_{c,c'} \frac{d|M_B|_{cc'}^2}{d\Phi_B} \sum_{i,j} \int_{x_1}^1 \frac{dz_1}{z_1} \int_{x_2}^1 \frac{dz_2}{z_2} f_i\left(k_{t1}, \frac{x_1}{z_1}\right) f_j\left(k_{t1}, \frac{x_2}{z_2}\right) \\ & \left(\delta_{ci}\delta_{c'j}\delta(1-z_1)\delta(1-z_2) \left(1 + \frac{\alpha_s(\mu_R)}{2\pi} H^{(1)}(\mu_R)\right) \right. \\ & \left. + \frac{\alpha_s(\mu_R)}{2\pi} \frac{1}{1-2\alpha_s(\mu_R)\beta_0 L} \left(C_{ci}^{(1)}(z_1)\delta(1-z_2)\delta_{c'j} + \{z_1 \leftrightarrow z_2; c, i \leftrightarrow c', j\} \right) \right), \end{aligned} \quad (3.20)$$

$$\begin{aligned} \mathcal{L}_{\text{N}^3\text{LL}}(k_{t1}) = & \sum_{c,c'} \frac{d|M_B|_{cc'}^2}{d\Phi_B} \sum_{i,j} \int_{x_1}^1 \frac{dz_1}{z_1} \int_{x_2}^1 \frac{dz_2}{z_2} f_i\left(k_{t1}, \frac{x_1}{z_1}\right) f_j\left(k_{t1}, \frac{x_2}{z_2}\right) \\ & \left\{ \delta_{ci}\delta_{c'j}\delta(1-z_1)\delta(1-z_2) \left(1 + \frac{\alpha_s(\mu_R)}{2\pi} H^{(1)}(\mu_R) + \frac{\alpha_s^2(\mu_R)}{(2\pi)^2} H^{(2)}(\mu_R)\right) \right. \\ & + \frac{\alpha_s(\mu_R)}{2\pi} \frac{1}{1-2\alpha_s(\mu_R)\beta_0 L} \left(1 - \alpha_s(\mu_R) \frac{\beta_1 \ln(1-2\alpha_s(\mu_R)\beta_0 L)}{\beta_0} \right) \\ & \times \left(C_{ci}^{(1)}(z_1)\delta(1-z_2)\delta_{c'j} + \{z_1 \leftrightarrow z_2; c, i \leftrightarrow c', j\} \right) \\ & + \frac{\alpha_s^2(\mu_R)}{(2\pi)^2} \frac{1}{(1-2\alpha_s(\mu_R)\beta_0 L)^2} \left(\left(C_{ci}^{(2)}(z_1) - 2\pi\beta_0 C_{ci}^{(1)}(z_1) \ln \frac{M^2}{\mu_R^2} \right) \delta(1-z_2)\delta_{c'j} \right. \\ & \left. + \{z_1 \leftrightarrow z_2; c, i \leftrightarrow c', j\} \right) + \frac{\alpha_s^2(\mu_R)}{(2\pi)^2} \frac{1}{(1-2\alpha_s(\mu_R)\beta_0 L)^2} \left(C_{ci}^{(1)}(z_1)C_{c'j}^{(1)}(z_2) + G_{ci}^{(1)}(z_1)G_{c'j}^{(1)}(z_2) \right) \\ & \left. + \frac{\alpha_s^2(\mu_R)}{(2\pi)^2} H^{(1)}(\mu_R) \frac{1}{1-2\alpha_s(\mu_R)\beta_0 L} \left(C_{ci}^{(1)}(z_1)\delta(1-z_2)\delta_{c'j} + \{z_1 \leftrightarrow z_2; c, i \leftrightarrow c', j\} \right) \right\}, \end{aligned} \quad (3.21)$$

where

$$x_1 = \frac{M}{\sqrt{s}} e^Y, \quad x_2 = \frac{M}{\sqrt{s}} e^{-Y}, \quad (3.22)$$

and Y is the rapidity of the colour singlet in the centre-of-mass frame of the collision at the Born level. $|M_B|_{cc'}^2$ is the Born squared matrix element, and $L = \ln(1/v_1)$, with $v_1 = k_{t1}/M$, $v = p_t/M$. Since we evaluated explicitly the sum over the emitting legs ℓ_i , the convolution of a regularised splitting kernel $\hat{P}^{(0)}$ with the NLL parton luminosity is now defined as

$$\hat{P}^{(0)} \otimes \mathcal{L}_{\text{NLL}}(k_{t1}) \equiv \sum_{c,c'} \frac{d|M_B|_{cc'}^2}{d\Phi_B} \left\{ \left(\hat{P}^{(0)} \otimes f \right)_c(k_{t1}, x_1) f_{c'}(k_{t1}, x_2) \right.$$

$$+ f_c(k_{t1}, x_1) \left(\hat{P}^{(0)} \otimes f \right)_{c'}(k_{t1}, x_2) \Big\}. \quad (3.23)$$

The term $\hat{P}^{(0)} \otimes \hat{P}^{(0)} \otimes \mathcal{L}_{\text{NLL}}(k_{t1})$ is to be interpreted in the same way. In the above expressions for the luminosity we have used the following expansions in powers of the strong coupling for the functions C , H and G , up to N³LL:

$$C_{ab}(\alpha_s(\mu)) = \delta(1-z)\delta_{ab} + \sum_{n=1}^2 \left(\frac{\alpha_s(\mu)}{2\pi} \right)^n C_{ab}^{(n)}(z), \quad (3.24)$$

$$H(\mu_R) = 1 + \sum_{n=1}^2 \left(\frac{\alpha_s(\mu_R)}{2\pi} \right)^n H^{(n)}(\mu_R), \quad (3.25)$$

$$G_{ab}(\alpha_s(\mu)) = \frac{\alpha_s(\mu)}{2\pi} G_{ab}^{(1)}(z), \quad (3.26)$$

where μ is the same scale at which the parton densities are evaluated, and μ_R is the renormalisation scale.

The expressions for $C^{(1)}$ and $H^{(1)}$ have been known for a long time, and are collected, for instance, in the appendix of ref. [54]. The hard-virtual coefficient $H(\mu_R)$ is defined as the finite part of the renormalised QCD form factor in the $\overline{\text{MS}}$ renormalisation scheme, divided by the underlying Born squared matrix element. The hard coefficients for gluonic processes up to $\mathcal{O}(\alpha_s^2)$ evaluated at the invariant mass of the colour singlet $H^{(1)}(M)$ and $H^{(2)}(M)$ read [58–60]

$$\begin{aligned} H_g^{(1)}(M) &= C_A \left(5 + \frac{7}{6}\pi^2 \right) - 3C_F, \\ H_g^{(2)}(M) &= \frac{5359}{54} + \frac{137}{6} \ln \frac{m_H^2}{m_t^2} + \frac{1679}{24}\pi^2 + \frac{37}{8}\pi^4 - \frac{499}{6}\zeta_3 + C_A \frac{16}{3}\pi\beta_0\zeta_3, \quad n_f = 5, \end{aligned} \quad (3.27)$$

where the last term in $H_g^{(2)}$ was deliberately left symbolic to stress its origin from Eq. (2.63). Analogously, for quark-initiated reactions one has [61–63]

$$\begin{aligned} H_q^{(1)}(M) &= C_F \left(-8 + \frac{7}{6}\pi^2 \right), \\ H_q^{(2)}(M) &= -\frac{57433}{972} + \frac{281}{162}\pi^2 + \frac{22}{27}\pi^4 + \frac{1178}{27}\zeta_3 + C_F \frac{16}{3}\pi\beta_0\zeta_3, \quad n_f = 5. \end{aligned} \quad (3.28)$$

The renormalisation-scale dependence of the first two hard-function coefficients is given by

$$\begin{aligned} H^{(1)}(\mu_R) &= H^{(1)}(M) + 2d_B\pi\beta_0 \ln \frac{\mu_R^2}{M^2}, \\ H^{(2)}(\mu_R) &= H^{(2)}(M) + 4d_B \left(\frac{1+d_B}{2}\pi^2\beta_0^2 \ln^2 \frac{\mu_R^2}{M^2} + \pi^2\beta_1 \ln \frac{\mu_R^2}{M^2} \right) \\ &\quad + 2(1+d_B)\pi\beta_0 \ln \frac{\mu_R^2}{M^2} H^{(1)}(M), \end{aligned} \quad (3.29)$$

$$(3.30)$$

where d_B is the strong-coupling order of the Born squared amplitude.

The $C^{(2)}$ and $G^{(1)}$ functions for gluon-fusion processes are obtained in refs. [22, 24], while for quark-induced processes they are derived in ref. [23]. In the present work we extract their expressions using the results of refs. [22, 23]. For gluon-fusion processes, the $C_{gq}^{(2)}$ and $C_{gg}^{(2)}$ coefficients normalised as in Eq. (3.24) are extracted from Eqs. (30) and (32) of ref. [22], respectively, where we use the hard coefficients of Eqs. (3.27) *without* the new term proportional to β_0 in the $H_g^{(2)}(M)$ coefficient.⁸

⁸These must be replaced by $H^{(1)} \rightarrow H^{(1)}/2$ and $H^{(2)} \rightarrow H^{(2)}/4$ to match the convention of refs. [22, 23].

The coefficient $G^{(1)}$ is taken from Eq. (13) of ref. [22]. Similarly, for quark-initiated processes, we extract $C_{qg}^{(2)}$ and $C_{qq}^{(2)}$ from Eqs. (32) and (34) of ref. [23], respectively, where the hard coefficients from Eqs. (3.28) we used, *without* the new term proportional to β_0 in the $H_q^{(2)}(M)$ coefficient.

Eq. (3.18) resums all logarithmic towers of $\ln(1/v)$ (with $v = p_t/M$) up to N³LL, therefore neglecting subleading-logarithmic terms of order $\alpha_s^n \ln^{2n-6}(1/v)$. Constant terms of order $\mathcal{O}(\alpha_s^3)$ relative to the Born will be extracted automatically from a matching to the N³LO cumulative cross section in Section 4. This will allow us to control all terms of order $\alpha_s^n \ln^{2n-6}(1/v)$ in the matched cross section, therefore neglecting terms $\mathcal{O}(\alpha_s^n \ln^{2n-7}(1/v))$. We have split the result as a sum of three terms. The first term (first line of Eq. (3.18)) starts at LL and contains the full NLL corrections. The second term of Eq. (3.18) (second to fourth lines) is necessary to achieve NNLL accuracy, while the third term (fifth to ninth lines) is purely N³LL.

Since Eq. (3.18) still contains subleading-logarithmic terms (i.e. starting at N⁴LL in $\ln(M/p_t)$), one could, even if not strictly required, perform further expansions on each of the terms of Eq. (3.18) in order to neglect at least some of the corrections beyond the desired logarithmic order. For instance, for a N³LL resummation, the full N³LL radiator is necessary in the first term of Eq. (3.18), while the radiator can be evaluated at NNLL in the second term, and at NLL in third term. Analogously, for a NNLL resummation, the NLL radiator suffices in the second term of Eq. (3.18). Furthermore, at NNLL, one could split $R'(k_{t1})$ into the sum of a NLL term $\hat{R}'(k_{t1})$ and a NNLL one $\delta\hat{R}'(k_{t1})$, and expand Eq. (3.18) about the former retaining only contributions linear in $\delta\hat{R}'(k_{t1})$. The last two considerations relate Eq. (3.18) to Eq. (9) of ref. [37] where this approach was first formulated at NNLL for the Higgs-boson transverse-momentum distribution.

Eq. (3.18) can be evaluated in its present form with fast Monte Carlo techniques, as we will discuss in Section 4.

3.2 Perturbative scaling in the $p_t \rightarrow 0$ regime

In this section we show that our formulation of the transverse-momentum resummation of Eq. (3.18) reproduces the correct scaling in the $p_t \rightarrow 0$ limit as first observed in [13]. Moreover, we obtain a correspondence between the logarithmic accuracy and the perturbative accuracy in this limit. To perform a comparison with the results of [13], we consider NLL resummation and neglect the evolution of the parton densities with the energy scale. However the same procedure can be easily extended to the general case. We have

$$\frac{d^2\Sigma(v)}{d^2\vec{p}_t d\Phi_B} = \sigma^{(0)}(\Phi_B) \int \frac{dk_{t1}}{k_{t1}} \frac{d\phi_1}{2\pi} e^{-R(k_{t1})} R'(k_{t1}) \int d\mathcal{Z}[\{R', k_i\}] \delta^{(2)}\left(\vec{p}_t - \left(\vec{k}_{t1} + \dots + \vec{k}_{t(n+1)}\right)\right), \quad (3.31)$$

where

$$\sigma^{(0)}(\Phi_B) \equiv \frac{d\sigma^{(0)}}{d\Phi_B}, \quad (3.32)$$

and $d\mathcal{Z}[\{R', k_i\}]$ is defined in Eq. (3.14). In order to evaluate the integral over $d\mathcal{Z}[\{R', k_i\}]$ analytically we proceed as in Sec. 2.4. After integrating over the azimuthal direction of \vec{p}_t we obtain

$$\begin{aligned} \frac{d^2\Sigma(v)}{dp_t d\Phi_B} &= \sigma^{(0)}(\Phi_B) p_t \int b db J_0(p_t b) \int \frac{dk_{t1}}{k_{t1}} e^{-R(k_{t1})} R'(k_{t1}) J_0(bk_{t1}) \\ &\quad \times \exp\left\{-R'(k_{t1}) \int_0^{k_{t1}} \frac{dk_t}{k_t} (1 - J_0(bk_t))\right\}. \end{aligned} \quad (3.33)$$

Before proceeding to the evaluation of Eq. (3.33), a remark is in order. At NLL one would be tempted to perform the replacement (see Sec. 2.4)

$$(1 - J_0(bk_t)) \simeq \Theta\left(k_t - \frac{b_0}{b}\right) + \dots, \quad (3.34)$$

and recast Eq. (3.33) as

$$\begin{aligned}
\frac{d^2\Sigma(v)}{dp_t d\Phi_B} &= \sigma^{(0)}(\Phi_B) p_t \int b db J_0(p_t b) \int \frac{dk_{t1}}{k_{t1}} e^{-R(k_{t1})} R'(k_{t1}) J_0(bk_{t1}) \left(\frac{b_0}{bk_{t1}}\right)^{R'(k_{t1})} \\
&= \sigma^{(0)}(\Phi_B) p_t \int \frac{dk_{t1}}{k_{t1}} e^{-R(k_{t1})} R'(k_{t1}) \left(\frac{b_0}{k_{t1}}\right)^{R'(k_{t1})} \frac{2^{1-R'(k_{t1})}}{(p_t^2 + k_{t1}^2)^{1-R'(k_{t1})/2}} \\
&\quad \times \frac{\Gamma(1-R'(k_{t1})/2)}{\Gamma(R'(k_{t1})/2)} {}_2F_1\left(\frac{2-R'(k_{t1})}{4}, 1 - \frac{R'(k_{t1})}{4}, 1, \frac{4p_t^2 k_{t1}^2}{(p_t^2 + k_{t1}^2)^2}\right). \quad (3.35)
\end{aligned}$$

The above result is singular for $R'(k_{t1}) \geq 2$, owing to the fact that the integrand scales as $b^{1-R'(k_{t1})}$ in the $b \rightarrow 0$ limit. This singular behaviour is however entirely due to the approximation in Eq. (3.34), where all power-suppressed terms are neglected, while Eq. (3.33) is regular, as the integral in its exponent vanishes as $\mathcal{O}(b^2)$ for small b . Therefore, when using Eq. (3.34) one must regularise the $b \rightarrow 0$ limit, for instance by means of modified logarithms as in ref. [15]. In our formalism, instead, Eq. (3.33) is evaluated numerically without further approximations so that the $b \rightarrow 0$ region is correctly described.

It is interesting to study the scaling of Eq. (3.33) in the small- p_t limit. In this limit, the dominant mechanism that produces a vanishing p_t involves several soft and collinear emissions with finite transverse momentum that mutually balance in the transverse plane. In this kinematic configuration one has $k_{t1} \gg p_t$, thus expanding k_{t1} about p_t in Eq. (3.33) is not allowed: such an operation would give rise to spurious singularities at $R'(p_t) \geq 2$, as reported several times in the literature [19, 36–38, 46, 64].

We therefore evaluate the b integral of Eq. (3.33) and observe that in the limit where $M \gg k_{t1} \gg p_t$ it gives

$$\int b db J_0(p_t b) J_0(bk_{t1}) \exp\left\{-R'(k_{t1}) \int_0^{k_{t1}} \frac{dk_t}{k_t} (1 - J_0(bk_t))\right\} \simeq 4 \frac{k_{t1}^{-2}}{R'(k_{t1})}, \quad (3.36)$$

namely it is constant in p_t in first approximation. In this regime Eq. (3.33) becomes

$$\frac{d^2\Sigma(v)}{dp_t d\Phi_B} = 4 \sigma^{(0)}(\Phi_B) p_t \int \frac{dk_{t1}}{k_{t1}^3} e^{-R(k_{t1})}. \quad (3.37)$$

In order to directly compare with the result of ref. [13], we specialise to the case of the Drell-Yan process, and compute $R(k_{t1})$ at the lowest order using the leading-order running coupling expressed in terms of the QCD scale Λ_{QCD} (with $n_f = 4$),

$$\alpha_s(k_t) = \frac{12}{25} \pi \frac{1}{\ln(k_t^2/\Lambda_{\text{QCD}}^2)}.$$

We obtain ($A^{(1)} = 2C_F$ in this case)

$$R(k_{t1}) = \frac{16}{25} \ln \frac{M^2}{\Lambda_{\text{QCD}}^2} \ln \left(\frac{\ln \frac{M^2}{\Lambda_{\text{QCD}}^2}}{\ln \frac{k_{t1}^2}{\Lambda_{\text{QCD}}^2}} \right) - \frac{16}{25} \ln \frac{M^2}{k_{t1}^2}.$$

We now integrate over k_{t1} in Eq. (3.37) from Λ_{QCD} up to the invariant mass of the Drell-Yan pair, obtaining

$$\frac{d^2\Sigma(v)}{dp_t d\Phi_B} = 4 \sigma^{(0)}(\Phi_B) p_t \int_{\Lambda_{\text{QCD}}}^M \frac{dk_{t1}}{k_{t1}^3} e^{-R(k_{t1})} \simeq 2 \sigma^{(0)}(\Phi_B) p_t \left(\frac{\Lambda_{\text{QCD}}^2}{M^2} \right)^{\frac{16}{25} \ln \frac{41}{16}}, \quad (3.38)$$

that reproduces the scaling of ref. [13].⁹

In order to study how this result is modified by the inclusion of higher-order logarithmic corrections, we evaluate Eq. (3.37) in the fixed-coupling-constant approximation. This is a simple toy model for the more complicated running coupling case. At lowest order one has

$$R(k_{t1}) = A^{(1)} \frac{\alpha_s}{\pi} L^2, \quad (3.39)$$

with $A^{(1)} = 2C$ (with $C = C_A$ for gluons and $C = C_F$ for quarks), and $L = \ln M/k_{t1}$. In the perturbative regime Eq. (3.37) therefore reads

$$\frac{d^2 \Sigma(v)}{dp_t d\Phi_B} \simeq 4 \sigma^{(0)}(\Phi_B) \frac{p_t}{M^2} \frac{\pi}{2} \frac{e^{\frac{\pi}{2C\alpha_s}}}{\sqrt{2C\alpha_s}} \left(1 + \text{Erf} \left(\frac{\sqrt{\pi}}{\sqrt{2C\alpha_s}} \right) \right). \quad (3.40)$$

Eq. (3.40) shows that in the small- p_t limit the differential spectrum features a non-perturbative scaling in α_s (see also Eq. (2.12) of ref. [13]¹⁰). However, the coefficient of this scaling can be systematically improved in perturbation theory: the inclusion of NLL terms $\alpha_s^n L^n$ in the right-hand side of Eq. (3.37) contributes an $\mathcal{O}(1)$ correction to the right-hand side of Eq. (3.40). Analogously, NNLL terms $\alpha_s^n L^{n-1}$ will produce an $\mathcal{O}(\alpha_s)$ correction relative to the non-perturbative factor $e^{\pi/(2C\alpha_s)}/\sqrt{2C\alpha_s}$, and so on. In particular, with our N³LL calculation we have control over the terms of relative order $\mathcal{O}(\alpha_s^2)$. From this scaling we deduce that the correspondence $L \sim 1/\alpha_s$ is still valid in the deep infrared regime. However, this does not mean that the above prediction is accurate in this limit: indeed non-perturbative effects due to soft-gluon radiation below Λ_{QCD} , as well as due to the intrinsic transverse momentum of the partons in the proton, feature a similar scaling. This is because the colour singlet's transverse momentum is sensitive to non-perturbative dynamics only through kinematical recoil, that is the same mechanism that drives the scaling (3.38).

4 Numerical implementation

In order to have a prediction that is valid across different kinematic regions of the spectrum, one needs to match the resummed calculation described above, valid in the small- v limit, to a fixed-order calculation that describes the hard (large- v) regions. In this section we discuss the matching of the result described in the previous sections, in particular Eq. (3.18), to a fixed-order prediction that is NNLO accurate in the hard region of the phase space. We then describe how to evaluate Eq. (3.18) exactly using a Monte Carlo Markov process, and discuss the implementation in a parton-level generator that is fully differential in the Born kinematics.

4.1 Unitarity constraint and resummation-scale dependence

In order to match the resummed calculation to a fixed-order prediction one has to ensure that the hard region of the phase space receives no contamination from resummation effects. We therefore need to modify Eq. (3.18) so that at large v ($v = p_t/M$ in the transverse-momentum case) all radiation effects vanish. At N³LL, it reduces to

$$\frac{d\Sigma(v)}{d\Phi_B} = \mathcal{L}_{\text{N}^3\text{LL}}(\mu_F)|_{L=0}, \quad (4.1)$$

where $\mathcal{L}_{\text{N}^3\text{LL}}$ is defined in Eq. (3.21). The unitarity constraint (4.1) can be implemented in several ways; in what follows we impose unitarity by modifying the structure of the logarithms L everywhere in Eq. (3.18), as commonly done for this observable in the literature.

⁹In the last step we have neglected a factor of $1/\Lambda_{\text{QCD}}^2 \ln(M^2/\Lambda_{\text{QCD}}^2)$, as done in ref. [13].

¹⁰Please note that only the leading contribution for $\alpha_s \ll 1$ is reported in the right-hand side of that equation.

Before defining the modified logarithms, it is convenient to have a way to estimate the resummation uncertainties due to higher-order logarithmic corrections that are not included in the calculation. To this aim, we introduce the dimensionless resummation scale x_Q by using the identity

$$L \equiv \ln \frac{1}{v_1} = \ln \frac{x_Q}{v_1} - \ln x_Q, \quad (4.2)$$

and then we expand the right-hand side about $\ln(x_Q/v_1)$ to the nominal logarithmic accuracy (in terms of $\ln(x_Q/v_1)$), neglecting subleading corrections. In the transverse-momentum case one has $v_1 = k_{t1}/M$ and $x_Q = Q/M$, where Q , the resummation scale, has mass dimensions. A variation of x_Q will therefore provide an estimate of the size of higher-order logarithmic corrections.

The unitarity constraint can now be imposed by replacing the resummed logarithms $\ln(x_Q/v_1)$ by

$$\ln \frac{x_Q}{v_1} \rightarrow \tilde{L} = \frac{1}{p} \ln \left(\left(\frac{x_Q}{v_1} \right)^p + 1 \right), \quad (4.3)$$

where the positive real parameter p is chosen in such a way that resummation effects vanish rapidly enough at $v_1 \sim x_Q$. Eq. (4.3) amounts to imposing unitarity by introducing in the resummed logarithms power-suppressed terms that scale as $(x_Q/v_1)^p$. Given that the spectrum tends to zero with a power law ($\sim v^{-n}$ with positive n) at large v , it follows that one should have $p \geq n$ in order not to affect the correct fixed-order scaling at large v . However, since we are interested in turning off the resummation at transverse momentum values of the order of the singlet's mass, the relevant scaling n to be considered in the choice of p is the one relative to the differential distribution in this region.

We notice that, with the prescription (4.3), the single-emission event in the first line of Eq. (3.18) is not a total derivative any longer. One can however restore this property by introducing the jacobian factor

$$\mathcal{J}(v_1/x_Q, p) = \left(\frac{x_Q}{v_1} \right)^p \left(1 + \left(\frac{x_Q}{v_1} \right)^p \right)^{-1} \quad (4.4)$$

in all integrals over $v_1 = k_{t1}/M$ in Eq. (3.18). This jacobian tends to one at small v_1 and therefore does not modify the logarithmic structure. Moreover, in the large- v region where the single-emission event dominates, this prescription prevents the proliferation of power-suppressed terms. The prescription (4.3) effectively maps the point at which the logarithms are turned off onto infinity. This also gives us the freedom to extend the upper bound of the integration over k_{t1} from M to ∞ in Eq. (3.18) without spoiling the logarithmic accuracy.

We therefore implement the prescription (4.3) in the Sudakov radiator and its derivatives. We denote all modified quantities by a ‘ \sim ’ superscript. The expansion about $\ln(x_Q/v)$ induces some constant terms in the Sudakov radiator that are expanded out up to $\mathcal{O}(\alpha_s^2)$ and included in the hard-function coefficients. The modified quantities in Eq. (3.18) are

$$\begin{aligned} \tilde{R}(k_{t1}) &= -\tilde{L}g_1(\alpha_s(\mu_R)\tilde{L}) - g_2(\alpha_s(\mu_R)\tilde{L}) - \frac{\alpha_s(\mu_R)}{\pi}g_3(\alpha_s(\mu_R)\tilde{L}) - \frac{\alpha_s^2(\mu_R)}{\pi^2}g_4(\alpha_s(\mu_R)\tilde{L}), \\ \tilde{H}^{(1)}(\mu_R, x_Q) &= H^{(1)}(\mu_R) + \left(-\frac{1}{2}A^{(1)} \ln x_Q^2 + B^{(1)} \right) \ln x_Q^2 \\ \tilde{H}^{(2)}(\mu_R, x_Q) &= H^{(2)}(\mu_R) + \frac{(A^{(1)})^2}{8} \ln^4 x_Q^2 - \left(\frac{A^{(1)}B^{(1)}}{2} + \frac{A^{(1)}}{3}\pi\beta_0 \right) \ln^3 x_Q^2 \\ &\quad + \left(\frac{-A^{(2)} + (B^{(1)})^2}{2} + \pi\beta_0 \left(B^{(1)} + A^{(1)} \ln \frac{x_Q^2 M^2}{\mu_R^2} \right) \right) \ln^2 x_Q^2 \\ &\quad - \left(-B^{(2)} + B^{(1)}2\pi\beta_0 \ln \frac{x_Q^2 M^2}{\mu_R^2} \right) \ln x_Q^2 + H^{(1)}(\mu_R) \ln x_Q^2 \left(-\frac{1}{2}A^{(1)} \ln x_Q^2 + B^{(1)} \right), \quad (4.5) \end{aligned}$$

where the functions g_i are given in Appendix B. All derivatives of the R function are to be consistently replaced by derivatives of \tilde{R} with respect to \tilde{L} . Notice that no constant terms are present in the radiator and therefore $g_i(0) = 0$.

The same replacement must be consistently performed in the parton densities. In addition, it is convenient to have the latter evaluated at a common factorisation scale μ_F at large v_1 , in order to match the fixed-order convention. Both steps can be implemented by expressing the parton densities f at the scale $\mu_F e^{-\tilde{L}}$, and expanding out the difference between $f(\mu_F e^{-\tilde{L}}, x)$ and $f(k_{t1}, x)$ neglecting regular terms as well as logarithmic terms beyond N³LL. The relevant terms in this expansion can be absorbed into a redefinition of the coefficient functions $C^{(i)}(z)$, thereby introducing an explicit dependence upon μ_F and x_Q . We obtain

$$\begin{aligned}\tilde{C}_{ij}^{(1)}(z, \mu_F, x_Q) &= C_{ij}^{(1)}(z) + \hat{P}_{ij}^{(0)}(z) \ln \frac{x_Q^2 M^2}{\mu_F^2}, \\ \tilde{C}_{ij}^{(2)}(z, \mu_F, x_Q) &= C_{ij}^{(2)}(z) + \pi \beta_0 \hat{P}_{ij}^{(0)}(z) \left(\ln^2 \frac{x_Q^2 M^2}{\mu_F^2} - 2 \ln \frac{x_Q^2 M^2}{\mu_F^2} \ln \frac{x_Q^2 M^2}{\mu_R^2} \right) + \hat{P}_{ij}^{(1)}(z) \ln \frac{x_Q^2 M^2}{\mu_F^2} \\ &\quad + \frac{1}{2} (\hat{P}^{(0)} \otimes \hat{P}^{(0)})_{ij}(z) \ln^2 \frac{x_Q^2 M^2}{\mu_F^2} + (C^{(1)} \otimes \hat{P}^{(0)})_{ij}(z) \ln \frac{x_Q^2 M^2}{\mu_F^2} - 2\pi \beta_0 C_{ij}^{(1)}(z) \ln \frac{x_Q^2 M^2}{\mu_R^2}.\end{aligned}\tag{4.6}$$

Finally, we also approximate the strong coupling in the terms proportional to $\alpha_s^2(k_{t1})$ in Eq. (3.18), featuring the convolution of one and two splitting functions with the NLL luminosity, by retaining only terms relevant to N³LL as

$$\alpha_s(k_{t1}) \simeq \frac{\alpha_s(\mu_R)}{1 - 2\alpha_s(\mu_R)\beta_0\tilde{L}}.\tag{4.7}$$

Summarising, the final formula that we employ in the matching to fixed order will be Eq. (3.18) with the following replacements:

$$\begin{aligned}L &\rightarrow \tilde{L}, & \frac{dk_{t1}}{k_{t1}} &\rightarrow \mathcal{J}(v_1/x_Q, p) \frac{dk_{t1}}{k_{t1}}, \\ R &\rightarrow \tilde{R}, & R' &\rightarrow d\tilde{R}/d\tilde{L}, & R'' &\rightarrow d\tilde{R}'/d\tilde{L}, & R''' &\rightarrow d\tilde{R}''/d\tilde{L}, \\ \mathcal{L}_{\text{NLL}} &\rightarrow \tilde{\mathcal{L}}_{\text{NLL}}, & \mathcal{L}_{\text{NNLL}} &\rightarrow \tilde{\mathcal{L}}_{\text{NNLL}}, & \mathcal{L}_{\text{N}^3\text{LL}} &\rightarrow \tilde{\mathcal{L}}_{\text{N}^3\text{LL}}.\end{aligned}\tag{4.8}$$

Moreover the coupling is treated according to Eq. (4.7) in the terms $\hat{P}^{(0)} \otimes \tilde{\mathcal{L}}_{\text{NLL}}$ and $\hat{P}^{(0)} \otimes \hat{P}^{(0)} \otimes \tilde{\mathcal{L}}_{\text{NLL}}$, and the upper bound of the k_{t1} integration in Eq. (3.18) is extended to infinity. The modified luminosity factors appearing in the previous equation are defined as

$$\tilde{\mathcal{L}}_{\text{NLL}}(k_{t1}) = \sum_{c, c'} \frac{d|M_B|_{cc'}^2}{d\Phi_B} f_c(\mu_F e^{-\tilde{L}}, x_1) f_{c'}(\mu_F e^{-\tilde{L}}, x_2),\tag{4.9}$$

$$\begin{aligned}\tilde{\mathcal{L}}_{\text{NNLL}}(k_{t1}) &= \sum_{c, c'} \frac{d|M_B|_{cc'}^2}{d\Phi_B} \sum_{i, j} \int_{x_1}^1 \frac{dz_1}{z_1} \int_{x_2}^1 \frac{dz_2}{z_2} f_i\left(\mu_F e^{-\tilde{L}}, \frac{x_1}{z_1}\right) f_j\left(\mu_F e^{-\tilde{L}}, \frac{x_2}{z_2}\right) \\ &\quad \left(\delta_{ci} \delta_{c'j} \delta(1 - z_1) \delta(1 - z_2) \left(1 + \frac{\alpha_s(\mu_R)}{2\pi} \tilde{H}^{(1)}(\mu_R, x_Q) \right) \right. \\ &\quad \left. + \frac{\alpha_s(\mu_R)}{2\pi} \frac{1}{1 - 2\alpha_s(\mu_R)\beta_0\tilde{L}} \left(\tilde{C}_{ci}^{(1)}(z_1, \mu_F, x_Q) \delta(1 - z_2) \delta_{c'j} + \{z_1 \leftrightarrow z_2; c, i \leftrightarrow c'j\} \right) \right),\end{aligned}\tag{4.10}$$

$$\begin{aligned}
\tilde{\mathcal{L}}_{\text{N}^3\text{LL}}(k_{t1}) &= \sum_{c,c'} \frac{d|M_B|_{cc'}^2}{d\Phi_B} \sum_{i,j} \int_{x_1}^1 \frac{dz_1}{z_1} \int_{x_2}^1 \frac{dz_2}{z_2} f_i\left(\mu_F e^{-\tilde{L}}, \frac{x_1}{z_1}\right) f_j\left(\mu_F e^{-\tilde{L}}, \frac{x_2}{z_2}\right) \\
&\left\{ \delta_{ci} \delta_{c'j} \delta(1-z_1) \delta(1-z_2) \left(1 + \frac{\alpha_s(\mu_R)}{2\pi} \tilde{H}^{(1)}(\mu_R, x_Q) + \frac{\alpha_s^2(\mu_R)}{(2\pi)^2} \tilde{H}^{(2)}(\mu_R, x_Q) \right) \right. \\
&+ \frac{\alpha_s(\mu_R)}{2\pi} \frac{1}{1-2\alpha_s(\mu_R)\beta_0\tilde{L}} \left(1 - \alpha_s(\mu_R) \frac{\beta_1}{\beta_0} \frac{\ln\left(1-2\alpha_s(\mu_R)\beta_0\tilde{L}\right)}{1-2\alpha_s(\mu_R)\beta_0\tilde{L}} \right) \\
&\times \left(\tilde{C}_{ci}^{(1)}(z_1, \mu_F, x_Q) \delta(1-z_2) \delta_{c'j} + \{z_1 \leftrightarrow z_2; c, i \leftrightarrow c', j\} \right) \\
&+ \frac{\alpha_s^2(\mu_R)}{(2\pi)^2} \frac{1}{(1-2\alpha_s(\mu_R)\beta_0\tilde{L})^2} \left(\tilde{C}_{ci}^{(2)}(z_1, \mu_F, x_Q) \delta(1-z_2) \delta_{c'j} + \{z_1 \leftrightarrow z_2; c, i \leftrightarrow c', j\} \right) \\
&+ \frac{\alpha_s^2(\mu_R)}{(2\pi)^2} \frac{1}{(1-2\alpha_s(\mu_R)\beta_0\tilde{L})^2} \left(\tilde{C}_{ci}^{(1)}(z_1, \mu_F, x_Q) \tilde{C}_{c'j}^{(1)}(z_2, \mu_F, x_Q) + G_{ci}^{(1)}(z_1) G_{c'j}^{(1)}(z_2) \right) \\
&\left. + \frac{\alpha_s^2(\mu_R)}{(2\pi)^2} \tilde{H}^{(1)}(\mu_R, x_Q) \frac{1}{1-2\alpha_s(\mu_R)\beta_0\tilde{L}} \left(\tilde{C}_{ci}^{(1)}(z_1, \mu_F, x_Q) \delta(1-z_2) \delta_{c'j} + \{z_1 \leftrightarrow z_2; c, i \leftrightarrow c', j\} \right) \right\}.
\end{aligned} \tag{4.11}$$

4.2 Matching to fixed order

To match the above result to a fixed-order calculation we design a scheme belonging to the class of multiplicative matchings [64, 65]. This, at present, is preferable to the more common additive R scheme [42], since the $\mathcal{O}(\alpha_s^3)$ constant terms of the cumulative cross section are currently unknown analytically (except for the three-loop corrections to the form factor that were computed in ref. [66–68]) and they can therefore be recovered numerically from our matching procedure. This ensures that our matched prediction controls all terms up to and including $\mathcal{O}(\alpha_s^n \ln^{2n-6}(1/v))$. Moreover, the multiplicative scheme is less sensitive to numerical instabilities of the fixed-order prediction close to the infrared and collinear regions.

However, the multiplicative scheme in hadronic collisions can give rise to higher-order terms in the high- p_t tail. These are effectively subleading and therefore they never spoil the perturbative accuracy, nevertheless they can be numerically non-negligible for processes featuring large K factors like Higgs production. In order to suppress such spurious terms, we introduce a factor Z defined as

$$Z = \left(1 - \left(\frac{v}{x_Q} \right)^u \right)^h \Theta(x_Q - v), \tag{4.12}$$

where h and u are positive parameters. h should be larger than two in order to avoid small kinks in the differential distribution. In our predictions below we set $h = 3$, and check that variations of ± 1 do not produce sizeable differences. The parameter u will be discussed shortly. In what follows, with a slight abuse of notation, we denote by $\Sigma(v, \Phi_B)$ the generic exclusive cross section $d\Sigma(v)/d\Phi_B$. We therefore define the matched cross section as

$$\Sigma_{\text{MAT}}(v, \Phi_B) = (\Sigma_{\text{RES}}(v, \Phi_B))^Z \frac{\Sigma_{\text{FO}}(v, \Phi_B)}{(\Sigma_{\text{EXP}}(v, \Phi_B))^Z}, \tag{4.13}$$

where Σ_{FO} is the fixed-order cross section at order α_s^n differential in the Born kinematics, and Σ_{EXP} is the expansion of the resummed cross section Σ_{RES} to $\mathcal{O}(\alpha_s^n)$. The factor Z ensures that the resummation is smoothly turned off for $v \geq x_Q$. We stress that at small v the factor Z leads to extra terms which are suppressed as $(v/x_Q)^u$. Therefore u can be chosen in order to make these terms arbitrarily small, although they are already very suppressed in the small- v region. In our case we simply set $u = 1$.

Up to N³LO we now express the fixed-order and the expanded cross sections as

$$\begin{aligned}
\Sigma_{\text{FO}}(v, \Phi_B) &= \sum_{i=0}^3 \Sigma_{\text{FO}}^{(i)}(v, \Phi_B), \\
\Sigma_{\text{FO}}^{(i)}(v, \Phi_B) &= \sigma^{(i)}(\Phi_B) - \int_v dv' \frac{d\Sigma_{\text{FO}}^{(i)}(v', \Phi_B)}{dv'} = \sigma^{(i)}(\Phi_B) + \bar{\Sigma}_{\text{FO}}^{(i)}(v, \Phi_B), \\
\Sigma_{\text{EXP}}(v, \Phi_B) &= \sum_{i=0}^3 \Sigma_{\text{EXP}}^{(i)}(v, \Phi_B),
\end{aligned} \tag{4.14}$$

where $\bar{\Sigma}_{\text{FO}}^{(0)}(v, \Phi_B) = 0$, $\Sigma_{\text{EXP}}^{(0)}(v, \Phi_B) = \sigma^{(0)}$, and we defined $\sigma^{(i)}(\Phi_B) = d\sigma^{(i)}/d\Phi_B$ as the i -th order of the total cross section differential in the Born kinematics

$$\sigma(\Phi_B) = \sum_{i=0}^3 \sigma^{(i)}(\Phi_B). \tag{4.15}$$

With this notation, Eq. (4.13) becomes

$$\begin{aligned}
\Sigma_{\text{MAT}}(v, \Phi_B) &= \left(\frac{\Sigma_{\text{RES}}(v, \Phi_B)}{\sigma^{(0)}(\Phi_B)} \right)^Z \left\{ \sigma^{(0)}(\Phi_B) + \sigma^{(1)}(\Phi_B) + \bar{\Sigma}_{\text{FO}}^{(1)}(v, \Phi_B) - Z \Sigma_{\text{EXP}}^{(1)}(v, \Phi_B) \right. \\
&+ \sigma^{(2)}(\Phi_B) + \bar{\Sigma}_{\text{FO}}^{(2)}(v, \Phi_B) - Z \Sigma_{\text{EXP}}^{(2)}(v, \Phi_B) + \frac{Z(1+Z)}{2} \frac{(\Sigma_{\text{EXP}}^{(1)}(v, \Phi_B))^2}{\sigma^{(0)}(\Phi_B)} \\
&- Z \Sigma_{\text{EXP}}^{(1)}(v, \Phi_B) \frac{\sigma^{(1)}(\Phi_B) + \bar{\Sigma}_{\text{FO}}^{(1)}(v, \Phi_B)}{\sigma^{(0)}(\Phi_B)} \\
&+ \sigma^{(3)}(\Phi_B) + \bar{\Sigma}_{\text{FO}}^{(3)}(v, \Phi_B) - Z \Sigma_{\text{EXP}}^{(3)}(v, \Phi_B) - Z \frac{(1+Z)(2+Z)}{6} \frac{(\Sigma_{\text{EXP}}^{(1)}(v, \Phi_B))^3}{(\sigma^{(0)}(\Phi_B))^2} \\
&+ \frac{Z(1+Z)}{2} \left(\Sigma_{\text{EXP}}^{(1)}(v, \Phi_B) \right)^2 \frac{\sigma^{(1)}(\Phi_B) + \bar{\Sigma}_{\text{FO}}^{(1)}(v, \Phi_B)}{(\sigma^{(0)}(\Phi_B))^2} - Z \Sigma_{\text{EXP}}^{(2)}(v, \Phi_B) \frac{\sigma^{(1)}(\Phi_B) + \bar{\Sigma}_{\text{FO}}^{(1)}(v, \Phi_B)}{\sigma^{(0)}(\Phi_B)} \\
&\left. + Z \Sigma_{\text{EXP}}^{(1)}(v, \Phi_B) \frac{(1+Z)\Sigma_{\text{EXP}}^{(2)}(v, \Phi_B) - \sigma^{(2)}(\Phi_B) - \bar{\Sigma}_{\text{FO}}^{(2)}(v, \Phi_B)}{\sigma^{(0)}(\Phi_B)} \right\}, \tag{4.16}
\end{aligned}$$

where terms contributing at different orders in α_s are separated by an extra blank line in the above equation.

To work out the expansion, we start from the three contributions of Eq. (3.18) with the replacements discussed in Sec. 4.1. The first contribution starts with a single emission, the second features at least two emissions, and the third contributes to events with at least three emissions. The single-emission term can be worked out analytically, since the integrand is a total derivative, while the remaining terms can be expanded to $\mathcal{O}(\alpha_s^3)$ at the integrand level and integrated over the real-emission phase space. When the integrand is expanded out, one can safely set $\epsilon = 0$ as the cancellation of all singularities is now manifest. The expanded result can be expressed as a linear combination in terms of the following three classes of integrals (we write them in terms of $v_1 = k_{t1}/M$):

$$\begin{aligned}
I_2^{(n,m)}(v) &= \int_0^\infty \frac{dv_1}{v_1} \int_0^{2\pi} \frac{d\phi_1}{2\pi} \int_0^1 \frac{d\zeta_2}{\zeta_2} \int_0^{2\pi} \frac{d\phi_2}{2\pi} \mathcal{J}(v_1/x_Q, p) \tilde{L}^n \ln^m \frac{1}{\zeta_2} \\
&\times \left\{ \Theta(v - V(\{\tilde{p}\}, k_1, k_2)) - \Theta(v - V(\{\tilde{p}\}, k_1)) \right\},
\end{aligned}$$

$$\begin{aligned}
I_3^{(n,m)}(v) &= \int_0^\infty \frac{dv_1}{v_1} \int_0^{2\pi} \frac{d\phi_1}{2\pi} \int_0^1 \frac{d\zeta_2}{\zeta_2} \int_0^{2\pi} \frac{d\phi_2}{2\pi} \int_0^1 \frac{d\zeta_3}{\zeta_3} \int_0^{2\pi} \frac{d\phi_3}{2\pi} \mathcal{J}(v_1/x_Q, p) \tilde{L}^n \left(\ln^m \frac{1}{\zeta_2} + \ln^m \frac{1}{\zeta_3} \right) \\
&\quad \times \left\{ \Theta(v - V(\{\tilde{p}\}, k_1, k_2, k_3)) - \Theta(v - V(\{\tilde{p}\}, k_1, k_2)) \right. \\
&\quad \quad \left. - \Theta(v - V(\{\tilde{p}\}, k_1, k_3)) + \Theta(v - V(\{\tilde{p}\}, k_1)) \right\}, \\
I_{3,R''}^{(n)}(v) &= \int_0^\infty \frac{dv_1}{v_1} \int_0^{2\pi} \frac{d\phi_1}{2\pi} \int_0^1 \frac{d\zeta_2}{\zeta_2} \int_0^{2\pi} \frac{d\phi_2}{2\pi} \int_0^1 \frac{d\zeta_3}{\zeta_3} \int_0^{2\pi} \frac{d\phi_3}{2\pi} \mathcal{J}(v_1/x_Q, p) \tilde{L}^n \ln \frac{1}{\zeta_2} \ln \frac{1}{\zeta_3} \\
&\quad \times \left\{ \Theta(v - V(\{\tilde{p}\}, k_1, k_2, k_3)) - \Theta(v - V(\{\tilde{p}\}, k_1, k_2)) \right. \\
&\quad \quad \left. - \Theta(v - V(\{\tilde{p}\}, k_1, k_3)) + \Theta(v - V(\{\tilde{p}\}, k_1)) \right\}, \quad (4.17)
\end{aligned}$$

where \tilde{L} and \mathcal{J} are defined in Eqs. (4.3) and (4.4), respectively. We stress that we extended the upper bound of the integration over v_1 to infinity, following the discussion of Sec. 4.1. The integral over v_1 can be evaluated analytically. The remaining integrations are carried out numerically and the final results are tabulated with fine grids as a function of v/x_Q .

4.3 Event generation

Before presenting a phenomenological application of this formalism, we comment briefly on how Eq. (3.18) is implemented numerically using a Monte Carlo method. We follow a variant of the procedure used in refs. [39, 41, 46]. For the first emission we generate v_1 uniformly according to the integration measure $dv_1/v_1 \mathcal{J}(v_1/x_Q, p)$, and assign it a weight in terms of the Sudakov radiator and parton luminosities. All the identical emissions belonging to the ensemble $d\mathcal{Z}[\{R', k_i\}]$ are generated via a shower ordered in v_i . This is done by expressing the term $\epsilon^{R'(k_{t1})}$ as

$$e^{-R'(k_{t1}) \ln \frac{1}{\epsilon}} = \prod_{i=2}^{n+2} e^{-R'(k_{t1}) \ln \frac{\zeta_{i-1}}{\zeta_i}}, \quad (4.18)$$

with $\zeta_1 = 1$ and $\zeta_{n+2} = \epsilon$. Each emission in $d\mathcal{Z}[\{R', k_i\}]$ now has a weight

$$\frac{d\zeta_i}{\zeta_i} R'(k_{t1}) e^{-R'(k_{t1}) \ln \frac{\zeta_{i-1}}{\zeta_i}},$$

and therefore it can be generated by solving for ζ_i the equation

$$e^{-R'(k_{t1}) \ln \frac{\zeta_{i-1}}{\zeta_i}} = r, \quad (4.19)$$

with r being a random number extracted uniformly in the range $[0, 1]$. The above equation has no solution for $\zeta_i > \zeta_{i-1}$, therefore this amounts to a shower ordered in ζ_i (or, equivalently, in v_i). The procedure is stopped as soon as a $\zeta_i < \epsilon$ is generated. The azimuthal angles are generated uniformly in the range $[0, 2\pi]$ for all emissions. Finally, the *special* emissions, denoted by the subscript s in Eq. (3.18), do not have an associated Sudakov suppression since their contribution is always finite in four dimensions. Therefore we generate them according to their phase-space measure and weight as they appear in the master formula.

This recipe is sufficient to evaluate Eq. (3.18), and it can be implemented in a fast numerical code. We stress that it is an exact procedure, meaning that no truncation at any perturbative order is involved. The algorithm leads to the generation of an arbitrary number of emissions with $\zeta_i > \epsilon$, while all unresolved emissions with $\zeta_i < \epsilon$ are accounted for analytically in the Sudakov radiator. This ensures that the whole singular part of the radiation phase space and all perturbative orders are treated exactly.

We generate Born events using the LO matrix elements and phase-space-integrator routines of MCFM [69], and we use HOPPET [70] to handle the evolution of the parton densities and the convolution with the various coefficient functions.

For each Born event we run the above algorithm to produce the initial-state radiation, and fill the histograms on the fly, thereby yielding $d\Sigma_{\text{RES}}(v)/d\Phi_B$. As a byproduct, this allows us to have exclusive events with N³LL accuracy for the observables treated in this article. For each Born event we also generate a histogram filled with the expansion counterterm, which is computed as described in the previous section. After the generation, the two histograms are combined with the corresponding fixed-order distribution according to Eq. (4.16).

We point out that the Sudakov radiator has a singularity in correspondence of the Landau pole at $2\alpha_s(\mu_R)\beta_0\tilde{L} = 1$ (see expressions in Appendix B). One could use different prescriptions to handle this singularity, all differing by power-suppressed terms in the perturbative expansion. We choose to set the result to zero below the singularity which, anyway, occurs at very small p_t values. We stress that other schemes can be adopted, and that this choice has no consequences above the scale of the singularity.

The resummation and matching as described above are implemented in the program RadISH that can simulate the production of any colour singlet with arbitrary phase-space cuts on the Born kinematics. The code will be released in due course.

4.4 Predictions for Higgs-boson production at 13 TeV pp collisions

We now apply the method described in the previous sections to obtain the inclusive transverse-momentum distribution of the Higgs boson at the LHC. We perform the calculation in the large-top-mass limit, and we match our N³LL result to the NNLO distribution that was computed in refs. [6, 7, 9]. In particular, here we use results obtained with the code of ref. [8] with a cut on the Higgs transverse momentum at 5 GeV. The matched distribution integrates to the inclusive N³LO cross section that is taken from ref. [3].

We consider 13 TeV collisions, and we use parton densities from the PDF4LHC15_nnlo_mc set [71–76]. The value of the parameter p appearing in the modified logarithms \tilde{L} is chosen considering that in the matching region, up to $\sim m_H$, the fixed-order spectrum falls roughly as $\sim 1/p_t^2$. p should thus be ≥ 2 in order to make the matching to the fixed order smooth in this region. On the other hand, its value should not be too large, in order to prevent the peak of the distribution from being artificially pushed upwards due to the unitarity constraint. We therefore set $p = 2$ as our reference value, but nevertheless checked that the choice $p = 3$ induces negligible differences.

As central scales we employ $\mu_R = \mu_F = m_H$, and $x_Q = Q/m_H = 1/2$. The perturbative uncertainty is estimated by performing a seven-scale variation of μ_R, μ_F by a factor of two in either direction, while keeping $1/2 < \mu_R/\mu_F < 2$ and $x_Q = 1/2$; moreover, for central μ_R and μ_F scales, x_Q is varied around its central value in a range that we now turn to discuss.

In the case of the transverse momentum p_t of a colour singlet of mass M , the resummation scale Q is introduced by splitting the resummed logarithms as

$$\ln \frac{M}{p_t} = \ln \frac{Q}{p_t} + \ln \frac{M}{Q}, \quad (4.20)$$

and subsequently assuming that

$$\ln \frac{Q}{p_t} \gg \ln \frac{M}{Q}. \quad (4.21)$$

The latter condition is true at small p_t , and it allows one to expand $\ln(M/p_t)$ about $\ln(Q/p_t)$, retaining only terms relevant to a given logarithmic accuracy. In this case, variations of Q give a handle to estimate the size of subleading-logarithmic terms in the region where all-order effects are important.

However, in the matching region $p_t \sim M/2$, condition (4.21) is violated for $p_t \gtrsim Q^2/M$. In this regime, the variation of the resummation scale is physically meaningless, since the logarithmic hierarchy it is based upon is not valid at these scales. In particular, for Higgs production, a

variation of Q by a factor of two around $m_H/2$ can have a couple of drawbacks. On the one hand, for $Q = m_H/4$, it leads to values of Q^2/m_H which are below the peak of the distribution, implying that the corresponding resummation-scale variation is technically reliable only to the left of the peak. On the other hand, for $Q = m_H$, resummation effects are allowed to survive up to the Higgs scale, which is a fairly hard region of the phase space, where one expects to be predictive with the sole fixed-order calculation. In practice, however, in our matching procedure the resummed contribution is subtracted up to the perturbative order one is matching to, which ensures that the residual variations of Q away from the region of large logarithms induce effects that are numerically very small.

For these two reasons, we believe that a more suitable variation range is given by $Q \in [m_H/3, 3m_H/4]$, which corresponds to a variation by a factor of $3/2$ around the central value $Q = m_H/2$. This range, that was already adopted in ref. [77], ensures that the resummation-scale variation is reliable in the peak region and that resummation effects are turned off well below the hard scale of the reaction, hence avoiding artifacts in the matched spectrum.

To study the impact of this choice, in the left panel of Figure 2 we show the comparison between the pure resummed N^3LL normalised spectra with two uncertainty prescriptions: in the green band, Q is varied by a factor of two around $m_H/2$, while the red band involves the aforementioned reduced variation by a factor of $3/2$; in both cases μ_R and μ_F undergo the seven-point variation described above. As expected, the choice $Q \in [m_H/3, 3m_H/4]$ reduces the impact of the resummation-scale uncertainty in the matching region where the logarithms are not large, while leaving the uncertainty unchanged in the small- p_t regime where the all-order treatment is necessary.

The right panel of Figure 2 shows the comparison between the two prescriptions for the matched $N^3LL+NLO$ distribution.¹¹ In the NLO matching, the resummed component is subtracted up to and including $\mathcal{O}(\alpha_s^2)$ terms relative to the Born. Therefore, in the region where the logarithms are moderate in size, the issues due to the large scale variation are suppressed by $\mathcal{O}(\alpha_s^3)$, and we indeed observe that the two bands differ only moderately at intermediate p_t values.

We conclude that the resummation-scale variation by a factor of $3/2$ still provides a wide enough variation range to probe the size of subleading-logarithmic corrections, while avoiding that some moderate resummation effects persist away from the region where the logarithms are large. We therefore adopt the modified variation in our prescription to estimate the perturbative uncertainty.

We next turn to the comparison with NNLL. The left panel of Figure 3 shows a comparison between the pure resummed predictions for the normalised spectrum at N^3LL and NNLL. The effect of the N^3LL correction on the central value of the distribution is about 10 – 15% for $p_t < 40$ GeV and it is partly driven by the $\mathcal{O}(\alpha_s^2)$ coefficient functions and virtual corrections to the form factor that are not included in the NNLL result. The inclusion of the N^3LL corrections also leads to a reduction in the scale uncertainty of the resummed prediction compared to the NNLL result.¹²

The right plot of Figure 3 shows the matching of the NNLL and N^3LL predictions to NLO. We observe that at the matched level, the N^3LL corrections amount to $\sim 10\%$ around the peak of the spectrum, and they get slightly larger for smaller p_t values ($\lesssim 10$ GeV). A reduction of the total scale uncertainty is observed for $p_t \lesssim 20$ GeV.

To conclude this section, in Figure 4 we report the $N^3LL+NNLO$ prediction for the normalised distribution. The latter is compared both to NNLL+NNLO and to the pure NNLO result. When matched to NNLO, the N^3LL corrections give rise to a few-percent shift of the central value with respect to the NNLL+NNLO prediction around the peak of the distributions, while they have a somewhat larger effect for $p_t \lesssim 10$ GeV. We observe that the matched N^3LL and NNLL predictions are only moderately different in their theoretical-uncertainty bands. While this is of course expected

¹¹Preliminary results at $N^3LL+NLO$ for this observable have been also shown at [78].

¹²An identical reduction in size is observed when varying Q by a factor of two around its central value.

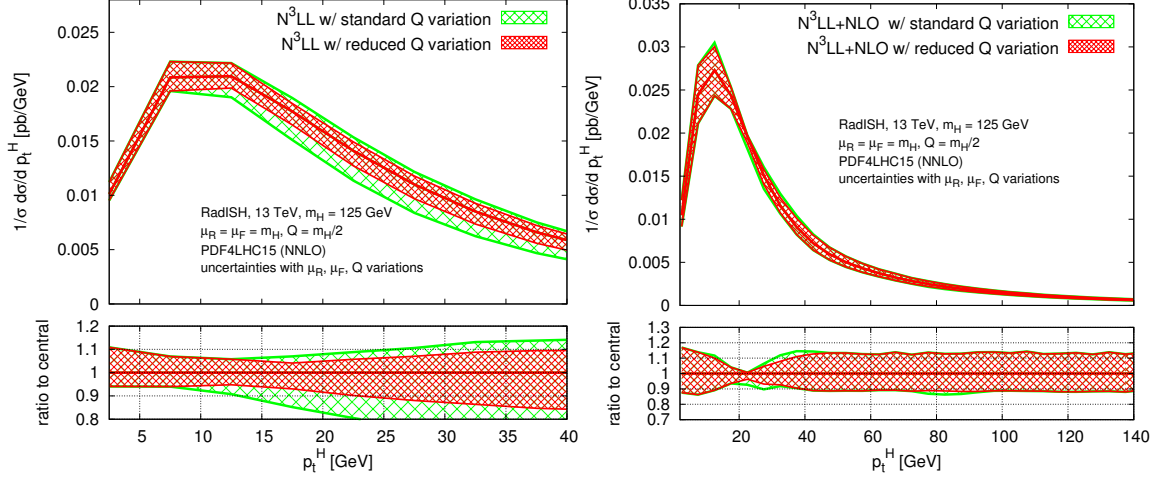


Figure 2. Comparison between two different prescriptions for the resummation-scale-variation range, as described in the text. The comparison is shown both at the resummation level (left) and with a matching to NLO (right).

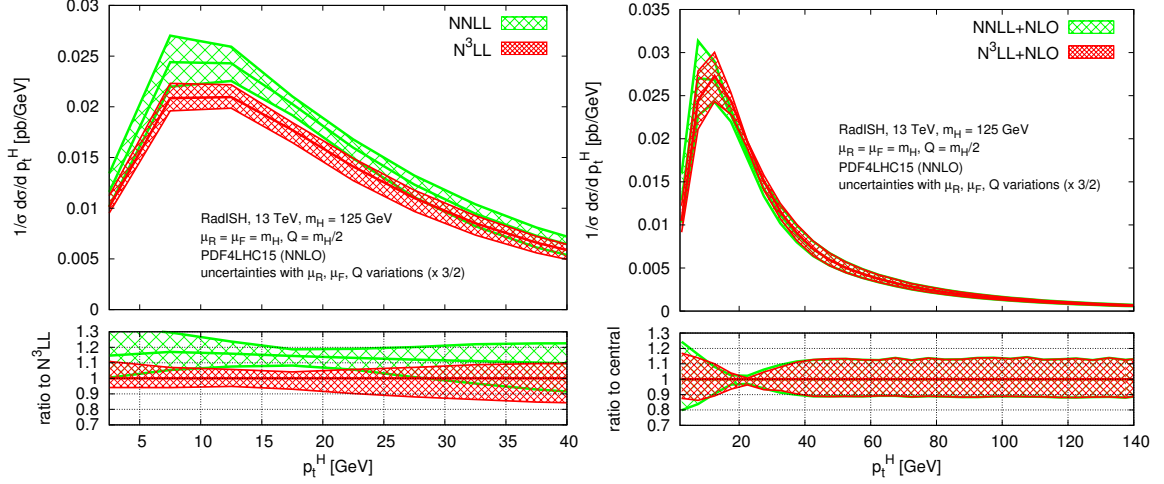


Figure 3. Left: comparison between the resummed distributions at N^3LL and NNLL; the lower panel shows the ratio of the two distributions. Right: comparison between the matched $N^3LL+NLO$ and the NNLL+NLO predictions for the inclusive Higgs spectrum; the lower panel shows the ratio of each distribution to its central value.

in the hard region of the spectrum, we point out that, in the region $p_t \lesssim 30$ GeV, the latter feature is due (and increasingly so at smaller p_t) to numerical instabilities of the fixed-order runs with one of the scales (μ_R or μ_F) set to $m_H/2$. It is indeed necessary to have stable fixed-order predictions down to very small p_t values in order to benefit from the uncertainty reduction due to the higher-order resummation. In particular, for the process under consideration, this requires dedicated runs with very high statistical precision that will be presented in due course.

5 Conclusions

In this article we presented a formulation of the momentum-space resummation for global, recursive infrared and collinear safe observables that vanish far from the Sudakov limit because of kinematic

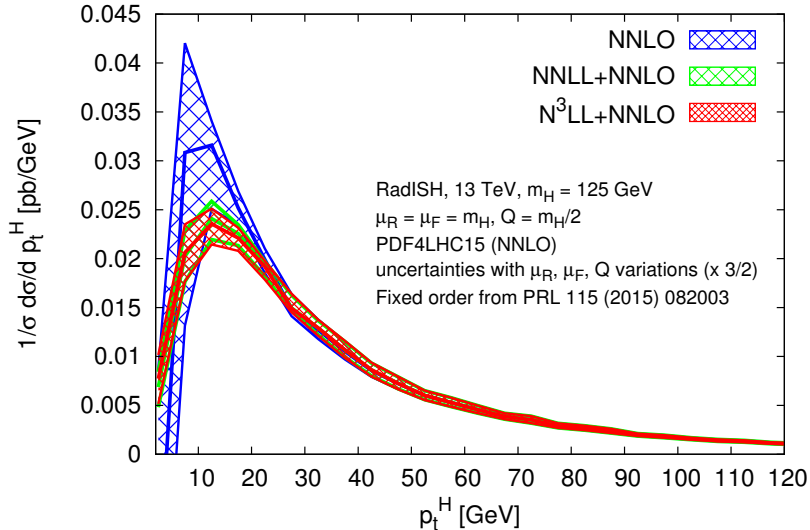


Figure 4. Comparison among the matched normalised distributions at $N^3\text{LL}+\text{NNLO}$, $\text{NNLL}+\text{NNLO}$, and NNLO . The uncertainties are obtained as described in the text.

cancellations implicit in the observable’s definition. In particular, we studied the class of inclusive observables that do not depend on the rapidity of the QCD radiation. Members of this class are, among others, the transverse momentum of a heavy colour singlet and the ϕ^* observable in Drell-Yan pair production. We obtained an all-order formula that is valid for all observables belonging to this class, and we explicitly evaluated it to $N^3\text{LL}$ up to effects due to the yet unknown four-loop cusp anomalous dimension. In the case of the transverse momentum of a colour singlet, we proved that our formulation is equivalent to the more common solution in impact-parameter space at this accuracy. This equivalence allowed us to extract the ingredients necessary to compute the Sudakov radiator at $N^3\text{LL}$ using the recently computed $B^{(3)}$ coefficient [25]. The radiator is universal for all observables of this class [41], which can therefore be resummed to this accuracy with our approach. The all-order result was shown to reproduce the correct power-like scaling in the small- p_t limit, where the perturbative component of the coefficient of the intercept can be systematically improved by including higher-order logarithmic corrections. We implemented our results in the exclusive generator **RadISH**, which performs the resummation and the matching to fixed order, and allows the user to apply arbitrary kinematic cuts on the Born phase space. Although we explicitly treated the case of Higgs production, the code developed here can automatically handle any colour-singlet system.

As a phenomenological application, we computed the Higgs transverse-momentum spectrum at the LHC. In comparison to the $\text{NNLL}+\text{NLO}$ prediction, we find that $N^3\text{LL}+\text{NLO}$ effects are moderate in size, and lead to $\mathcal{O}(10\%)$ corrections near the peak of the distribution and they are somewhat larger for $p_t \lesssim 10\text{ GeV}$. The scale uncertainty of the matched calculation is reduced by the inclusion of the $N^3\text{LL}$ corrections in the small transverse-momentum region. When matched to NNLO , the effect of the $N^3\text{LL}$ is pushed towards lower p_t values, leading to a few percent correction to the previously known $\text{NNLL}+\text{NNLO}$ prediction [37] around the peak, and to more sizeable effects at smaller p_t values. In order to further improve the theoretical control in the small-medium transverse momentum region, it will be necessary to consider the deviations from the large- m_t approximation. Recently, progress has been made in this respect by computing the NLO corrections to the top-bottom interference [12]. Higher-order effects due to the leading tower of logarithms of p_t/m_b were addressed in ref. [79] and were found to be moderate in size. The

procedure for the inclusion of mass effects in the context of transverse-momentum resummation is a debated topic. While some prescriptions are available [80, 81], further studies are necessary to estimate these effects in the logarithmic region at this level of accuracy.

6 Acknowledgements

We wish to thank A. Banfi, G. Salam, G. Zanderighi for stimulating discussions on the topics treated here and very valuable comments on the manuscript. We also thank F. Caola for providing us with the fixed-order runs for the Higgs transverse-momentum spectrum at NNLO. The work of LR is supported by the European Research Council Starting Grant PDF4BSM, WB is supported by the European Research Council grant 614577 HICCUP (High Impact Cross Section Calculations for Ultimate Precision), and the work of ER is supported by a Maria Skłodowska-Curie Individual Fellowship of the European Commission's Horizon 2020 Programme under contract number 659147 PrecisionTools4LHC. PM would like to thank the Erwin Schrödinger Institute of Vienna for hospitality and support while part of this work was carried out. PT would like to thank CERN's Theoretical Physics Department for hospitality during the development of this work.

A Connection with the backward-evolution algorithm at NLL

It is interesting to relate our formulation for the transverse-momentum resummation to a NLL-accurate backward-evolution algorithm [82–84]. We start from Eq. (2.48), that was deduced by considering only flavour-conserving real splitting kernels, for the sake of clarity. We briefly comment on the general flavour case below.

After neglecting the effect of the hard and coefficient functions, which starts at NNLL, we recast the NLL partonic cross section as

$$\begin{aligned} \hat{\Sigma}_{N_1, N_2}^{c_1, c_2}(v) &= \mathbb{1}^{(c_1, c_2)} \int_0^M \frac{dk_{t1}}{k_{t1}} \int_0^{2\pi} \frac{d\phi_1}{2\pi} e^{-\mathbf{R}(\epsilon k_{t1})} \exp \left\{ - \sum_{\ell=1}^2 \int_{\epsilon k_{t1}}^{\mu_0} \frac{dk_t}{k_t} \frac{\alpha_s(k_t)}{\pi} \Gamma_{N_\ell}(\alpha_s(k_t)) \right\} \\ &\sum_{\ell_1=1}^2 \left(\mathbf{R}'_{\ell_1}(k_{t1}) + \frac{\alpha_s(k_{t1})}{\pi} \Gamma_{N_{\ell_1}}(\alpha_s(k_{t1})) \right) \sum_{n=0}^{\infty} \frac{1}{n!} \prod_{i=2}^{n+1} \int_{\epsilon}^1 \frac{d\zeta_i}{\zeta_i} \int_0^{2\pi} \frac{d\phi_i}{2\pi} \\ &\times \sum_{\ell_i=1}^2 \left(\mathbf{R}'_{\ell_i}(k_{ti}) + \frac{\alpha_s(k_{ti})}{\pi} \Gamma_{N_{\ell_i}}(\alpha_s(k_{ti})) \right) \Theta(v - V(\{\tilde{p}\}, k_1, \dots, k_{n+1})), \end{aligned} \quad (\text{A.1})$$

where $\mathbb{1}^{(c_1, c_2)}$ enforces the flavour of the two parton densities to be identical to that entering the Born process, i.e. $\mathbf{f}^T \mathbb{1}^{(c_1, c_2)} \mathbf{f} = f_{c_1} f_{c_2}$. At NLL order, the emission probabilities involve only tree-level splitting functions, whose coupling we evaluate in the CMW scheme, as discussed in Sec. 2.1:

$$\frac{\alpha_s(k_t)}{\pi} \rightarrow \frac{\alpha_s^{\text{CMW}}(k_t)}{\pi} = \frac{\alpha_s(k_t)}{\pi} \left(1 + \frac{\alpha_s(k_t)}{2\pi} K \right), \quad (\text{A.2})$$

where K is defined in Eq. (2.18). In order to perform the inverse Mellin transform of Eq. (A.1), we observe that, when inverted into z space, each of the real-emission probabilities acts on a generic parton distribution $f(x_{\ell_i})$ as described in Section 2.3:

$$\begin{aligned} &\left(R'_{\ell_i}(k_{ti}) + \frac{\alpha_s(k_{ti})}{\pi} \gamma_{N_{\ell_i}}^{(0)}(\alpha_s(k_{ti})) \right) f_{N_{\ell_i}}(\mu) \\ &\rightarrow \frac{\alpha_s^{\text{CMW}}(k_{ti})}{\pi} \left(\int_0^{1-k_{ti}/M} dz_i^{(\ell_i)} P^{(0)}(z_i^{(\ell_i)}) f(\mu, x_{\ell_i}) + \int_{x_{\ell_i}}^1 dz_i^{(\ell_i)} \frac{\hat{P}^{(0)}(z_i^{(\ell_i)})}{z_i^{(\ell_i)}} f(\mu, \frac{x_{\ell_i}}{z_i^{(\ell_i)}}) \right), \end{aligned} \quad (\text{A.3})$$

where we reintroduced the regular terms in the hard-collinear contribution to R'_ℓ , whose $z^{(\ell)}$ upper limit was set to 1 in Section 2.3.

Similarly, we can now restore the remaining power-suppressed terms in the single-emission probability that we neglected in our discussion of Section 2.3, and recast the right-hand side of Eq. (A.3) in terms of the unregularised splitting function as¹³

$$\frac{\alpha_s^{\text{CMW}}(k_{ti})}{\pi} \int_{x_{\ell_i}}^{1-k_{ti}/M} dz_i^{(\ell_i)} \frac{P^{(0)}(z_i^{(\ell_i)})}{z_i^{(\ell_i)}} f\left(\mu, \frac{x_{\ell_i}}{z_i^{(\ell_i)}}\right). \quad (\text{A.4})$$

We furthermore introduce the shower Sudakov form factor $\Delta(Q_i)$, that at NLL reads

$$\Delta(Q_i) = \exp \left\{ - \sum_{\ell=1}^2 \int_{\epsilon k_{t1}}^{Q_i} \frac{dk_t}{k_t} \int_0^{1-k_t/M} dz^{(\ell)} \frac{\alpha_s^{\text{CMW}}(k_t)}{\pi} P^{(0)}(z^{(\ell)}) \right\}, \quad (\text{A.5})$$

such that $\Delta(M) = \exp \{-R_{\text{NLL}}(\epsilon k_{t1})\}$ up to non-logarithmic terms included in Δ but not in $\exp \{-R\}$.

As shown in the main text, in the all-order picture, the correct $z^{(\ell)}$ bounds for each emission depend on the radiation that was emitted before it. Following the discussion of Section 2.1, however, we recall that these effects contribute beyond NLL accuracy, and therefore can be neglected in the present case. We then plug Eq. (A.1) into Eq. (2.47) and perform the inverse Mellin transform as just described, obtaining

$$\begin{aligned} \frac{d\Sigma(v)}{d\Phi_B} &= \frac{d|M_B|_{c_1 c_2}^2}{d\Phi_B} \\ &\times \int_0^M \frac{dk_{t1}}{k_{t1}} \int_0^{2\pi} \frac{d\phi_1}{2\pi} \frac{\Delta(M)}{\Delta(k_{t1})} \sum_{\ell_1=1}^2 \int_{x_{\ell_1}}^{1-k_{t1}/M} dz_1^{(\ell_1)} \frac{\alpha_s^{\text{CMW}}(k_{t1})}{\pi} \frac{P^{(0)}(z_1^{(\ell_1)})}{z_1^{(\ell_1)}} \sum_{n=0}^{\infty} \frac{1}{n!} \prod_{i=2}^{n+1} \int_{\epsilon}^1 \frac{d\zeta_i}{\zeta_i} \int_0^{2\pi} \frac{d\phi_i}{2\pi} \\ &\times \frac{\Delta(k_{t(i-1)})}{\Delta(k_{ti})} \sum_{\ell_i=1}^2 \int_{w_{\ell_i}}^{1-\zeta_i k_{t1}/M} dz_i^{(\ell_i)} \frac{\alpha_s^{\text{CMW}}(k_{ti})}{\pi} \frac{P^{(0)}(z_i^{(\ell_i)})}{z_i^{(\ell_i)}} f_{c_1}(\epsilon k_{t1}, \bar{x}_1) f_{c_2}(\epsilon k_{t1}, \bar{x}_2) \\ &\times \Theta(v - V(\{\tilde{p}\}, k_1, \dots, k_{n+1})), \quad (\text{A.6}) \end{aligned}$$

with $\Delta(\epsilon k_{t1}) = 1$ and

$$w_{\ell_i} = x_{\ell_i} / \left(\prod_{\substack{j=1 \\ \ell_j=\ell_i}}^{i-1} z_j^{(\ell_j)} \right), \quad \bar{x}_1 = x_1 / \left(\prod_{\substack{j=1 \\ \ell_j=1}}^{n+1} z_j^{(\ell_j)} \right), \quad \bar{x}_2 = x_2 / \left(\prod_{\substack{j=1 \\ \ell_j=2}}^{n+1} z_j^{(\ell_j)} \right). \quad (\text{A.7})$$

We stress again that the $z_i^{(\ell)}$ limits in Eq. (A.6) are obtained in the approximation of soft kinematics which is valid at NLL accuracy. To implement Eq. (A.6) in a Markov process we can now impose an ordering in the transverse momentum of the emissions, which amounts to performing the following replacement in Eq. (A.6) (we remind that $\zeta_i = k_{ti}/k_{t1}$)

$$\frac{1}{n!} \prod_{i=2}^{n+1} \int_{\epsilon}^1 \frac{d\zeta_i}{\zeta_i} \rightarrow \int_{\epsilon}^1 \frac{d\zeta_2}{\zeta_2} \int_{\epsilon}^{\zeta_2} \frac{d\zeta_3}{\zeta_3} \dots \int_{\epsilon}^{\zeta_n} \frac{d\zeta_{n+1}}{\zeta_{n+1}}. \quad (\text{A.8})$$

With this replacement, Eq. (A.6) reproduces the backward-evolution equation for a shower of primary gluons emitted off the two initial-state legs (see e.g. Eq. (49) of ref. [84]), ordered in transverse

¹³We recall that Eq. (A.4) in the case of $g \rightarrow gg$ splitting also requires an extra symmetry factor of 2 to account for the fact that the total probability to find a gluon with momentum fraction $z^{(\ell)}$ is the sum of the probability to find either of the two gluons involved in the branching, as in Eq. (2.34).

momentum. The only relevant difference with the common parton-shower formulation is in the fact that, unlike a parton shower, Eq. (A.6) does not contain a no-emission event. This term is indeed infinitely suppressed in our case and therefore it does not contribute to the final result. As a consequence, the cutoff (represented by ϵk_{t1} in our formula) is replaced by a fixed cut Q_0 in the trasverse momentum of the emissions. In order for Eq. (A.6) to be NLL accurate for the transverse-momentum distribution, the recoil of all initial-state emissions must be entirely absorbed by the colour singlet. This shows that a branching algorithm for initial-state radiation that fulfils the above conditions is NLL accurate for this observable (see also [45]). Analogous considerations apply to other rIRC safe, global observables of the type (2.5). To extend the above discussion to the generic flavour case, the same comment made in Section 3.1 applies. It is indeed easier to reformulate the evolution in an angular-ordered way which is what colour coherence imposes. It is possible to show that the backward-evolution algorithm reproduces the resulting evolution formula in that case as well, and it is therefore NLL accurate.

B Analytic formulae for the N³LL radiator

In this Appendix we report the expressions for some of the quantities used in the article. The RGE equation for the QCD coupling reads

$$\frac{d\alpha_s(\mu)}{d\ln\mu^2} = \beta(\alpha_s) \equiv -\alpha_s (\beta_0\alpha_s + \beta_1\alpha_s^2 + \beta_2\alpha_s^3 + \beta_3\alpha_s^4 + \dots). \quad (\text{B.1})$$

The coefficients of the β function (with n_f active flavours) are

$$\beta_0 = \frac{11C_A - 2n_f}{12\pi}, \quad \beta_1 = \frac{17C_A^2 - 5C_An_f - 3C_Fn_f}{24\pi^2}, \quad (\text{B.2})$$

$$\beta_2 = \frac{2857C_A^3 + (54C_F^2 - 615C_FC_A - 1415C_A^2)n_f + (66C_F + 79C_A)n_f^2}{3456\pi^3}, \quad (\text{B.3})$$

$$\begin{aligned} \beta_3 = \frac{1}{(4\pi)^4} & \left\{ C_A C_F n_f^2 \frac{1}{4} \left(\frac{17152}{243} + \frac{448}{9} \zeta_3 \right) + C_A C_F^2 n_f \frac{1}{2} \left(-\frac{4204}{27} + \frac{352}{9} \zeta_3 \right) \right. \\ & + \frac{53}{243} C_A n_f^3 + C_A^2 C_F n_f \frac{1}{2} \left(\frac{7073}{243} - \frac{656}{9} \zeta_3 \right) + C_A^2 n_f^2 \frac{1}{4} \left(\frac{7930}{81} + \frac{224}{9} \zeta_3 \right) \\ & + \frac{154}{243} C_F n_f^3 + C_A^3 n_f \frac{1}{2} \left(-\frac{39143}{81} + \frac{136}{3} \zeta_3 \right) + C_A^4 \left(\frac{150653}{486} - \frac{44}{9} \zeta_3 \right) \\ & + C_F^2 n_f^2 \frac{1}{4} \left(\frac{1352}{27} - \frac{704}{9} \zeta_3 \right) + 23C_F^3 n_f + n_f \frac{d_F^{abcd} d_A^{abcd}}{N_A} \left(\frac{512}{9} - \frac{1664}{3} \zeta_3 \right) \\ & \left. + n_f^2 \frac{d_F^{abcd} d_F^{abcd}}{N_A} \left(-\frac{704}{9} + \frac{512}{3} \zeta_3 \right) + \frac{d_A^{abcd} d_A^{abcd}}{N_A} \left(-\frac{80}{9} + \frac{704}{3} \zeta_3 \right) \right\}, \quad (\text{B.4}) \end{aligned}$$

where

$$\begin{aligned} \frac{d_F^{abcd} d_F^{abcd}}{N_A} &= \frac{N_c^4 - 6N_c^2 + 18}{96N_c^2}, \\ \frac{d_F^{abcd} d_A^{abcd}}{N_A} &= \frac{N_c(N_c^2 + 6)}{48}, \\ \frac{d_A^{abcd} d_A^{abcd}}{N_A} &= \frac{N_c^2(N_c^2 + 36)}{24}, \end{aligned}$$

and $C_A = N_c$, $C_F = \frac{N_c^2 - 1}{2N_c}$, and $N_c = 3$.

The lowest-order regularised Altarelli-Parisi splitting functions in four dimensions are

$$\begin{aligned}
\hat{P}_{qq}^{(0)}(z) &= C_F \left[\frac{1+z^2}{(1-z)_+} + \frac{3}{2} \delta(1-z) \right], \\
\hat{P}_{qg}^{(0)}(z) &= \frac{1}{2} [z^2 + (1-z)^2], \\
\hat{P}_{gq}^{(0)}(z) &= C_F \frac{1+(1-z)^2}{z}, \\
\hat{P}_{gg}^{(0)}(z) &= 2C_A \left[\frac{z}{(1-z)_+} + \frac{1-z}{z} + z(1-z) \right] + 2\pi\beta_0 \delta(1-z),
\end{aligned} \tag{B.5}$$

where the plus prescription is defined as

$$\int_0^1 dz \frac{f(z)}{(1-z)_+} = \int_0^1 dz \frac{f(z) - f(1)}{1-z}. \tag{B.6}$$

The corresponding unregularised Altarelli-Parisi splitting functions in four dimensions are

$$\begin{aligned}
P_{qq}^{(0)}(z) &= C_F \frac{1+z^2}{1-z}, \\
P_{qg}^{(0)}(z) &= \frac{1}{2} [z^2 + (1-z)^2], \\
P_{gq}^{(0)}(z) &= C_F \frac{1+(1-z)^2}{z}, \\
P_{gg}^{(0)}(z) &= C_A \left[\frac{z}{1-z} + \frac{1-z}{z} + z(1-z) \right].
\end{aligned} \tag{B.7}$$

Next we report the functions that enter the definition of the Sudakov radiator (Eq. (4.5)) up to NNLL. To simplify the notation we set $\lambda = \alpha_s(\mu_R)\beta_0 L$. They read

$$g_1(\alpha_s L) = \frac{A^{(1)} 2\lambda + \ln(1-2\lambda)}{\pi\beta_0 2\lambda}, \tag{B.8}$$

$$\begin{aligned}
g_2(\alpha_s L) &= \frac{1}{2\pi\beta_0} \ln(1-2\lambda) \left(A^{(1)} \ln \frac{1}{x_Q^2} + B^{(1)} \right) - \frac{A^{(2)} 2\lambda + (1-2\lambda) \ln(1-2\lambda)}{4\pi^2\beta_0^2 (1-2\lambda)} \\
&\quad + A^{(1)} \left(-\frac{\beta_1}{4\pi\beta_0^3} \frac{\ln(1-2\lambda)((2\lambda-1)\ln(1-2\lambda)-2)-4\lambda}{1-2\lambda} \right. \\
&\quad \left. - \frac{1}{2\pi\beta_0} \frac{(2\lambda(1-\ln(1-2\lambda))+\ln(1-2\lambda))}{1-2\lambda} \ln \frac{\mu_R^2}{x_Q^2 M^2} \right),
\end{aligned} \tag{B.9}$$

$$\begin{aligned}
g_3(\alpha_s L) &= \left(A^{(1)} \ln \frac{1}{x_Q^2} + B^{(1)} \right) \left(-\frac{\lambda}{1-2\lambda} \ln \frac{\mu_R^2}{x_Q^2 M^2} + \frac{\beta_1}{2\beta_0^2} \frac{2\lambda + \ln(1-2\lambda)}{1-2\lambda} \right) \\
&\quad - \frac{1}{2\pi\beta_0} \frac{\lambda}{1-2\lambda} \left(A^{(2)} \ln \frac{1}{x_Q^2} + B^{(2)} \right) - \frac{A^{(3)}}{4\pi^2\beta_0^2} \frac{\lambda^2}{(1-2\lambda)^2} \\
&\quad + A^{(2)} \left(\frac{\beta_1}{4\pi\beta_0^3} \frac{2\lambda(3\lambda-1) + (4\lambda-1)\ln(1-2\lambda)}{(1-2\lambda)^2} - \frac{1}{\pi\beta_0} \frac{\lambda^2}{(1-2\lambda)^2} \ln \frac{\mu_R^2}{x_Q^2 M^2} \right) \\
&\quad + A^{(1)} \left(\frac{\lambda(\beta_0\beta_2(1-3\lambda) + \beta_1^2\lambda)}{\beta_0^4(1-2\lambda)^2} + \frac{(1-2\lambda)\ln(1-2\lambda)(\beta_0\beta_2(1-2\lambda) + 2\beta_1^2\lambda)}{2\beta_0^4(1-2\lambda)^2} \right. \\
&\quad \left. + \frac{\beta_1^2}{4\beta_0^4} \frac{(1-4\lambda)\ln^2(1-2\lambda)}{(1-2\lambda)^2} - \frac{\lambda^2}{(1-2\lambda)^2} \ln^2 \frac{\mu_R^2}{x_Q^2 M^2} \right. \\
&\quad \left. - \frac{\beta_1}{2\beta_0^2} \frac{(2\lambda(1-2\lambda) + (1-4\lambda)\ln(1-2\lambda))}{(1-2\lambda)^2} \ln \frac{\mu_R^2}{x_Q^2 M^2} \right).
\end{aligned} \tag{B.10}$$

The new N³LL g_4 coefficient reads

$$\begin{aligned}
g_4(\alpha_s L) = & \frac{A^{(4)}(3-2\lambda)\lambda^2}{24\pi^2\beta_0^2(2\lambda-1)^3} \\
& + \frac{A^{(3)}}{48\pi\beta_0^3(2\lambda-1)^3} \left\{ 3\beta_1(1-6\lambda)\ln(1-2\lambda) + 2\lambda \left(\beta_1(5\lambda(2\lambda-3) + 3) \right. \right. \\
& \quad \left. \left. + 6\beta_0^2(3-2\lambda)\lambda \ln \frac{\mu_R^2}{x_Q^2 M^2} \right) + 12\beta_0^2(\lambda-1)\lambda(2\lambda-1) \ln \frac{1}{x_Q^2} \right\} \\
& + \frac{A^{(2)}}{24\beta_0^4(2\lambda-1)^3} \left\{ 32\beta_0\beta_2\lambda^3 - 2\beta_1^2\lambda(\lambda(22\lambda-9) + 3) \right. \\
& \quad + 12\beta_0^4(3-2\lambda)\lambda^2 \ln^2 \frac{\mu_R^2}{x_Q^2 M^2} + 6\beta_0^2 \ln \frac{\mu_R^2}{x_Q^2 M^2} \times \\
& \quad \left(\beta_1(1-6\lambda)\ln(1-2\lambda) + 2(\lambda-1)\lambda(2\lambda-1) \left(\beta_1 + 2\beta_0^2 \ln \frac{1}{x_Q^2} \right) \right) \\
& \quad + 3\beta_1 \left(\beta_1 \ln(1-2\lambda)(2\lambda + (6\lambda-1)\ln(1-2\lambda) - 1) \right. \\
& \quad \left. \left. - 2\beta_0^2(2\lambda-1)(2(\lambda-1)\lambda - \ln(1-2\lambda)) \ln \frac{1}{x_Q^2} \right) \right\} \\
& + \frac{\pi A^{(1)}}{12\beta_0^5(2\lambda-1)^3} \left\{ \beta_1^3(1-6\lambda)\ln^3(1-2\lambda) + 3\ln(1-2\lambda) \left(\beta_0^2\beta_3(2\lambda-1)^3 \right. \right. \\
& \quad + \beta_0\beta_1\beta_2(1-2\lambda)(8\lambda^2-4\lambda+3) + 4\beta_1^3\lambda^2(2\lambda+1) \\
& \quad + \beta_0^2\beta_1 \ln \frac{\mu_R^2}{x_Q^2 M^2} \left(\beta_0^2(1-6\lambda) \ln \frac{\mu_R^2}{x_Q^2 M^2} - 4\beta_1\lambda \right) \\
& \quad + 3\beta_1^2 \ln^2(1-2\lambda) \left(2\beta_1\lambda + \beta_0^2(6\lambda-1) \ln \frac{\mu_R^2}{x_Q^2 M^2} \right) \\
& \quad + 3\beta_0^2(2\lambda-1) \ln \frac{1}{x_Q^2} \left(-\beta_1^2 \ln^2(1-2\lambda) + 2\beta_0^2\beta_1 \ln(1-2\lambda) \ln \frac{\mu_R^2}{x_Q^2 M^2} \right. \\
& \quad \left. + 4\lambda \left(\lambda(\beta_1^2 - \beta_0\beta_2) + \beta_0^4(\lambda-1) \ln^2 \frac{\mu_R^2}{x_Q^2 M^2} \right) \right) \\
& \quad + 2\lambda \left(\beta_0^2\beta_3((15-14\lambda)\lambda-3) + \beta_0\beta_1\beta_2(5\lambda(2\lambda-3) + 3) \right. \\
& \quad + 4\beta_1^3\lambda^2 + 2\beta_0^6(3-2\lambda)\lambda \ln^3 \frac{\mu_R^2}{x_Q^2 M^2} + 3\beta_0^4\beta_1 \ln^2 \frac{\mu_R^2}{x_Q^2 M^2} \\
& \quad \left. \left. + 6\beta_0^2\lambda(2\lambda+1)(\beta_0\beta_2 - \beta_1^2) \ln \frac{\mu_R^2}{x_Q^2 M^2} - 8\beta_0^6(4\lambda^2 - 6\lambda + 3)\zeta_3 \right) \right\} \\
& + \frac{B^{(3)}(\lambda-1)\lambda}{4\pi\beta_0(1-2\lambda)^2} + \frac{B^{(2)} \left(\beta_1 \ln(1-2\lambda) - 2(\lambda-1)\lambda \left(\beta_1 - 2\beta_0^2 \ln \frac{\mu_R^2}{x_Q^2 M^2} \right) \right)}{4\beta_0^2(1-2\lambda)^2} \\
& + \frac{\pi B^{(1)}}{4\beta_0^3(1-2\lambda)^2} \left\{ 4\lambda \left(\lambda(\beta_1^2 - \beta_0\beta_2) + \beta_0^4(\lambda-1) \ln^2 \frac{\mu_R^2}{x_Q^2 M^2} \right) \right\}
\end{aligned}$$

$$\left. -\beta_1^2 \ln^2(1-2\lambda) + 2\beta_0^2 \beta_1 \ln(1-2\lambda) \ln \frac{\mu_R^2}{x_Q^2 M^2} \right\}. \quad (\text{B.11})$$

References

- [1] ATLAS collaboration, G. Aad et al., *Observation of a new particle in the search for the Standard Model Higgs boson with the ATLAS detector at the LHC*, *Phys. Lett.* **B716** (2012) 1–29, [[1207.7214](#)].
- [2] CMS collaboration, S. Chatrchyan et al., *Observation of a new boson at a mass of 125 GeV with the CMS experiment at the LHC*, *Phys. Lett.* **B716** (2012) 30–61, [[1207.7235](#)].
- [3] C. Anastasiou, C. Duhr, F. Dulat, F. Herzog and B. Mistlberger, *Higgs Boson Gluon-Fusion Production in QCD at Three Loops*, *Phys. Rev. Lett.* **114** (2015) 212001, [[1503.06056](#)].
- [4] C. Anastasiou, C. Duhr, F. Dulat, E. Furlan, T. Gehrmann, F. Herzog et al., *High precision determination of the gluon fusion Higgs boson cross-section at the LHC*, *JHEP* **05** (2016) 058, [[1602.00695](#)].
- [5] M. Bonvini, S. Marzani, C. Muselli and L. Rottoli, *On the Higgs cross section at $N^3\text{LO}+N^3\text{LL}$ and its uncertainty*, *JHEP* **08** (2016) 105, [[1603.08000](#)].
- [6] R. Boughezal, F. Caola, K. Melnikov, F. Petriello and M. Schulze, *Higgs boson production in association with a jet at next-to-next-to-leading order*, *Phys. Rev. Lett.* **115** (2015) 082003, [[1504.07922](#)].
- [7] R. Boughezal, C. Focke, W. Giele, X. Liu and F. Petriello, *Higgs boson production in association with a jet at NNLO using jetiness subtraction*, *Phys. Lett.* **B748** (2015) 5–8, [[1505.03893](#)].
- [8] F. Caola, K. Melnikov and M. Schulze, *Fiducial cross sections for Higgs boson production in association with a jet at next-to-next-to-leading order in QCD*, *Phys. Rev.* **D92** (2015) 074032, [[1508.02684](#)].
- [9] X. Chen, J. Cruz-Martinez, T. Gehrmann, E. W. N. Glover and M. Jaquier, *NNLO QCD corrections to Higgs boson production at large transverse momentum*, *JHEP* **10** (2016) 066, [[1607.08817](#)].
- [10] K. Melnikov, L. Tancredi and C. Wever, *Two-loop $gg \rightarrow Hg$ amplitude mediated by a nearly massless quark*, *JHEP* **11** (2016) 104, [[1610.03747](#)].
- [11] K. Melnikov, L. Tancredi and C. Wever, *Two-loop amplitudes for $qg \rightarrow Hq$ and $q\bar{q} \rightarrow Hg$ mediated by a nearly massless quark*, *Phys. Rev.* **D95** (2017) 054012, [[1702.00426](#)].
- [12] J. M. Lindert, K. Melnikov, L. Tancredi and C. Wever, *Top-bottom interference effects in Higgs plus jet production at the LHC*, [1703.03886](#).
- [13] G. Parisi and R. Petronzio, *Small Transverse Momentum Distributions in Hard Processes*, *Nucl. Phys.* **B154** (1979) 427–440.
- [14] J. C. Collins, D. E. Soper and G. F. Sterman, *Transverse Momentum Distribution in Drell-Yan Pair and W and Z Boson Production*, *Nucl. Phys.* **B250** (1985) 199–224.
- [15] G. Bozzi, S. Catani, D. de Florian and M. Grazzini, *The $q(T)$ spectrum of the Higgs boson at the LHC in QCD perturbation theory*, *Phys. Lett.* **B564** (2003) 65–72, [[hep-ph/0302104](#)].
- [16] G. Bozzi, S. Catani, D. de Florian and M. Grazzini, *Transverse-momentum resummation and the spectrum of the Higgs boson at the LHC*, *Nucl. Phys.* **B737** (2006) 73–120, [[hep-ph/0508068](#)].
- [17] S. Catani, D. de Florian and M. Grazzini, *Universality of nonleading logarithmic contributions in transverse momentum distributions*, *Nucl. Phys.* **B596** (2001) 299–312, [[hep-ph/0008184](#)].
- [18] T. Becher, M. Neubert and D. Wilhelm, *Higgs-Boson Production at Small Transverse Momentum*, *JHEP* **05** (2013) 110, [[1212.2621](#)].

- [19] T. Becher and M. Neubert, *Drell-Yan Production at Small q_T , Transverse Parton Distributions and the Collinear Anomaly*, *Eur. Phys. J.* **C71** (2011) 1665, [[1007.4005](#)].
- [20] M. G. Echevarria, A. Idilbi and I. Scimemi, *Factorization Theorem For Drell-Yan At Low q_T And Transverse Momentum Distributions On-The-Light-Cone*, *JHEP* **07** (2012) 002, [[1111.4996](#)].
- [21] D. Neill, I. Z. Rothstein and V. Vaidya, *The Higgs Transverse Momentum Distribution at NNLL and its Theoretical Errors*, *JHEP* **12** (2015) 097, [[1503.00005](#)].
- [22] S. Catani and M. Grazzini, *Higgs Boson Production at Hadron Colliders: Hard-Collinear Coefficients at the NNLO*, *Eur. Phys. J.* **C72** (2012) 2013, [[1106.4652](#)].
- [23] S. Catani, L. Cieri, D. de Florian, G. Ferrera and M. Grazzini, *Vector boson production at hadron colliders: hard-collinear coefficients at the NNLO*, *Eur. Phys. J.* **C72** (2012) 2195, [[1209.0158](#)].
- [24] T. Gehrmann, T. Luebbert and L. L. Yang, *Calculation of the transverse parton distribution functions at next-to-next-to-leading order*, *JHEP* **06** (2014) 155, [[1403.6451](#)].
- [25] Y. Li and H. X. Zhu, *Bootstrapping Rapidity Anomalous Dimensions for Transverse-Momentum Resummation*, *Phys. Rev. Lett.* **118** (2017) 022004, [[1604.01404](#)].
- [26] H.-n. Li, *Unification of the $k(T)$ and threshold resummations*, *Phys. Lett.* **B454** (1999) 328–334, [[hep-ph/9812363](#)].
- [27] E. Laenen, G. F. Sterman and W. Vogelsang, *Recoil and threshold corrections in short distance cross-sections*, *Phys. Rev.* **D63** (2001) 114018, [[hep-ph/0010080](#)].
- [28] A. Kulesza, G. F. Sterman and W. Vogelsang, *Joint resummation for Higgs production*, *Phys. Rev.* **D69** (2004) 014012, [[hep-ph/0309264](#)].
- [29] S. Marzani, *Combining Q_T and small- x resummations*, *Phys. Rev.* **D93** (2016) 054047, [[1511.06039](#)].
- [30] S. Forte and C. Muselli, *High energy resummation of transverse momentum distributions: Higgs in gluon fusion*, *JHEP* **03** (2016) 122, [[1511.05561](#)].
- [31] F. Caola, S. Forte, S. Marzani, C. Muselli and G. Vita, *The Higgs transverse momentum spectrum with finite quark masses beyond leading order*, *JHEP* **08** (2016) 150, [[1606.04100](#)].
- [32] G. Lusterians, W. J. Waalewijn and L. Zeune, *Joint transverse momentum and threshold resummation beyond NLL*, *Phys. Lett.* **B762** (2016) 447–454, [[1605.02740](#)].
- [33] S. Marzani and V. Theeuwes, *Vector boson production in joint resummation*, *JHEP* **02** (2017) 127, [[1612.01432](#)].
- [34] C. Muselli, S. Forte and G. Ridolfi, *Combined threshold and transverse momentum resummation for inclusive observables*, *JHEP* **03** (2017) 106, [[1701.01464](#)].
- [35] R. K. Ellis and S. Veseli, *W and Z transverse momentum distributions: Resummation in q_T space*, *Nucl. Phys.* **B511** (1998) 649–669, [[hep-ph/9706526](#)].
- [36] S. Frixione, P. Nason and G. Ridolfi, *Problems in the resummation of soft gluon effects in the transverse momentum distributions of massive vector bosons in hadronic collisions*, *Nucl. Phys.* **B542** (1999) 311–328, [[hep-ph/9809367](#)].
- [37] P. F. Monni, E. Re and P. Torrielli, *Higgs Transverse-Momentum Resummation in Direct Space*, *Phys. Rev. Lett.* **116** (2016) 242001, [[1604.02191](#)].
- [38] M. A. Ebert and F. J. Tackmann, *Resummation of Transverse Momentum Distributions in Distribution Space*, *JHEP* **02** (2017) 110, [[1611.08610](#)].
- [39] A. Banfi, G. P. Salam and G. Zanderighi, *Principles of general final-state resummation and automated implementation*, *JHEP* **03** (2005) 073, [[hep-ph/0407286](#)].
- [40] A. Banfi, S. Redford, M. Vesterinen, P. Waller and T. R. Wyatt, *Optimisation of variables for studying dilepton transverse momentum distributions at hadron colliders*, *Eur. Phys. J.* **C71** (2011) 1600, [[1009.1580](#)].

- [41] A. Banfi, H. McAslan, P. F. Monni and G. Zanderighi, *A general method for the resummation of event-shape distributions in e^+e^- annihilation*, *JHEP* **05** (2015) 102, [[1412.2126](#)].
- [42] S. Catani, L. Trentadue, G. Turnock and B. R. Webber, *Resummation of large logarithms in e^+e^- event shape distributions*, *Nucl. Phys.* **B407** (1993) 3–42.
- [43] S. Catani and L. Trentadue, *Resummation of the QCD Perturbative Series for Hard Processes*, *Nucl. Phys.* **B327** (1989) 323–352.
- [44] A. Banfi, G. P. Salam and G. Zanderighi, *Generalized resummation of QCD final state observables*, *Phys. Lett.* **B584** (2004) 298–305, [[hep-ph/0304148](#)].
- [45] S. Catani, B. R. Webber and G. Marchesini, *QCD coherent branching and semiinclusive processes at large x* , *Nucl. Phys.* **B349** (1991) 635–654.
- [46] A. Banfi, G. P. Salam and G. Zanderighi, *Semi-numerical resummation of event shapes*, *JHEP* **01** (2002) 018, [[hep-ph/0112156](#)].
- [47] A. Banfi, H. McAslan, P. F. Monni and G. Zanderighi, *The two-jet rate in e^+e^- at next-to-next-to-leading-logarithmic order*, *Phys. Rev. Lett.* **117** (2016) 172001, [[1607.03111](#)].
- [48] R. K. Ellis, W. J. Stirling and B. R. Webber, *QCD and collider physics*, *Camb. Monogr. Part. Phys. Nucl. Phys. Cosmol.* **8** (1996) 1–435.
- [49] V. N. Gribov and L. N. Lipatov, *Deep inelastic $e p$ scattering in perturbation theory*, *Sov. J. Nucl. Phys.* **15** (1972) 438–450.
- [50] G. Altarelli and G. Parisi, *Asymptotic Freedom in Parton Language*, *Nucl. Phys.* **B126** (1977) 298–318.
- [51] Y. L. Dokshitzer, *Calculation of the Structure Functions for Deep Inelastic Scattering and e^+e^- Annihilation by Perturbation Theory in Quantum Chromodynamics.*, *Sov. Phys. JETP* **46** (1977) 641–653.
- [52] S. Catani and M. Grazzini, *QCD transverse-momentum resummation in gluon fusion processes*, *Nucl. Phys.* **B845** (2011) 297–323, [[1011.3918](#)].
- [53] S. Catani, D. de Florian, M. Grazzini and P. Nason, *Soft gluon resummation for Higgs boson production at hadron colliders*, *JHEP* **07** (2003) 028, [[hep-ph/0306211](#)].
- [54] A. Banfi, P. F. Monni, G. P. Salam and G. Zanderighi, *Higgs and Z-boson production with a jet veto*, *Phys. Rev. Lett.* **109** (2012) 202001, [[1206.4998](#)].
- [55] D. de Florian and M. Grazzini, *The Structure of large logarithmic corrections at small transverse momentum in hadronic collisions*, *Nucl. Phys.* **B616** (2001) 247–285, [[hep-ph/0108273](#)].
- [56] C. T. H. Davies and W. J. Stirling, *Nonleading Corrections to the Drell-Yan Cross-Section at Small Transverse Momentum*, *Nucl. Phys.* **B244** (1984) 337–348.
- [57] P. F. Monni, T. Gehrmann and G. Luisoni, *Two-Loop Soft Corrections and Resummation of the Thrust Distribution in the Dijet Region*, *JHEP* **08** (2011) 010, [[1105.4560](#)].
- [58] M. Kramer, E. Laenen and M. Spira, *Soft gluon radiation in Higgs boson production at the LHC*, *Nucl. Phys.* **B511** (1998) 523–549, [[hep-ph/9611272](#)].
- [59] K. G. Chetyrkin, B. A. Kniehl and M. Steinhauser, *Hadronic Higgs decay to order α_s^4* , *Phys. Rev. Lett.* **79** (1997) 353–356, [[hep-ph/9705240](#)].
- [60] R. V. Harlander, *Virtual corrections to $g g \rightarrow H$ to two loops in the heavy top limit*, *Phys. Lett.* **B492** (2000) 74–80, [[hep-ph/0007289](#)].
- [61] G. Kramer and B. Lampe, *Two Jet Cross-Section in e^+e^- Annihilation*, *Z. Phys.* **C34** (1987) 497.
- [62] T. Matsuura, S. C. van der Marck and W. L. van Neerven, *The Calculation of the Second Order Soft and Virtual Contributions to the Drell-Yan Cross-Section*, *Nucl. Phys.* **B319** (1989) 570–622.

- [63] T. Gehrmann, T. Huber and D. Maitre, *Two-loop quark and gluon form-factors in dimensional regularisation*, *Phys. Lett.* **B622** (2005) 295–302, [[hep-ph/0507061](#)].
- [64] M. Dasgupta and G. P. Salam, *Resummation of the jet broadening in DIS*, *Eur. Phys. J.* **C24** (2002) 213–236, [[hep-ph/0110213](#)].
- [65] V. Antonelli, M. Dasgupta and G. P. Salam, *Resummation of thrust distributions in DIS*, *JHEP* **02** (2000) 001, [[hep-ph/9912488](#)].
- [66] P. A. Baikov, K. G. Chetyrkin, A. V. Smirnov, V. A. Smirnov and M. Steinhauser, *Quark and gluon form factors to three loops*, *Phys. Rev. Lett.* **102** (2009) 212002, [[0902.3519](#)].
- [67] R. N. Lee, A. V. Smirnov and V. A. Smirnov, *Analytic Results for Massless Three-Loop Form Factors*, *JHEP* **04** (2010) 020, [[1001.2887](#)].
- [68] T. Gehrmann, E. W. N. Glover, T. Huber, N. Ikizlerli and C. Studerus, *The quark and gluon form factors to three loops in QCD through to $O(\epsilon^2)$* , *JHEP* **11** (2010) 102, [[1010.4478](#)].
- [69] J. M. Campbell, R. K. Ellis and C. Williams, *Vector boson pair production at the LHC*, *JHEP* **07** (2011) 018, [[1105.0020](#)].
- [70] G. P. Salam and J. Rojo, *A Higher Order Perturbative Parton Evolution Toolkit (HOPPET)*, *Comput. Phys. Commun.* **180** (2009) 120–156, [[0804.3755](#)].
- [71] J. Butterworth et al., *PDF4LHC recommendations for LHC Run II*, *J. Phys.* **G43** (2016) 023001, [[1510.03865](#)].
- [72] S. Dulat, T.-J. Hou, J. Gao, M. Guzzi, J. Huston, P. Nadolsky et al., *New parton distribution functions from a global analysis of quantum chromodynamics*, *Phys. Rev.* **D93** (2016) 033006, [[1506.07443](#)].
- [73] NNPDF collaboration, R. D. Ball et al., *Parton distributions for the LHC Run II*, *JHEP* **04** (2015) 040, [[1410.8849](#)].
- [74] L. A. Harland-Lang, A. D. Martin, P. Motylinski and R. S. Thorne, *Parton distributions in the LHC era: MMHT 2014 PDFs*, *Eur. Phys. J.* **C75** (2015) 204, [[1412.3989](#)].
- [75] S. Carrazza, J. I. Latorre, J. Rojo and G. Watt, *A compression algorithm for the combination of PDF sets*, *Eur. Phys. J.* **C75** (2015) 474, [[1504.06469](#)].
- [76] G. Watt and R. S. Thorne, *Study of Monte Carlo approach to experimental uncertainty propagation with MSTW 2008 PDFs*, *JHEP* **08** (2012) 052, [[1205.4024](#)].
- [77] A. Banfi, F. Caola, F. A. Dreyer, P. F. Monni, G. P. Salam, G. Zanderighi et al., *Jet-vetoed Higgs cross section in gluon fusion at $N^3LO+NNLL$ with small- R resummation*, *JHEP* **04** (2016) 049, [[1511.02886](#)].
- [78] H. X. Zhu, *Transverse-momentum resummation for Higgs production at N^3LL* , Talk given at *LoopFest XV* (2016) .
- [79] K. Melnikov and A. Penin, *On the light quark mass effects in Higgs boson production in gluon fusion*, *JHEP* **05** (2016) 172, [[1602.09020](#)].
- [80] M. Grazzini and H. Sargsyan, *Heavy-quark mass effects in Higgs boson production at the LHC*, *JHEP* **09** (2013) 129, [[1306.4581](#)].
- [81] A. Banfi, P. F. Monni and G. Zanderighi, *Quark masses in Higgs production with a jet veto*, *JHEP* **01** (2014) 097, [[1308.4634](#)].
- [82] T. Sjostrand, *A Model for Initial State Parton Showers*, *Phys. Lett.* **B157** (1985) 321–325.
- [83] T. D. Gottschalk, *BACKWARDS EVOLVED INITIAL STATE PARTON SHOWERS*, *Nucl. Phys.* **B277** (1986) 700–738.
- [84] G. Marchesini and B. R. Webber, *Monte Carlo Simulation of General Hard Processes with Coherent QCD Radiation*, *Nucl. Phys.* **B310** (1988) 461–526.